LEONARD WOOD INSTITUTE COLLABORATIVE RESEARCH PROJECT
FINAL REPORT

LWI Subaward Number:	LWI 61042
Project Title:	Demonstration Mobile Seismic Unit for Detecting Subterranean Passageways
Principal Investigator:	Dr. Neil Anderson
Co-Investigator	Dr. Steve Grant
Period of Report:	Final Report

1. PROJECT OVERVIEW/ABSTRACT

A mobile seismic unit for detecting shallow subterranean passageways was designed and constructed. The unit was successfully field tested and/or demonstrated at six known tunnel sites (tunnel diameters ranged from 0.6–4.0 m; tunnel depths ranged from 0.3–1.5 m). The locations of the six tunnels were determined with an average accuracy of 0.5 m; on average, one false positive was identified on each of the six test site data sets.

The mobile unit consists of an ATV, a 24-channel seismograph, an acoustic weight drop source, a 17 m-long land streamer, a camera, a GPS system, a survey wheel and a laptop computer. The demonstration unit can be operated by non-technical personnel and is capable of acquiring ~0.5 km of field data per day. The data can be interpreted in the field by non-technical personnel using fully-automated built-in interpretational software.

2. PROJECT SCHEDULE

All seven tasks identified in the original proposal were completed as anticipated (Table 1). All project milestones were achieved. The unit was successfully field tested and demonstrated.

Task	**N**	**D**	**J**	**F**	**M**	**A**	**M**	**J**	**J**	**A**	**S**	**O**	**N**	**D**
Task I: Physical construction of basic mobile unit	**X**	**X**												
Task II: Interfacing of modularized components	**X**	**X**	**X**	**X**										
Task III: Acquisition of test data	**X**	**X**	**X**	**X**	**X**	**X**	**X**	**X**	**X**	**X**				
Task IV: Selection and refinement of basic surface wave processing software	**X**	**X**	**X**	**X**	**X**	**X**	**X**	**X**						
Task V: Refinement of pattern recognition processing software	**X**	**X**	**X**	**X**	**X**	**X**	**X**	**X**	**X**	**X**	**X**	**X**		
Task VI: Field demonstration testing of mobile unit				**X**	**X**	**X**	**X**	**X**	**X**	**X**	**X**	**X**	**X**	
Task VII: Creation and maintenance of a project website	**X**	**X**	**X**	**X**	**X**	**X**	**X**	**X**	**X**	**X**	**X**	**X**	**X**	**X**

Table 1: A 14-month schedule for the seven main tasks (starting November 1, 2007)

Report Documentation Page

Form Approved
OMB No. 0704-0188

1. REPORT DATE	2. REPORT TYPE	3. DATES COVERED
JAN 2009		

4. TITLE AND SUBTITLE	5a. CONTRACT NUMBER
Demonstration Mobile Seismic Unit For Detecting Subterranean Passageways	5b. GRANT NUMBER
	5c. PROGRAM ELEMENT NUMBER
6. AUTHOR(S)	5d. PROJECT NUMBER
	5e. TASK NUMBER
	5f. WORK UNIT NUMBER
7. PERFORMING ORGANIZATION NAME(S) AND ADDRESS(ES) **Missouri University of Science & Technology (MS&T),Department of Earth Sciences & Engineering,1870 Miner Circle,Rolla,MO,65473**	8. PERFORMING ORGANIZATION REPORT NUMBER
9. SPONSORING/MONITORING AGENCY NAME(S) AND ADDRESS(ES)	10. SPONSOR/MONITOR'S ACRONYM(S)
	11. SPONSOR/MONITOR'S REPORT NUMBER(S)

12. DISTRIBUTION/AVAILABILITY STATEMENT
Approved for public release; distribution unlimited.

13. SUPPLEMENTARY NOTES
The original document contains color images.

14. ABSTRACT

15. SUBJECT TERMS

16. SECURITY CLASSIFICATION OF:			17. LIMITATION OF ABSTRACT	18. NUMBER OF PAGES	19a. NAME OF RESPONSIBLE PERSON
a. REPORT	b. ABSTRACT	c. THIS PAGE			
unclassified	**unclassified**	**unclassified**		**164**	

3. PROJECT OUTCOMES

3A. Deliverables

1. Information about the design of the modularized mobile demonstration seismic unit, including information about all purchased/built equipment/components, is posted on the Project Website:

   http://web.mst.edu/~nanders/LWI/Leonard%20Wood%20Institute%20(LWI)%20Project.html

2. Information about all purchased hardware and electronics is posted on the Project Website.

3. Information about all purchased or specially designed software is posted on the Project Website.

4. Information about the interfacing of all equipment, electronics, hardware and software is posted on the Project Website.

5. Displays of the data acquired at the test sites (complete with descriptions of all test sites, including target specifications, subsurface geology, surficial topography, operating conditions, length of time required to acquire data) are posted on the Project Website.

6. A summary of the "official" demonstration of the mobile seismic unit at FLW on October 4th is posted on the Project Website. An abbreviated summary is presented in sub-section 3C (**Demonstrations conducted**) of this Final report.

7. Recommendations for enhancing the utility of the unit are summarized in Section 5 (**WAY AHEAD**) of this Final Report

3B. Publications/presentations

1. Putnam, N. H., 2008, *Preliminary Analysis of Surface Waves to Detect Shallow Manmade Tunnels*, 2008 Symposium on Applications Geophysics on Engineering and Environmental Problems, Philadelphia Pennsylvania, Session on Karst & Tunnel Detection, (http://www.eegs.org/sageep/techsessions.html#s19Karst).

2. Putnam, N. H., 2008, *Preliminary Analysis of Surface Waves to Detect Shallow Manmade Tunnels*, Seismological Society of America Annual Meeting, v. 79:2, Santa Fe, NM, p. 279 (http://www.seismosoc.org/meetings/2008/program.html).

3. Anderson N. & Putnam N., 2008, *Analysis Using Surface Wave Methods to Detect Shallow Manmade Tunnels*: Army Science Conference, Orlando, FL, Poster Session AP-10, (http://www.asc2008.com/sessions/sessiona.htm).

4. Putnam, N.H., 2008, *Analysis Using Surface Wave Methods to Detect Shallow Manmade Tunnels*: Proceedings of the Fifth Highway Geophysics -NDE Conference, Charlotte, NC, pp 404-412, (http://www.ncdot.org/doh/preconstruct/highway/geotech/geophysicsconference/).

5. Putnam, N.H., 2009, Attenuation Analysis of Surface Waves used to Locate Shallow Manmade Tunnels: American Rock Mechanics Association, Ashville, NC, Abstract Submitted, (http://www.armasymposium.org/).

3C. Demonstrations conducted

The mobile seismic unit was "officially" demonstrated at Fort Leonard Wood on Saturday, October 4th, 2008. Three external reviewers were in attendance:

1. Larry Allen (ERDC)
2. LTC R. Tucker (MSBL)
3. Stephen Tupper (MST-FLW Federal Liaison)

The mobile seismic unit acquired demonstration field data along a ~30 m-long traverse that overlaid a known metal culvert (diameter of ~0.6 m; depth of ~0.3 m). When the mobile seismic unit reached the end of the traverse, the acquired field data were automatically interpreted. The automated interpretation software indicated that there was a high-probability that the traverse was underlain by a single tunnel. The "estimated" location of the tunnel, as calculated by the automated software and displayed on the computer screen, was within 0.5 m of the actual tunnel location. No false positives were recorded at the demonstration site.

The external reviewers completed brief questionnaires. Their responses are posted on the Project Website (http://web.mst.edu/~nanders/LWI/Leonard%20Wood%20Institute%20(LWI)%20Project.html). All three reviewers circled response B to the question #10:

Question #10: What is your overall recommendation?

A. Deploy and test "as is" (pending training/manual)
B. <u>Good potential; create superior prototype and retest</u>
C. Test demonstration was inconclusive
D. Little potential

3D. STTR/SBIR Phase I proposal submissions

STTR/SBIR Phase I proposals have neither been prepared nor submitted.

3E. Intellectual properties

With the exception of the landstreamer, the physical components of the mobile seismic unit (ATV, seismograph and cables, computer, geophones, weight drop source, camera, GPS system, survey wheel) are available from commercial vendors. Commercially-available software was used to operate the computer, the camera, the seismograph, and the GPS unit.

The landstreamer (as described on the Project Website) was designed and constructed by the investigators. The investigators do not intend to apply for a patent for the landstreamer.

The automated interpretation software, comprised of the Surface Wave Common Offset (SWCO) module, the Spiking Filter (SF) module and the Attenuation Analysis of Raleigh Waves (AARW) module, is the intellectual property of the investigators. Descriptions of these modules are posted on the Project Website under the heading "Post-Processing Algorithm Summary" (http://web.mst.edu/~nanders/LWI/Leonard%20Wood%20Institute%20(LWI)%20Project.html).

3F. Shortcomings and the associated cause or problem area as applicable:

1. The man-made tunnels at the six test and/or demonstration sites were no deeper than 1.5 m and no less than 0.5 m in diameter. We did not attempt to image deeper tunnels because of availability issues and because our current landstreamer (re: short geophone spacing) was designed to image shallow targets. We do not know, with certainty, if our unit is capable of imaging comparable or larger tunnels at significantly greater depths (~5 m).

2. The mobile seismic unit was tested successfully at six different sites in central Missouri. The unit is capable of imaging shallow tunnels overlain by grass, asphalt or concrete and encased in fairly uniform clayey silty soils. However, we do not know if our unit is capable of imaging comparable tunnels encased within dry partially-cemented sandy soils.

3. The mobile seismic unit was able to locate all of the tunnels at all of the test sites with an average accuracy of 0.5 m. With minimal modifications, the interpretational software should be capable of providing reliable estimates of tunnel widths and tunnel depths.

4. OVERALL ASSESSMENT OF PROJECT

From our perspective, the Project was very successful. The mobile seismic unit (Figure 1) is capable of identifying and locating shallow subsurface tunnels with a reasonably high degree of precision and a minimal number of false positives. The mobile seismic unit is user-friendly and can be operated by non-specialists. Data interpretation is automated; the output is a plan view map (on computer screen) showing the locations of probable tunnels (Figure 2).

From the perspective of the external reviewers, the mobile seismic unit (or a modified version thereof) is practical for military operational use in semi-permissive/austere environments and could be operated by a soldier with minimal training.

The current technology (mobile seismic unit complete with interpretational software) could be transferred to military personnel immediately. However, we believe it would be more prudent to invest a bit more time and money into the project, with the expectation a significantly superior product will be ready for military use in a matter of months.

Figure 1: The mobile seismic unit in operation at Ber Juan Park test site.

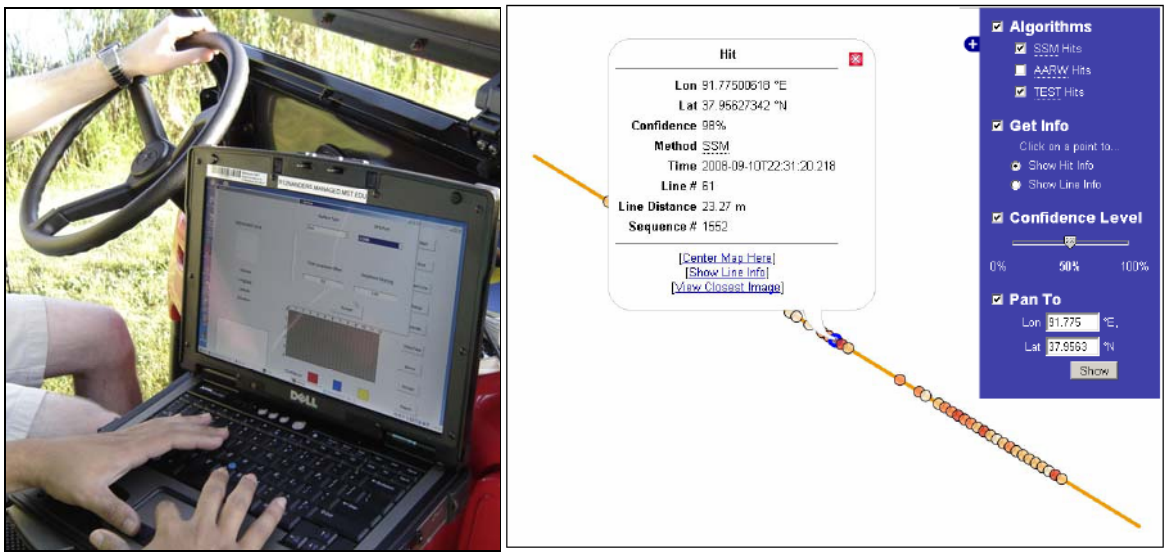

Figure 2: (a) Laptop with Seismic Interpretation Software. The operator is entering field parameters. (b) Mapping Tool (Screen Capture). Displays location of probable tunnel(s) based on automated interpretation of the field data.

5. WAY AHEAD

Our mobile seismic unit could be field-tested by non-technical military personnel "as is". However, we recommend that we be provided with a follow-up award of $200,000 and be given an additional nine months to develop and rigorously test a superior prototype that better meets of needs of the military in terms of accuracy, width/depth estimates, robustness, speed, overall utility, defined capabilities, and user-friendliness.

The modified prototype would be significantly superior to the current unit for several reasons:

Accuracy: To improve accuracy and minimize false interpretations, we developed three separate interpretation modules [Surface Wave Common Offset (SWCO) module, Spiking Filter (SF) module, and Attenuation Analysis of Raleigh Waves (AARW) module]. Incoming field data are automatically and simultaneously analyzed by all three modules; tunnel locations are identified on the basis of the statistical analyses of the output of all three modules. At this point in time, AARW provides the most accurate results, in large part because this analytical tool was developed first. It is our opinion that the SWCO approach is extremely promising and that our interpretation system will be significantly improved if we are given more time to further develop and fine-tune this approach. Our SF module will also benefit significantly from "fine-tuning".

Width/depth estimates: The current unit is capable of estimating tunnels locations to within 0.5 m, but is not capable of automatically estimating tunnel widths and depths. We anticipate that our interpretational software, with minimal modifications, will be capable of providing reliable estimates of tunnel widths and tunnel depths.

Robustness: Our current unit functions well under friendly environmental conditions (moderate temperatures, dust-free, sunny skies). We would like to have the opportunity to redesign our unit so that it is capable of functioning well under more difficult environmental conditions.

Speed: The current unit is capable of acquiring about 0.5 km of data per day. It is anticipated that the modified prototype will be capable of acquiring more than 1 km of data per day.

Overall utility: Two of the three reviewers indicated that the mobile seismic unit would be of much more utility to the military if the acquired surface wave data could be automatically transformed into shear-wave velocity profiles. These shear-wave velocity profiles would provide military engineers with critical information about the nature subsurface to depths on the order of 15+ m (including shear strength, depth to bedrock, heterogeneity, etc.). If these capabilities are integrated into the existing system, the unit could be used for routine geotechnical investigation purposes (in addition to tunnel detection purposes). The

transformation technology (software) is available. It is simply a matter of integrating it into our existing system.

Defined capabilities: The current unit is capable of imaging shallow tunnels. The proposed modified prototype will be thoroughly tested under diverse field conditions (soil conditions and tunnel depth) so that the potential user is fully aware of the strengths and limitations of the system.

User-friendliness: Our current unit has been successfully operated by non-geophysicists. The system is fairly user-friendly. However, there are a number of modifications that can be made (software mostly) to improve the usability of the mobile seismic unit.

Project Technical Report
LWI 61042

DEMONSTRATION MOBILE SEISMIC UNIT FOR DETECTING SUBTERRANEAN PASSAGEWAYS

Submitted to:

Leonard Wood Institute (LWI)

Submitted by:

Neil Anderson, Niklas Putnam, Steven Grant, Ali Nasseri-Moghaddam, Peng Xie, Oleg Kovin, Preetam Modur, Colin Stagner and Evginey Torgashov

Missouri University of Science & Technology

January 15th, 2009

TECHNICAL REPORT DOCUMENTATION PAGE

1. Report No. LWI 61042	2. Government Accession No.	3. Recipient's Catalog No.
4. Title and Subtitle Demonstration Mobile Seismic Unit for Detecting Subterranean Passageways		5. Report Date January 15, 2009
		6. Performing Organization Code Missouri University Missouri-Rolla
7. Author(s) Anderson, N., Putnam, N., Grant, S., Nasseri-Moghaddam, A., Xie, P., Kovin, O., Modur, P., Stagner, C., and Torgashov, E.		8. Performing Organization Report No. LWI Project 61042
9. Performing Organization Name and Address Department of Earth Sciences & Engineering Missouri University of Science & Technology (MS&T) 1870 Miner Circle Rolla, MO 65409		10. Work Unit No.
		11. Contract or Grant No. LWI Project 61042
12. Sponsoring Agency Name and Address Leonard Wood Institute 197 Replacement Avenue Fort Leonard, MO 65473-9089		13. Type of Report and Period Covered Final Report
		14. Sponsoring Agency Code Leonard Wood Institute (LWI)
15. Supplementary Notes This investigation was conducted by the Missouri University of Science & Technology through the Fort Leonard Wood Institute for the U.S. Army Research Laboratory.		

16. Abstract

The Missouri University of Science & Technology, through the auspices of the Leonard Wood Institute, built and demonstrated a mobile seismic unit designed to rapidly and reliably locate shallow man-made subterranean passageways. The demonstration mobile seismic unit acquired active surface (Rayleigh) wave data at regular and irregular intervals as it was driven across an area of interest, visually displaying the location and coordinates of anomalous ground signals. Three conventional and/or newly developed signal processing algorithms were integrated for determining the location of voids. The three methods, listed below, were evaluated individually and then comparatively in terms of accuracy, functionality and overall utility.

- Surface Wave Common Offset (SWCO)
- Spiking Filter (SF)
- Attenuation Analysis of Raleigh Waves (AARW)

In addition, a 2-D (plan view) mapping are used to geospatially locate the voids for visual display. Additional data (along parallel traverses) can be acquired for confirmation and/or delineation purposes. This work includes physical construction/optimization of the demonstration mobile seismic unit hardware, acquisition test data, description of pattern recognition algorithms and software, and conclusions through comparisons to field measurements and complementary geophysical data. Assessment, problem areas, and recommendations are summarized at the end of this report.

17. Key Words surface waves, seismic, Rayleigh waves, common offset, spiking filter, Attenuation Analysis of Rayleigh Waves, AARW, tunnel, void, Mobile Seismic Unit, land streamer, seismic impact source, multi-method seismic, MATLAB	18. Distribution Statement No restrictions. This document is available to the public through the Leonard Wood Institute, Fort Leonard Wood, MO 65473

19. Security Classification (of report) Unclassified	20. Security Classification (of this page) Unclassified	21. No. of Pages 142	22. Price

EXECUTIVE SUMMARY

The Missouri University of Science & Technology (MS&T) received a contract from the Leonard Wood Institute (LWI) to build a demonstration mobile seismic unit designed to rapidly and reliably locate shallow man-made subterranean passageways. The results of field testing and data analysis indicate that Rayleigh wave multi-algorithm interpretation software is a viable approach to detecting man-made subterranean passageways that supports force protection applications and is self-contained. If the demonstration mobile seismic unit is utilized for routine geophysical reconnaissance, risks to clandestine tunneling are reduced by active and change detection in the Earth's shallow subsurface. Additionally, the mobile demonstration unit is flexible as it is self-contained and designed for employment by non-geotechnical personnel.

The MS&T, in collaboration with Dr. Ali Nasseri-Moghaddam, evaluated three conventional and/or newly developed signal processing algorithms for determining the location of shallow tunnels/culverts:

- Surface Wave Common Offset (SWCO)
- Spiking Filter (SF)
- Attenuation Analysis of Rayleigh Waves (AARW)

Fundamentally, direct examination of Surface Wave data, without application of standard dispersion curves used for processing in Multi-channel Analysis of Surface Wave Method, provides the capability to detect anomalous changes associated with linear void space in the Earth's subsurface. Field seismic data, collected along a traverse, is interpreted using automated pattern-recognition type software. The software identifies anomalous patterns, potentially generated by subsurface voids, then plots the location of the same on a plan view map of the traverse, complete with an estimated probability factor. The probability factor being an estimate of the likelihood that a specific anomaly was generated by a tunnel. The operator can select one or all of the three algorithms and toggle an anomaly sensitivity button to increase reduce the number of detections based on the probability factor.

The sample the target set was nominally one meter depth and void diameter of one meter. The demonstration mobile seismic unit outputs for the target set when compared to field location is an average of 0.5m (meter) accuracy. Average of false positives using a 90% anomaly discrimination setting is estimated at 2:1 given relative heterogeneous soil.

Although the demonstration mobile seismic unit is capable of rapidly and reliably detecting shallow man-made passageways, we recommend further tests to increase detection depth and in broader geological settings (e.g. hard rock). While the demonstration mobile seismic unit is not the single solution to detect shallow tunnels, it is potentially a subsurface screening tool that can optimally survey 500 lineal meters per day.

ACKNOWLEDGEMENTS

The work presented in this report was the product of many collaborators at the Missouri University of Science & Technology. The authors would like to thank Dr. Ali Nasseri-Moghaddam, Inspec Sol, Inc., Mr. Steven Tupper, MS&T Liason, and the Leonard Wood Institute for their efforts in supporting this effort to facilitate this research and development towards implementation for the customer.

The financial support from the Leonard Wood Institute via Contract LWI Project 61042 is also acknowledged.

TABLE OF CONTENTS

LIST OF FIGURES

LIST OF TABLES

1. INTRODUCTION

1.1 Statement of Problem

A demonstration mobile seismic unit (DMSU) is required to rapidly and reliably locate shallow man-made subterranean passageways. The detection unit must have the following capabilities:

- It must be capable of rapidly and reliably locating and mapping man-made shallow subterranean passageways.
- The tunnel identification process (interpretation software) must be automated to the point where the system can be operated by non-specialists.
- False interpretations must be minimal.
- The system must be mobile, self-contained and afford protection to its occupants.
- The unit must be capable of operating under different physiographic and climatic conditions.

1.2 Scope of Work/Objectives

The Missouri University of Science & Technology (MS&T) designed, built and demonstrated a mobile seismic unit consisting of an all-terrain vehicle (ATV), a towed trailer with an acoustic impact source, a towed streamer consisting of a fire hose with 24 geophones, a GPS sensor, a 24-channel engineering seismograph, and a dedicated laptop computer and automated surface wave interpretation software (Figure 1.1).

Figure 1.1: Demonstration Mobile Seismic Unit (DMSU) designed to rapidly and reliably locate shallow man-made subterranean passageways.

The GEOStrike (acoustic impact source) trailer is towed by the ATV. In turn, the land streamer (firehose housing the 24 geophones and cable) are coupled to the rear of the trailer and towed. The GPS unit and seismograph are mounted to the outside of the ATV. The rearview camera, and laptop computer / operator's station are located in the cab of the ATV.

The following three conventional and/or newly developed signal processing algorithms were evaluated individually and also comparatively in terms of accuracy, functionality and overall utility for determining the location of shallow tunnels / culverts:

- Surface Wave Common Offset (SWCO)
- Spiking Filter (SF)
- Attenuation Analysis of Rayleigh Waves (AARW)

The evaluations of these three algorithms were based on comparisons to field measurements and complementary geophysical methods. The first battery of field surveys were conducted at Ber Juan Park in Rolla, MO for purposes of optimizing hardware geometry to detect a 1 meter diameter tunnel not to exceed 2 meters in depth from the Earth's Surface to the crown / top of the tunnel.

In order to demonstrate the utility of respective algorithms, a 2D (plan view) mapping tool depicting location(s) of detected anomalies associated with voids was plotted along the survey line (Figure 1.2.b).

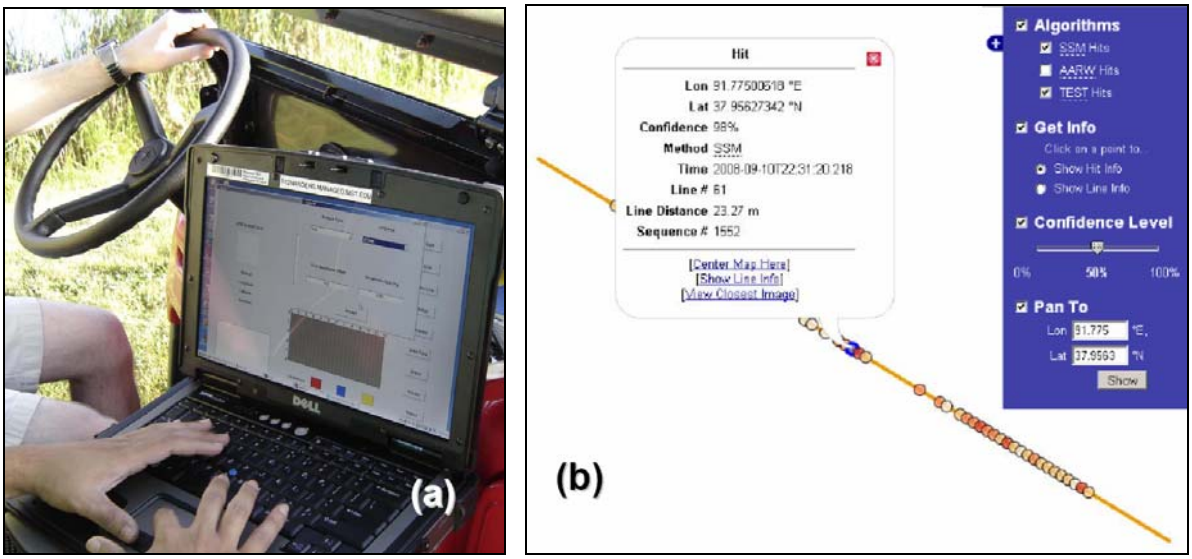

Figure 1.2: (a) Laptop with Seismic Interpretation Software: Here the operator is setting the parameters (e.g. length of the line and location of the unit) before beginning the survey; (b) Mapping Tool (Screen Capture) that plots anomaly based on AARW and Spiking Filter where certainty is based on relative algorithm strength value of the anomaly.

1.3 Deliverables

There are six deliverables:

1. The first deliverable is detailed information about the design of the modularized demonstration mobile seismic unit, including information about all purchased and built equipment.

2. The second deliverable is detailed information about all purchased and built hardware and electronics.

3. The third deliverable is detailed information about all purchased and specially designed software.

4. The fourth deliverable is detailed information about the interfacing of all equipment, electronics, hardware and software.

5. The fifth deliverable is all of the experimental and test surface wave data acquired during the course of this investigation, complete with descriptions of all test sites, including target specifications, subsurface lithology, etc.

6. The sixth deliverable is a suite of comprehensively documentation demonstrations of the utility of the DMSU for detecting shallow man-made tunnels and estimating their locations.

Deliverables 1 through 4 are contained in the DMSU Operations Manual: TAB A. A summary of deliverables 5 and 6 are outlined in this report. All supporting data for deliverables 5 and 6 are available upon request from Missouri University of Science & Technology by contacting Dr. Neil Anderson at 573-341-4852 or E-mail nanders@mst.edu.

The DMSU has limitations that can be addressed in subsequent re-designs.

1. The land streamer may not function effectively when towed across highly irregular surfaces, because some of its geophones might not be effectively coupled to the ground surface.

2. The demonstration unit and its occupants will not be armor-protected.

3. The demonstration unit will be manned by two-persons. However, subsequent designs could be operated entirely by remote control.

1.4 Demonstration Mobile Seismic Unit (DMSU) Concept

The mobile demonstration unit will be capable of acquiring active surface (Rayleigh) wave data at regular or irregular intervals as it is driven across an area of interest (along the fenced periphery of a prison, for example). At selected observation locations, the unit will be halted momentarily (few seconds) and the impact source will generate high-amplitude surface waves. These surface waves will be recorded by the seismograph, and automatically processed and interpreted. The automated pattern recognition interpretation software will analyze the field records and discriminate underground passageways from undisturbed soil/rock on the basis of back-scattered (diffracted) surface-wave energy, frequency-dependent surface-wave amplitude attenuation and decreased group velocity. This automated analysis will take only a few seconds for each station.

At the completion of the respective sets of shots (on a relative straight line distance along an area of interest) on a set of survey lines (typically 3 parallel lines) the seismic data is analyzed by the software with the results available in virtual real time. The location and coordinates of the anomalous ground will be visually displayed, along with estimates of passageway depth. The acquiring of sets of three parallel traverses allows for elimination of false positives and increases confidence and delineates tunnel orientation.

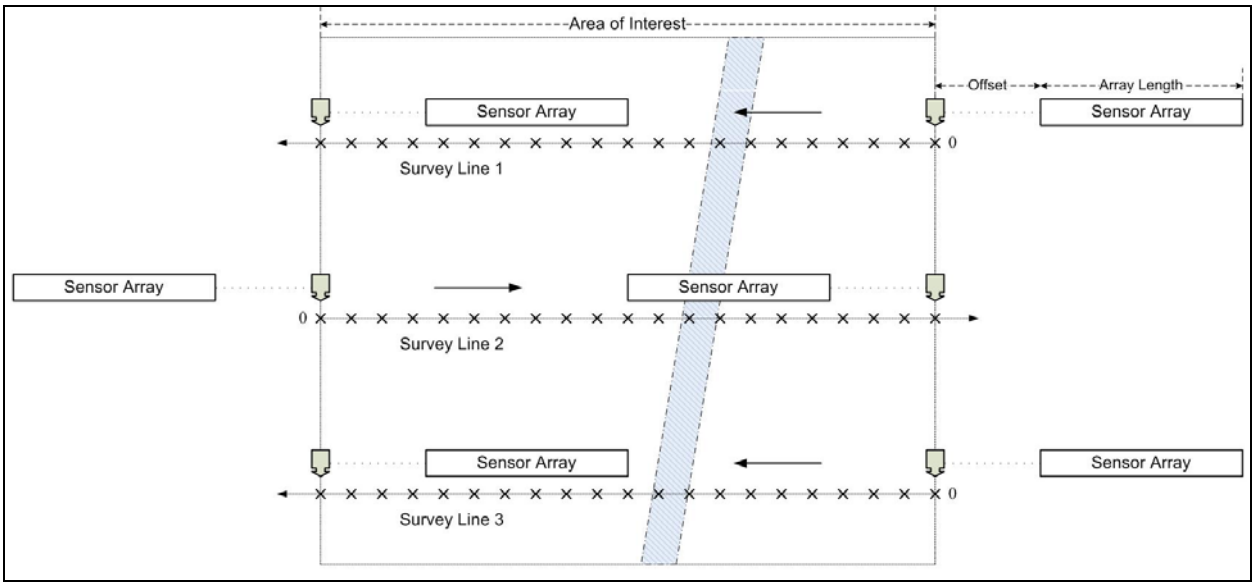

Figure 1.3: Diagram of a standard survey pattern used to detect subterranean passageways. The diagram depicts survey lines run in parallel oriented perpendicular to the likely center-line orientation of the shallow manmade tunnel.

1.5 Work Plan

1.5.1 Summary of Work Plan

The DMSU is a self-contained unit that deployed to six selected test site locations that met the nominal one meter diameter and one meter depth target requirements (Table 1.1). The hardware geometry and algorithm was optimization at the first test site (Ber Juan Park in Rolla, MO) before further sites were surveyed. Continued iterative optimization improvements were made throughout the field testing. The three conventional and/or newly developed signal processing algorithms were integrated into MATLAB construct with graphic output was available at the end of each survey using the 2D mapping tool. Along with 'blue prints' and field measurements, complementary geophysical methods were used to further corroborate the interpretations:

Algorithms:

- Pre-Processing / Common Offset (RAS-24)
- Spiking Filter (SF)
- Attenuation Analysis of Rayleigh Waves (AARW)

Complementary methods:

- Resistivity (Soil)
- Ground Penetrating Radar (GPR) (Pavement)
- Shear Wave Velocity Profile (Pseudo Boring Log)

Table 1.1 summarizes seismic survey field work conducted in chronological order. The Ber Juan Park spillway tunnel in Rolla, Missouri was used prior to July 2008 to determine optimal geophone natural frequency, geophone spacing, source to first receiver offset, and seismic impact source configuration for the given target set(s) of interest. Pertinent optimization subjects are outlined in Chapter 2. The field work plan was devised with the expectation that we would have sufficient data for the purposes of evaluation and comparative analyses.

Location (Date)	Lithology	Depth of Void (m)	Dimension(s) of Void (m)
Ber Juan JUN08	**Clay**	**0.90**	**0.96**
Physics Bldg SEP08	**Pavement**	**1.00**	**0.80 height x 0.60 width (0.73 width at cos35^{o})**
Tech Park OCT08	**Mixed Soil**	**0.30**	**0.60**
Tech Park OCT08	**Pavement**	**0.43**	**0.84**
Wilson Lib. NOV08	**Mixed Soil**	**1.00**	**1.93 height x 1.20 width**
Bishop St. NOV08	**Pavement**	**1.23**	**2.80 height x 3.15 width**

Table 1.1: Summary of field work plan

1.5.2 Generation of 2D Graphics (Length versus Depth)

In order to demonstrate the utility of the DMSU hardware and interpretation software, a suite of 2D cross sections from field measurements, shear wave velocity profiles, and resistivity / ground Penetrating Radar (GPR) were used for the respective test sites (Chapter 6) were prepared for comparison. A Graphic User Interface (GUI) was developed for the DMSU for the operator while collecting seismic data. At the completion of collecting seismic data on a survey line, the data was compiled with interpreted locations plotted using a 2D mapping tool along the survey line.

The DMSU hardware used to gather seismic data consist of five major components:

- Polaris Ranger 500 Series ATV 4X4
- GEO Strike Acoustic 100 lb. Impact Source
- Seistronix RAS-24 Seismograph (Hardware & Software)
- Streamer Array using Sunfull Weihai 4.5 Hz Geophones (fabricated fire hose and Geophone Plate Housings)
- Dell XFR D630 Toughbook

The generation of the suite of automated operator user interface and interpretation software and mapping tools involved the following:

- Dr. Ali Nasseri - Attenuation Analysis of Rayleigh Waves (AARW) Algorithm
- Missouri University of Science & Technology
  - Itasca FLAC 3D v.3 Modeling Software
  - RAS-24 Seismic Collection Software (Seistronix Inc.)
  - Mathworks MATLAB 2007B
  - Trimble GPS Pathfinder ProXT Receiver
- Other public and commercial sources
  - Digital satellite images (USGS Mapserver)
  - Ber Juan Park Earthen Dam Construction Blueprints
  - Fort Leonard Wood Directorate of Public Works Post-construction geologic boring logs
  - MS&T Digital Campus Facility Maps
  - 2D Mapping Tool (Conglomerate of Shareware)
  - AGFA Digital Video Camera DV-5000G

Some problems were encountered when using the Trimble GPS software in obtaining accurate geospatial locations. It was necessary in many cases to individually review the survey line records and manually input the location(s) of points on the line. The adjusted survey lines could then be used to locate the anomalous signals associated with manmade tunnels.

2. TEST LOCATIONS

There were a total of six test sites. Sites were successively selected and tested based on increasing complexity in host material and depths of culvert / tunnel. Hence the tests are presented in chronological order. For purposes of simplicity the culvers / tunnels will simply be referred to as tunnels. As summarized previously, the first test site was located at Ber Juan Park Spillway Tunnel, Rolla, Missouri. Two test sites were located at the Missouri University Technical Park at Fort Leonard Wood, Missouri. Three test sites were located on the campus of MS&T, Rolla, Missouri. The general location of the sites can be readily accessed by vehicle off of U.S. Interstate Highway 44 about 120 miles south west of St. Louis, Missouri (Figure 2.1).

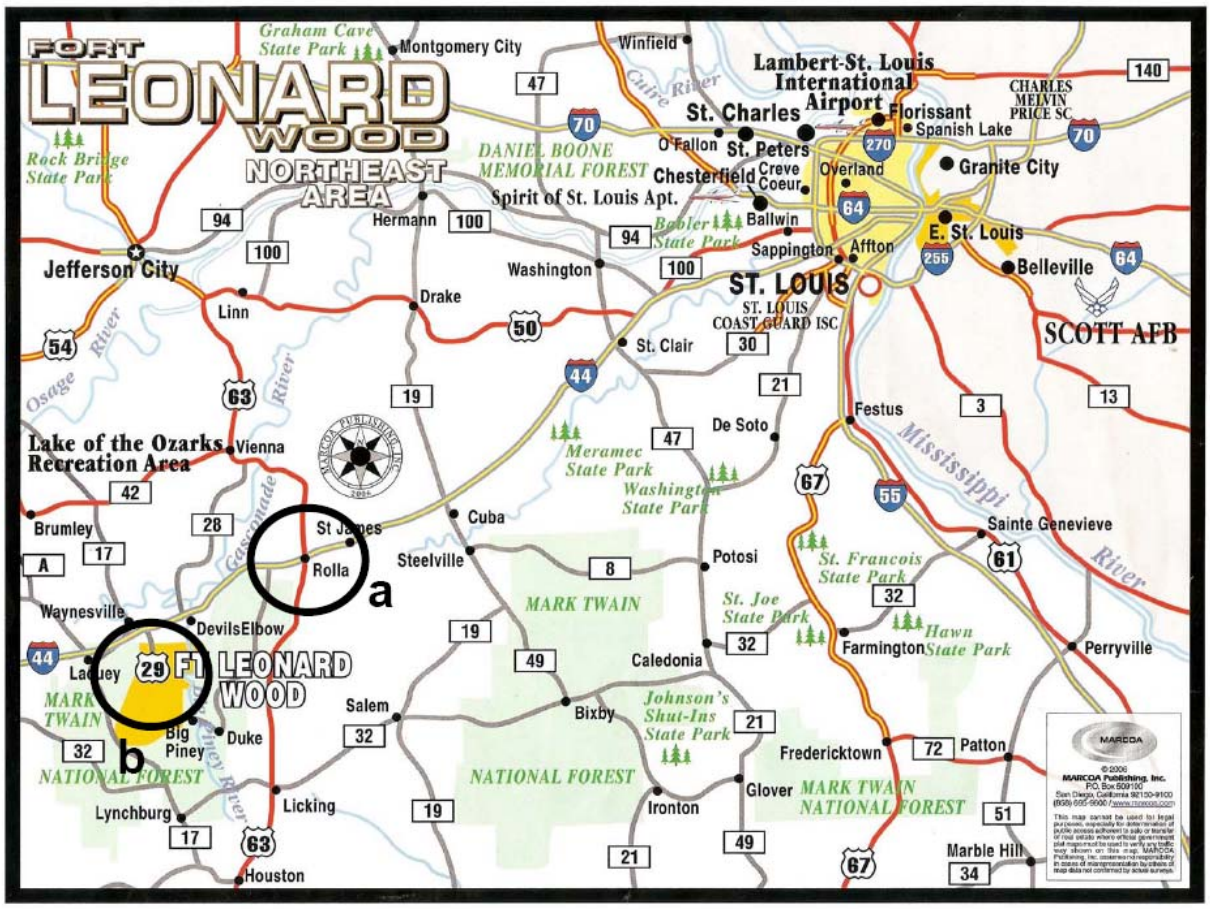

Figure 2.1: The DMSU test sites were all located in south-west Missouri in (a) the City of Rolla & on the Missouri University of Science& Technology Campus; and (b) on Fort Leonard Wood at the University of Missouri Industrial Technology Park.

2.1 Tunnel Geometry Limits

The target set was bounded by geometric criteria to ensure there is some reasonable expectation by the customer and of performance by the developers. Investigation of sites to confidently detect manmade subterranean passageways is said to be a relatively horizontal (to the Earth's surface) cylindrical to box shaped linear void between 1.5 to 2.5 meters in diameter or length / width at embedment depth (top of tunnel) between 0.25 and 2.0 meters. It is assumed that clandestine manmade tunnels are oriented generally perpendicular to a fence or border between points of ingress /egress.

2.2 Ber Juan Park Spillway Tunnel, Rolla, Missouri

The Ber Juan Spillway Tunnel is located at Ber Juan Municipal Park off of Missouri State Highway BB in the City of Rolla (Figure 2.2). The Ber Juan Spillway Tunnel was selected as the first study area because of the near heterogeneous soil conditions, availability of engineering blueprints, and availability for multiple geophysical survey runs. This site was used for feasibility and proximal to distal studies beginning in August 2007. The LWI proposal for this study was submitted due to the encouraging results in detecting the tunnel using seismic methods at this location.

Figure 2.2: Location of Ber Juan Spillway Tunnel that provides an overflow to the pond immediately north west of the conduit. The location of the center-line of the tunnel at 1 meter embedment depth is Longitude -91^{o} 45' 26" W Latitude 37^{o} 57' 07" N.

2.3 Campus of Missouri University of Science & Technology, Rolla, Missouri

Three sites provided test beds to validate the DMSU's capabilities and provided additional data sets for statistical analysis. These sites are at the following locations (Figure 2.3):

- Adjacent to the Physics Building on 14th (asphalt pavement) Street; Longitude -91° 46' 25" W Latitude 37° 57' 19" N
- Bishop Street Student Access Tunnel (Pavement) near McNutt Hall Longitude -91° 46' 37" W Latitude 37° 57' 19" N
- Utility Tunnel (Mixed Soil) below the University Quadrangle; Longitude -91° 45' 25" W Latitude 37° 57' 16" N

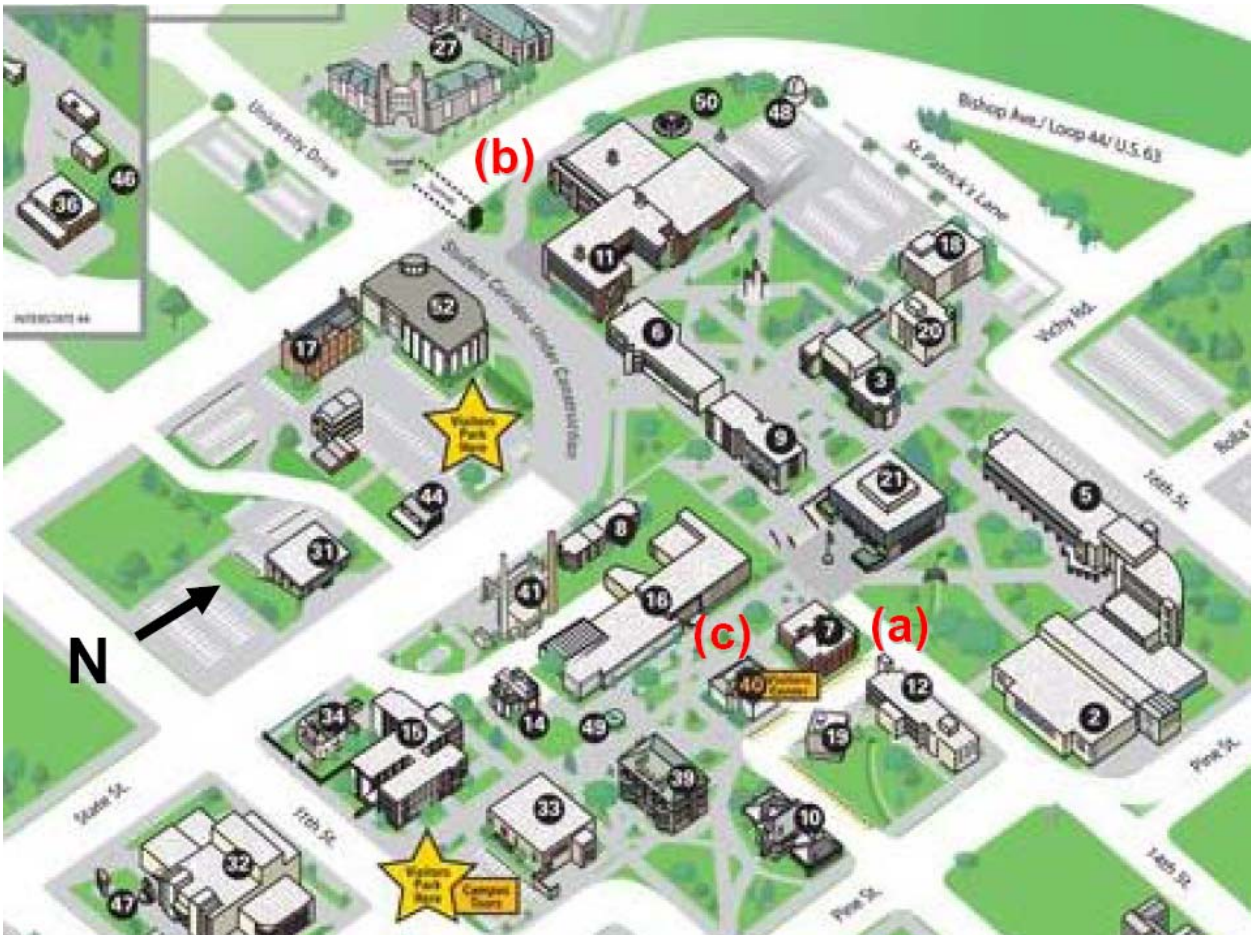

Figure 2.3: Location of (a) Physics Building (Pavement); (b) Bishop Street Student Access Tunnel (Pavement); and (c) Utility Tunnel (Soil) survey sites.

2.4 University of Missouri Technology Park, Fort Leonard Wood, Missouri

Two tunnels located on the premises of the University of Missouri Technology Park at Fort Leonard Wood, Missouri were used to demonstrate the capability of the MSU to impartial observers on behalf of the customer. The address of the location is 197 Replacement Avenue, Fort Leonard Wood, Missouri 65473 (Figure 2.4). Both of the respective sites were within 50 meters of each other:

- Technical Park (Mixed Soil) south side of the office building; Longitude -92° 06' 25" W Latitude 37° 45' 37" N
- Technical Park (Pavement) west side of the office building; Longitude -92° 06' 26" W Latitude 37° 45' 38" N

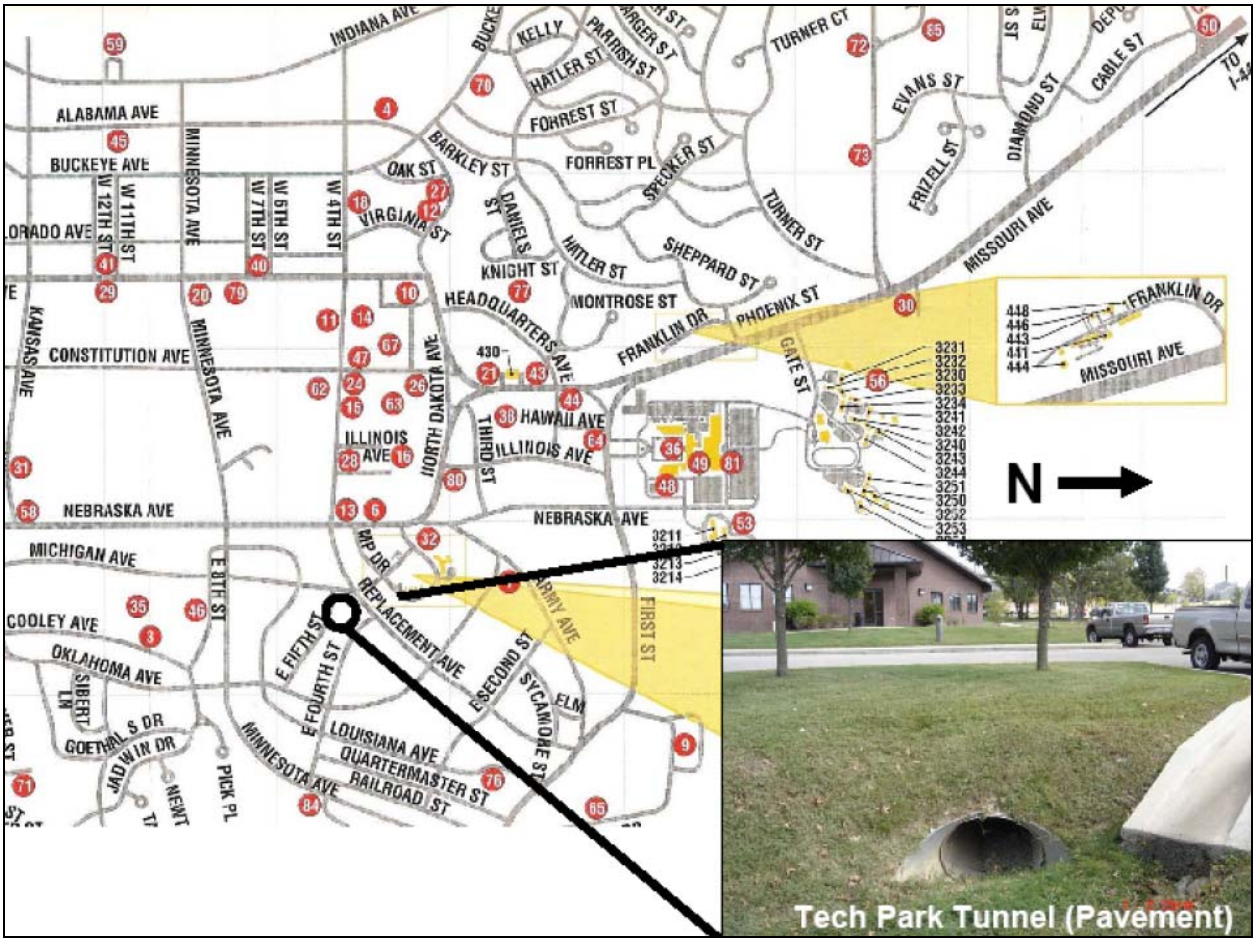

Figure 2.4: Location of University of Missouri Technology Park, Fort Leonard Wood, Missouri with inset of the tunnel beneath cement pavement.

3. HARDWARE PARAMETERS AND OPTIMIZATION

Chapter 3 outlines the fundamental seismic system parameters and geometry selected for the DMSU to detecting shallow manmade tunnels in the Earth's subsurface. The selection was then optimized based on preliminary surface wave modeling and field tests at Ber Juan Park to validate the utility of SWCO, SF & AARW algorithms to detect the tunnel.

Originally, the problem set included manmade tunnels or culverts to an embedment depth of down to 3 meters. An embedment depth is defined here as the crown, roof, or top part of a tunnel nearest to the ground surface. The preliminary field tests at Ber Juan Park of the spillway tunnel failed to conclusively locate a 1 meter diameter tunnel at 2 and 3 meters depth respectively. This rationale was addressed in the technical article *Analysis Using Surface Wave Methods to Detect Shallow Manmade Tunnels,* Putnam et. al., 2007. Therefore, a decision was made by the DMSU Team to focus on tunnels at less than 2 meters embedment depth as site selection criteria for further testing the DMSU. Therefore, the DMSU Team selected tunnels based on the following bounding criteria:

- The diameter of the tunnel nominally 1 meter
- The embedment depth of the tunnel less than 2 meters
- Tunnels are lined with concrete or corrugated metal
- The host material containing the tunnel is homogenous fill
- The surface was generally flat (grade less than 10^{o}) soil or pavement

Assumption:

- The ingress and egress of a clandestine manmade tunnel is the shortest straight line distance between two concealed portals underneath a security perimeter. The orientation of a tunnel in relation to the DMSU is generally perpendicular to the traverse of the survey line.

The engineering geophysics community has recently focused on the use of Rayleigh wave methods, such as Multichannel Analysis of Surface Waves (MASW) and Refraction Micrometer (ReMi), to detect manmade tunnels in the Earth's shallow subsurface (Miller et al, 2006). Successful applications of the method in detection of underground cavities have been reported; however, the research conducted here by the Missouri University of Science & Technology (MS&T) herein using SWCO, SF & AARW demonstrates equal if not increased capability to detect voids associated with shallow man-made tunnels over other surface wave methods currently used. The research and subsequent development of the DMSU is based on the use of both back-scattered energy and attenuation analysis to locate known tunnels and culverts in a 1 m diameter range. This integrated seismic multi-method approach is predicated on obtaining robust seismic data sets for Rayleigh wave single shot and Common Offset gathers. Selection of geophones, impact source, and the geometric inter-relationship to the tunnel are a requisite in obtaining the appropriate seismic data for further post-processing.

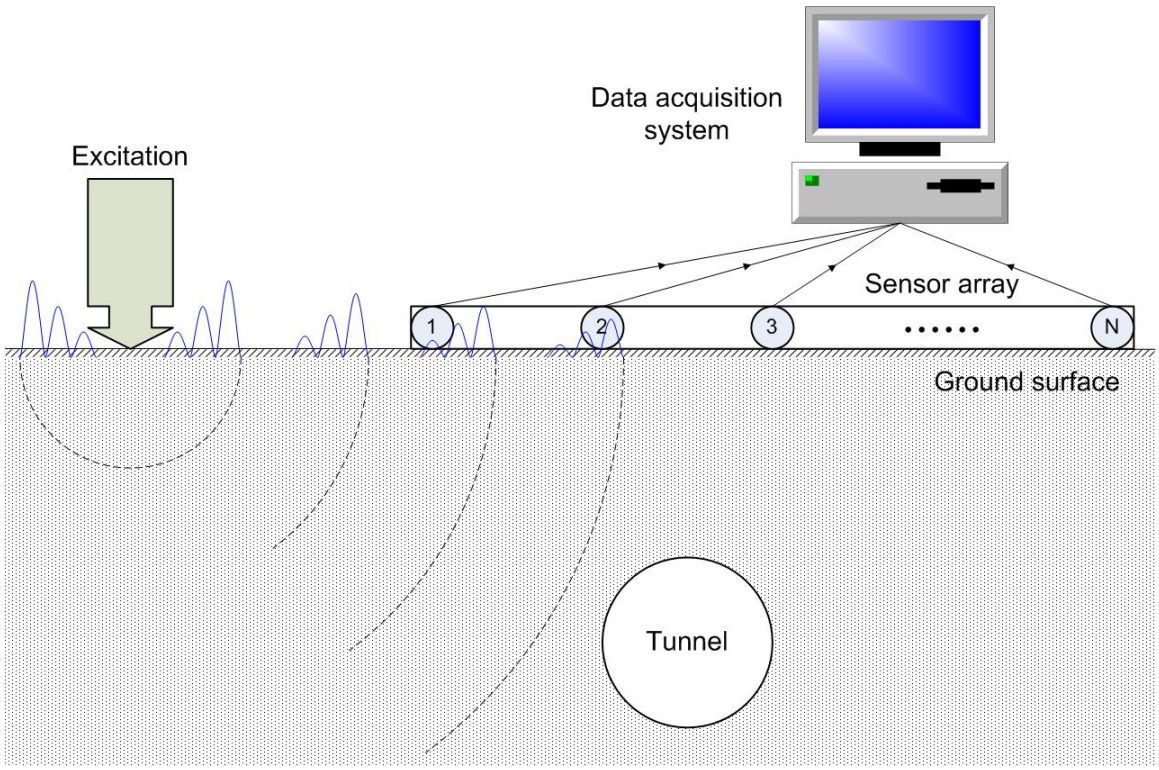

Figure 3.1: Simplified field configuration of Rayleigh Wave data set using an array of 24 low-frequency geophones. The preliminary phase involves the selection of geophones, impact source, an optimal geometric (distance) between impact source (excitation) to first geophone (offset), and geophone spacing, all in relation to the tunnel (bounding) criteria.

3.1 Geophone Selection & Calibration

Geophone Selection. The selection of the vertical 4.5 Hz natural frequency geophone for the DMSU was based on its wide use in surface wave void detection applications (Kansas Geological Survey, University of Waterloo - Canada, among others). A 4.5 Hz geophone improves the registration of the low-frequency surface waves providing deeper penetration. A 4.5 Hz Geophone reduces spurious noise at higher frequency. It is also relatively inexpensive compared to other natural frequency geophones (e.g. 10 Hz). Its disadvantage is an inability to function properly on surfaces with a grade of more than 10^{o}.

In an internal DMSU preliminary In-Progress Review, a comparison of 100, 14, & 4.5 Hz natural frequency 24-geophone arrays all detected the spillway tunnel at 1m depth (07 OCT 2007). However, the 100 Hz geophones were not able to detect the tunnel at 2 and 3m depth using currently deployed software.

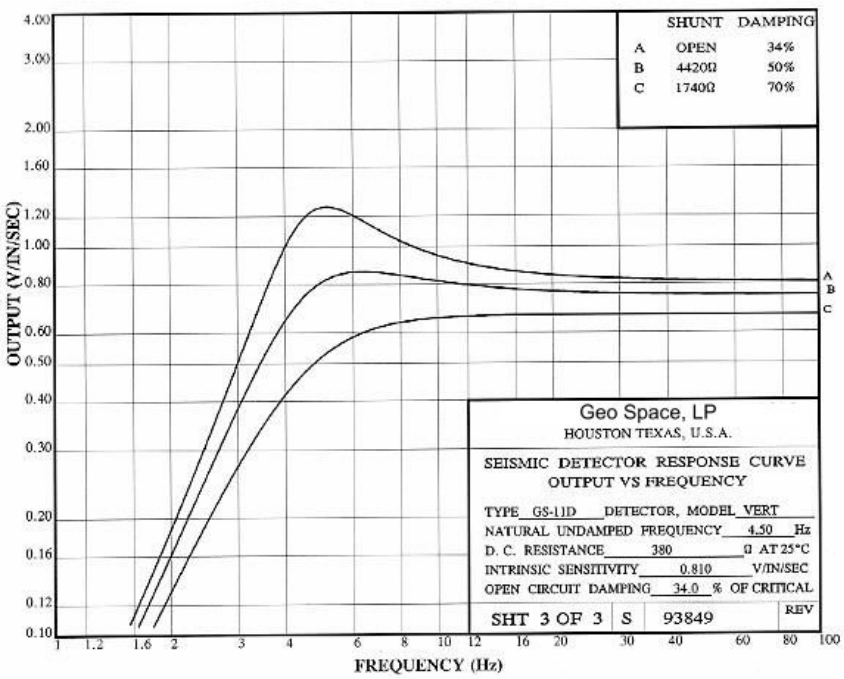

Figure 3.2: Graphic representation of a 4.5 Hz natural frequency geophone.

Figure 3.3: (a) 4.5 Hz geophone array over a tunnel structure at a Ber Juan Park in Rolla, Mo.: Graduate student Amos Wamweya assists by striking a sledge hammer to a plate on the ground that generates the seismic energy that will be measured by the geophones. (b) Cross-section blueprint and on site survey measurements of the Ber Juan spillway tunnel is compared to the geophysical field data to determine agreement of approximated void location using the respective Rayleigh Wave geophysical cross section(s).

In order to ensure the flexibility of the DMSU to extend its depth and use in a variety of geology, an abbreviated analysis was performed for the selection of the 4.5 Hz geophone. Surface wave velocities geologic materials are derived from P-wave velocities from Reynolds, John, 1997. *An Introduction to Applied and Environmental Geophysics*. John Wiley & Sons, England, p. 221. The approximate surface wave velocities of materials conducive to clandestine manmade tunneling are summarized below:

Material	Vp (m/s)	Vs (m/s)
Soil	200-500	118-294
Landfill	400-750	235-442
Clay	1000-2500	588-1470
Sandstone	1400-4500	824-2647
Limestone	1700-4200	1000-2470

Table 3.1: Material Velocities of soft to medium velocity soil.

The following assumptions are applied to the problem set as per the customer. 1) The target range of depth for the proximal to distal study is 1 to 3 meters in depth. The void ranges from 0.5 to 2 meters and may be circular, ovate, or rectangular in cross section. The tunnels are generally parallel and horizontal in orientation to the Earth's surface. Using the relation V (velocity) = F (frequency in Hz) * w (wavelength) we select a set of geophones with the best center frequency for a maximum void depth of 3 meters for this project and is summarized.

Center Frequency (Hz)	Upper Velocity Range of Limestone (2,500 m/s)	Lower Velocity Range of Unconsolidated (100 m/s)
4.5	555.6 m	22.2 m
14	178.6 m	7.14 m
28	89.3 m	3.58 m
100	25.0 m	1.0 m

Table 3.2: Tabularized results of the geophone natural frequency analysis. Note that for Rayleigh Waves that empirical effective penetration depth is ½ lambda or half wavelength (Miller, et al, 2006). Therefore, we estimate that 4.5Hz geophone can plausibly detect a void down to 11 meters in depth under ideal conditions.

Geophone Calibration. There are several methods and standards by which to test geophones to ensure they are within specification tolerance.

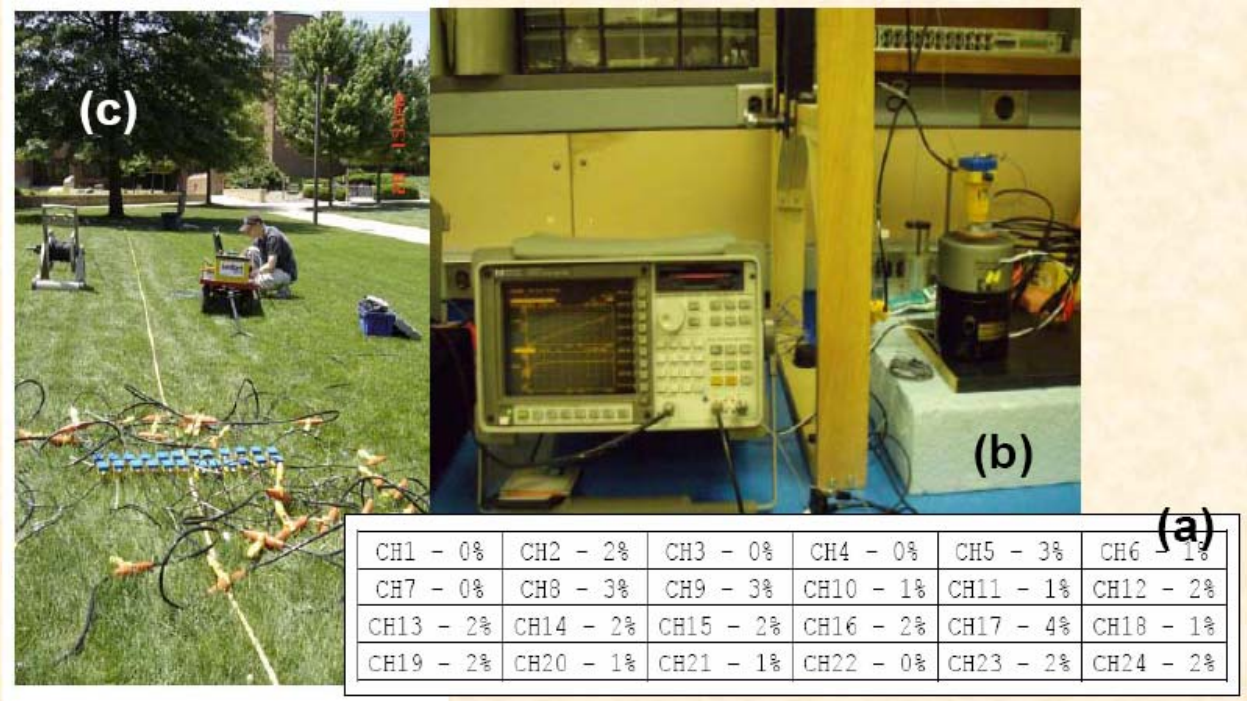

Figure 3.4: (a) Dissimilarity Test below 5%, (b) Shaker Table Test SD = 6.5 mV/cm/s, (c) Amplitude trace comparison of 24 geophone suite showed no discernable difference when comparing seismic traces side-by-side.

Dissimilarity Test. The RAS-24 geophone dissimilarity test software provides an evaluation of geophone condition. It is effective at spotting damaged phones, phones that are planted off vertical axis, and phones that have not been properly damped (e.g. damping resistor not installed or wrong value).

To arrive at the percentages displayed by the RAS-24, the software computes the Root Mean Square (RMS) energy of the reference geophone over about a 150ms interval after it is pulsed and compares this to the same number generated for each geophone under test. It applies a 100μa current source to each individual phone for about 4ms which displaces the coil. It then removes the current source and begins sampling at 0.25ms sample rate. To calculate the dissimilarity, it multiplies each sample of the reference geophone by the corresponding sample of the geophone under test, summing the resultant values from the 28th sample to the 600th sample (7ms to 150ms). The final sum of the geophone under test is then divided by the number of sums (573) and the square root is taken. Finally, this is expressed as a percentage of the reference geophone energy over the same interval and can perform the same RMS calculation on the reference geophone.

The default setting for the RAS-24 Dissimilarity Test is 5 (%). The test was conducted prior to a second seismic survey at Ber Juan Park Spillway Tunnel in Rolla, Missouri in June, 2008. A facsimile of the screen capture is as follows:

```
- - - - - - - - - - - - - - - - - - - - - - - - - - - -
RAS-24 TEST  - - Dissimilarity (%)
- - - - - - - - - - - - - - - - - - - - - - - - - - - -
Date: 05-28-2008        Time: 14:45:17          RAS-24 Serial Number:
Total Boxes: 1                (24 Channels)
PreAmp Gain = 12 db
Sample rate = .25ms
Maximum acceptable value:  5%
- - - - - - - - - - - - - - - - - - - - - - - - - - - -
Dissimilarity (%)       Box: 1                        SN: 31014
```

CH1 – 0%	CH2 – 2%	CH3 – 0%	CH4 – 0%	CH5 – 3%	CH6 – 1%
CH7 – 0%	CH8 – 3%	CH9 – 3%	CH10 – 1%	CH11 – 1%	CH12 – 2%
CH13 – 2%	CH14 – 2%	CH15 – 2%	CH16 – 2%	CH17 – 4%	CH18 – 1%
CH19 – 2%	CH20 – 1%	CH21 – 1%	CH22 – 0%	CH23 – 2%	CH24 – 2%

```
All Channels Passed
- - - - - - - - - - - - - - - - - - - - - - - - - - - -
```

Table 3.3: Tabularized RAS-24 Dissimilarity Test

Shaker Table Test. The shaker table test is often used for scientific tolerance tests of the geophones but not for practical use by operators in the field (as expedient calibration). The equipment used for the geophone calibration included a signal analyzer (HP Dynamic Signal Analyzer Model 35670A), a shaker (Labworks Inc. Electric Transducer Model NV-ET-26B), and an accelerometer (Dytran Instruments Inc. Model 3035BG). The equipment setup is illustrated in Figure 3.5. Crazy glue was used to firmly attach the accelerometer to the geophone, and the geophone to the shaker.

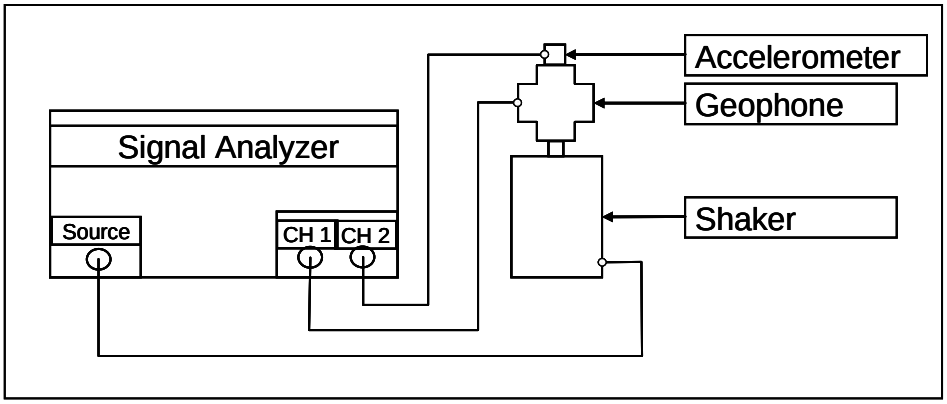

Figure 3.5: Shaker table test equipment set-up (University of Waterloo, 2008).

The source was set to random noise to excite the geophone and accelerometer through a broad spectrum of frequencies. Four sets of data were captured and transferred to a computer for analysis. These included the ratio of the accelerometer response to the geophone response (response magnitude ratio) with respect to the frequency of excitation from 1 to 400 Hz and 1 to 100 Hz, and the response signal phase difference between the accelerometer and the geophone with respect to frequency from 1 to 400 Hz and 1 to 100 Hz. The results are tabularized as follows for Geophone Sensitivity (Sg) in mV/cm/s:

Range	Sg Range	Sg Average	Sg Waterloo	SD
1 to 400	293.60 to 274.94	287.29	298.29	6.43
1 to 100	300.42 to 283.14	295.17	306	6.34

Table 3.4: Tabularized results of the Shaker Table Test. The standard deviations are calculated for a sample set of 4 geophones from the DMSU geophone set of 24.

Of all the algorithms used in the DMU, AARW is most sensitive to error in interpreting the void location. With a SD of 6.43 the error is +/- 3.22%. According to Dr. Ali Nasseri, who is the subject matter expert on AARW, the maximum tolerable error allowed for confidently interpreting void dimensions is +/- 5%. Therefore, the standard deviation is within tolerance for AARW.

Expedient Geophone Calibration. The 24 each 4.5 Hz geophones were tested in the upper lawn in the vicinity of the McNutt Mineral Engineering Building on the Missouri University of Science & Technology in Rolla, Missouri on 28 May, 2008 (see figure 3.5). The premise of the experiment was to group the 24 geophones at approximately the same distance from the energy source using spikes for coupling. Single shot gather readings were taken at 6, 10, 20, and 30 meter offset respectively for distance comparisons. The assumption being that the 24 new geophones adhere to factory specifications.

A Seistronix RAS-24 (channel) seismic recorder was used with an 18 lb sledge hammer and 0.5 inch thick, 6 by 6 inch metal plate as the seismic source. The condition of the ground at the site was generally dry at the surface. Software settings were set at a sample rate of 0.125 ms and a gain of 12 db. As demonstrated in the layout pictured above (Figure 3.4.a), the primary analysis is to compare each respective geophone wavelet to the other 23 that should be identical in amplitude & phase over time (Figure 3.6).

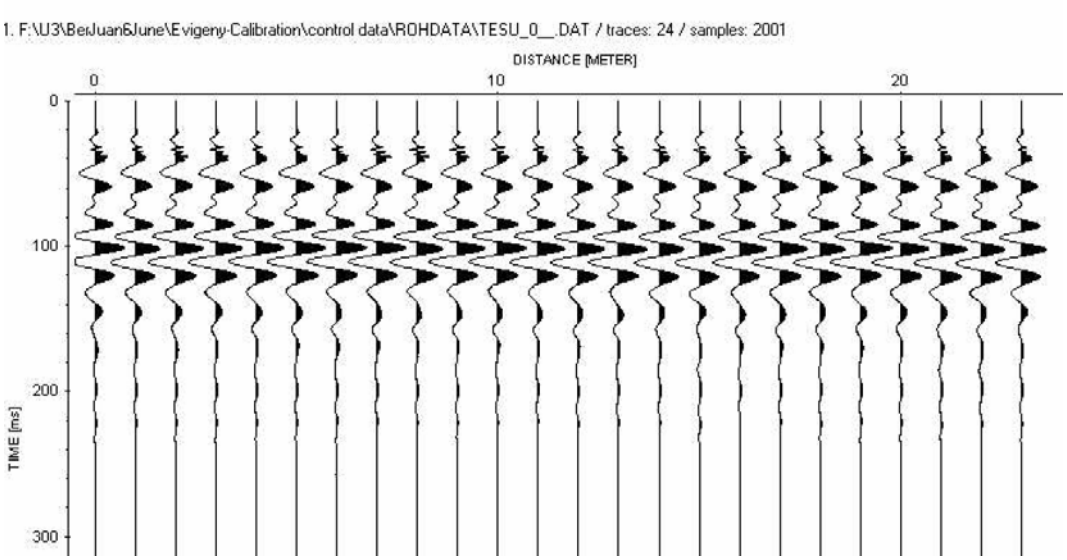

Figure 3.6: 25 geophone trace record using the 6m source offset data. Here each geophone records seismic energy as a positive or negative motion of a magnet suspended in a spring (phase) & intensity of that energy (amplitude) along the trace downward (time). Note that there are no discernable differences between the wavelets.

Recommendation. The geophones 'pass' all three tolerance tests in accordance with a +/-5% error recommended by Dr. Ali Nasseri for AARW interpretation purposes. The dissimilarity test is provided by RAS-24 and is included in the user manual as an equipment check after shipping the DMSU and before conducting the first survey. Likewise, 'calibration of low-frequency geophones for use in surface wave geophysical survey can be ascertained directly from the wavelet traces (Dr. Miller, 2008). Suspect geophones that consistently fail the test should be removed from the array and replaced. Shock and weather resistant storage will mitigate the degradation of geophones.

3.2 Streamer Array

The standard distance between each geophone in the array was set at 0.5m. Since surface wave energy generally cannot propagate through voids or water, the dispersion, attenuation, and reflections that occur at the interface of the void increase approaching and over the void. Given, shallow manmade tunnels are approximately 1m in diameter; two geophones along the array should be vertically positioned over its location. By lengthening the array to cover more area, a single geophone detecting an anomaly may be a result of spurious noise and increases false positives significantly. To the contrary, a geophone spacing of 0.25m doubles the amount of time required to survey a given line or area.

A significant challenge is the coupling of the surface laid geophone plates to the Earth's surface. Geophones are screwed into metal fabricated plates that are fastened to a durable fire hose. The firehose is dragged along the surface at predetermined intervals before stopping and taking seismic measurements. Coupling becomes more effective as weight is applied downward on the plate attachment surface. Pavements were more effective at transferring energy to the plates. Vegetation attenuated energy at the surface and created greater variation depending upon thickness of growth, detritus material, and the natural undulation in topography. Digging skates welded to the bottom of plates were considered but caused undue damage to manicured lawns as well as a possible trench digging effect causing variations in coupling along the array. The DMSU streamer array incorporated 2 each 2.5 lb. cast iron weights are used per geophone plate housing to increase coupling.

Figure 3.7: Missouri S&T Graduate Student Preetam Modur screws a geophone into the geophone plate. A firehose acts as a semi-rigid construct where a cast iron weight was spot welded to the top of the geophone adapter plate. As the project progressed, a second cast iron weight was added.

3.3 Seismic Impact Source

The seismic impact source is a vertical electrically powered 100lb strike hammer housed on a two wheel trailer. It is powered by a Marine 12V battery and manually operated by an extension cable into the cab of the ATV. The hammer is assisted by additional force once release from he up position by an elastic band that is tightened by the operator before the beginning of a survey. The hammer can be configured for pavements with a rubberized foot or with a hard hammer head that strikes a steel plate dragged behind the ATV and directly under the hammer.

Figure 3.8: The seismic impact source that imparts seismic energy into the ground is an active seismic system. The energy propagates through the ground and is measured by the geophones embedded along the yellow firehouse streamer. Note the rubberized foot configuration as to avoid damaging the thin concrete sidewalk.

Source to First Receiver Offset. The impact source (excitation) to first geophone off set is determined as the minimum distance required for the surface wave to propagate its wavelength consummate of the depth of interest. It is an important parameter because the first geophone trace is important for visual identification of voids using SWCO and SF analysis. For the simple case, the minimum horizontal shot to (first) receiver offset is 1 vertical wavelength or depth of investigation. For our purposes, a wavelength should reach a 1m diameter tunnel at 3m depth to include 1m below the tunnel floor (or lowest part of the void). The additional meter is for AARW calculations. As a general rule of thumb, the minimum distance for the offset is 5m using surface waves in a soil or slow velocity medium (Nasseri, 2006.)

In June, 2007 the DMSU Team conducted a set of seismic surveys at Ber Juan Park to validate a best source to receiver offset based on field data. 1, 2, and 3m depths were surveyed using manual plate, hammer, and spiked geophone streamer array beginning using a 3m surface wave common offset (SWCO). Review of the SWCO offset records visually demonstrated best results in the 6 to 10m common offsets range for the three embedment depths.

For the visual examination of the different source to receiver SWCO records we note that the advance of the DMSU was left to right approaching the void. This method does not require processing where the survey cross-section (length versus depth) is constructed by adding a wavelet from the first geophone at each successive shot at 0.5m intervals. This avoids aliasing problems sometimes encountered when software attempts to shift wavelets to their assumed proper geospatial position on the seismograph.

The red downward arrow signifies the field location of the geophone over the centerline of the tunnel. The visual phenomenon as the geophone approaches the tunnel is a ‘pull up’ of the peak amplitude wavelets forming a hyperbolic curve with its apex at the tunnel centerline. Attenuation of energy is seen directly below the traces as noticeably absent. As the geophone continues to advance to the right, the tunnel continues to damp the energy from the acoustic source. The source is over the tunnel at trace 31 that corresponds to the 6m off-set, trace 35 that corresponds to the 8m offset, and 39 that corresponds to the 10m off-set respectively.

Visual examination yields that 6 and 8m offsets appear optimal. However, the geophone cable length was constrained by a length of 6m from impact source to the first geophone taking into account 3m of additional slack required to plug into the seismograph. Therefore, the maximum allowable length was adopted as the standard shot to receiver offset for the DMSU. The side-by-side common offset comparison of the wavelet trace analysis is graphically displayed in Figures 3.9 & 3.10.

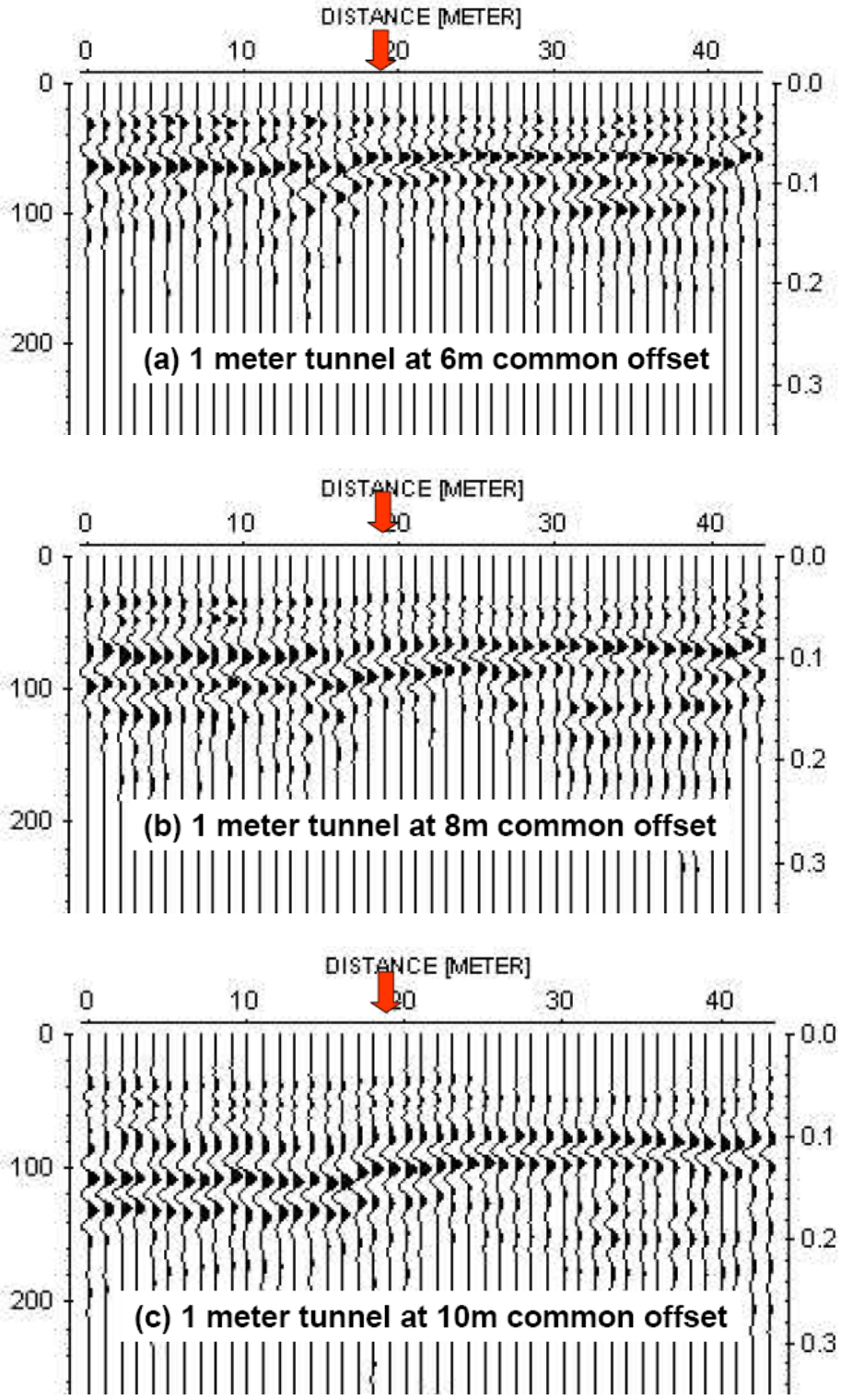

Figure 3.9: Common offset analysis of the 1 meter diameter tunnel at a depth of 1 meter at Ber Juan Park. The red arrow inset is the location of the geophone over the center line of the tunnel at (a) 6m; (b) 8m; and (c) 10m shot to receiver offset.

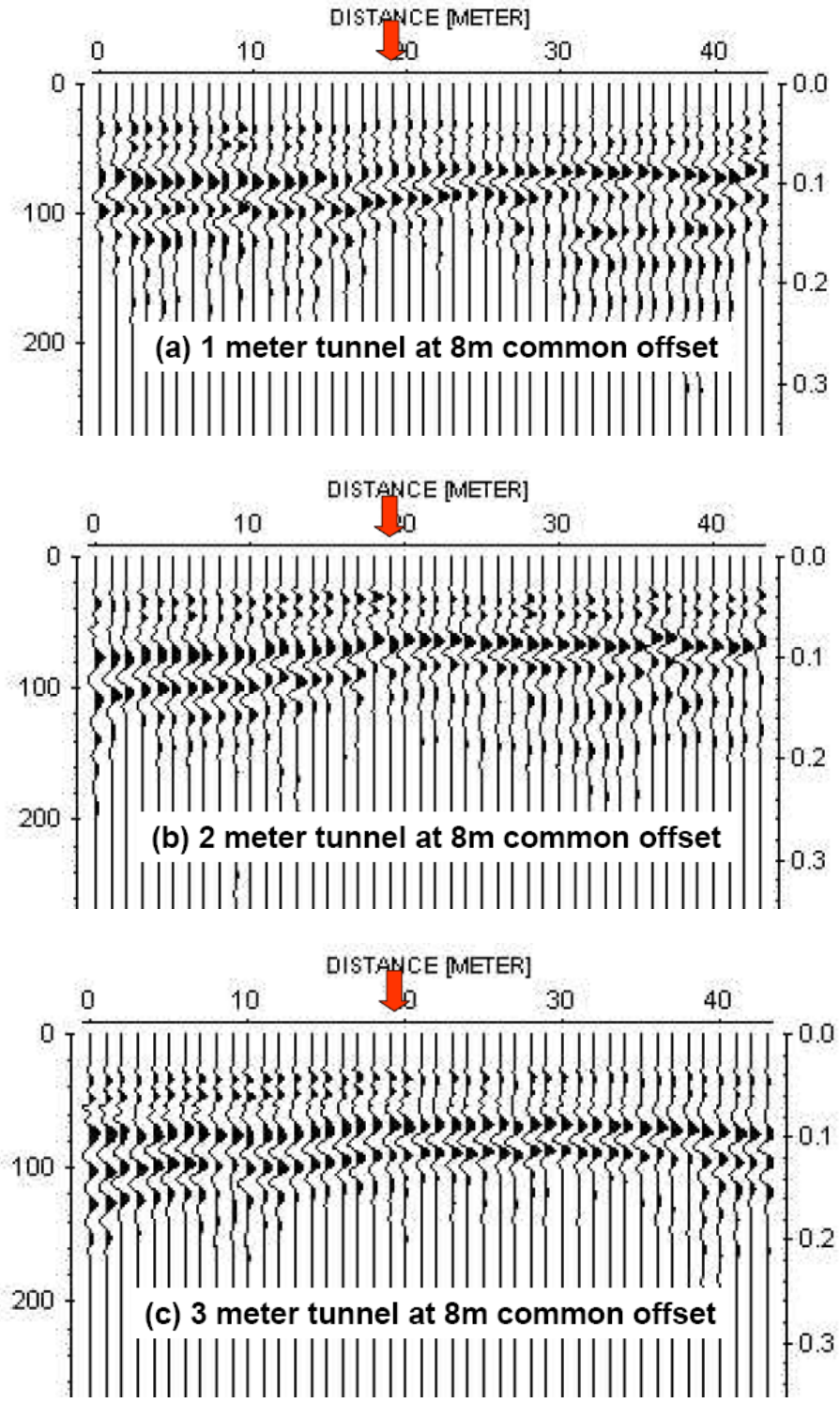

Figure 3.10: Common offset analysis of the 1m diameter tunnel at shot to receiver offset of 8 meters at Ber Juan Park. The red arrow inset is the location of the geophone over the center line of the tunnel at (a) 1m; (b) 2m; and (c) 3m embedment depths respectively.

The array length itself is another consideration for common shot analysis since the entire array is post-processed for use in reflection analysis and later by AARW. This affects the advance rate of the DMSU as a trade off between linear ground surveyed and certainty as a function of the sub-array (discussed in chapter 5, AARW) through redundant statistical anomaly validation. Similarly, other data processing programs such as SURFSIS rely on the combined shot gather of the 24 geophone array to conduct inversion of the dispersion curve as example. For these analyses the maximum resolvable wavelength (and thus depth penetration) is about 0.4 of the spread length (O'Neill, et al, 2008). Hence, we can estimate that our maximum effective depth capability of the 11.5m array is down to 4.6m.

3.4 Summary of Hardware Geometry

- 24 each 4.5 natural frequency geophones are used in the seismic sensor array.
- Geophone spacing is 0.5m.
- Source to first receiver offset is 6.0m.
- The advance of the DMSU between shots is 0.5m.
- The preferred seismic source configuration is the plate & steel hammer head.

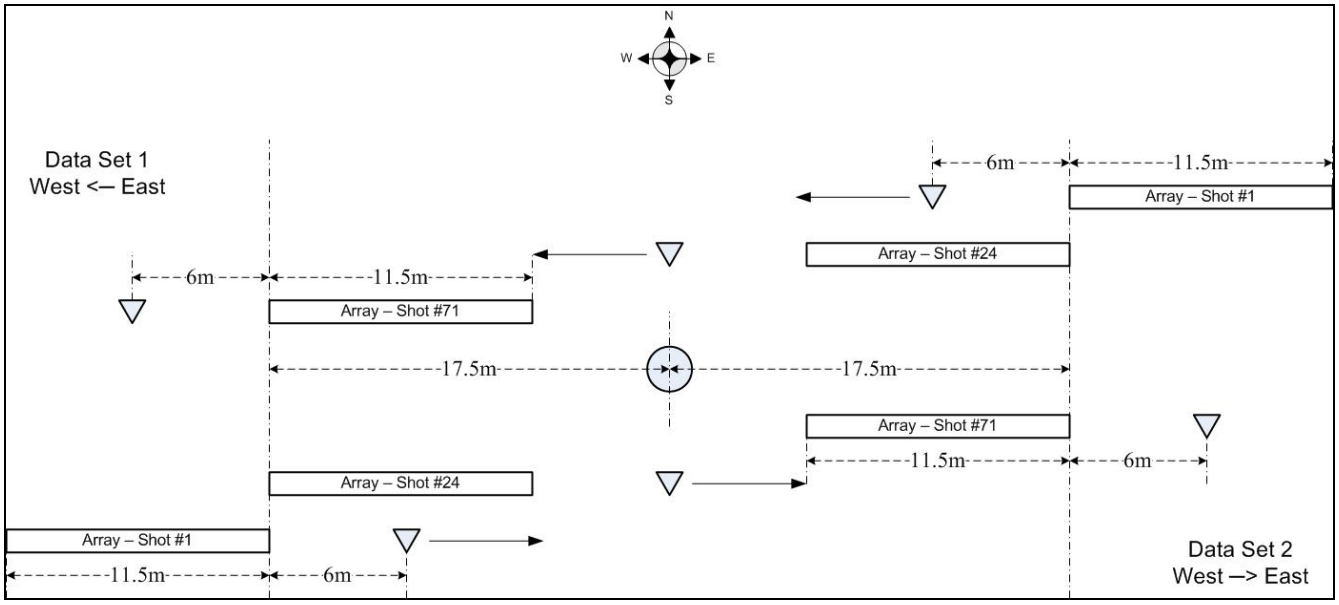

Figure 3.11: Diagram of the Standard Operating Procedure for the DMSU survey generally perpendicular to the direction of the tunnel. The procedure entails conducting two survey lines opposite in direction. The tunnel is the circle in the center and the down turned triangle represents the acoustic impact source. The minimum distance from the known tunnel at the start of the survey line is 6m (less as site constraints dictate).

4. PRE-PROCESSING SOFTWARE OPTIMIZATION

This chapter outlines the data acquisition software settings to facilitate required resolution for direct seismic interpretation and further post-processing at the most expeditious rate possible. Pre-processing is a term used for the gathering and sorting seismic data on a seismograph. The signals are gained & filtered on the seismograph in analog form using related electronic circuits. No digital processing is done. The signal is gained, filtered, digitized and written to the file. Pre-processing is limited in scope and uses instrumental software that is installed on the laptop.

Once the laptop / software operator accepts the seismic data, that RAS-24 software stores the record in SEG2 format in a historical batch file for further algorithm processing. Very experienced operators can visually estimate the location of a void anomaly apparent from the seismograph from the common shot gathers. However, the common shot gather traces are largely displayed to ensure the geophones are connected, operating properly, and spurious noise is not interfering with the shot (e.g. truck rolling by at the time of the shot). A non-geotechnical laptop / software operator is more likely to rely on SWCO that is built by a succession of shots. The SWCO is completed and then displayed at the end of a survey line for visual interpretation.

4.1 Overview of Rayleigh Waves

Rayleigh waves propagate along the free surface of the Earth's surface, with particle motions that decay exponentially with depth (Figure 4.1). The lower component frequencies of Rayleigh waves involve particle motion at greater depths. In a homogenous (non-dispersive) medium, Rayleigh wave phase velocities are constant and can be determined using the following equation:

$$V_R^6 - 8\,\beta^2\,V_R^4 + (24 - 16\,\beta^2/\alpha^2)\,\beta^4\,V_R^2 + 16\,(\beta^2/\alpha^2 - 1)\,\beta^6 = 0$$

where:

V_R is the Rayleigh wave velocity within the uniform medium
β is the shear-wave velocity within the uniform medium (also denoted as Vs)
α is the compressional wave velocity within the uniform medium (also denoted as Vp)

Rayleigh wave velocities, as noted in the equation above, are a function of both shear-wave velocity and compressional wave velocity in the subsurface. In heterogeneous earth, shear-wave and compressional-wave velocities vary with depth. Hence, the different component frequencies of Rayleigh waves (involving particle motion over different depth ranges) exhibit different phase velocities (Bullen, 1963). The phase velocities of each component frequency being a function of the variable body wave velocities over the vertical depth range associated with that specific wavelength.

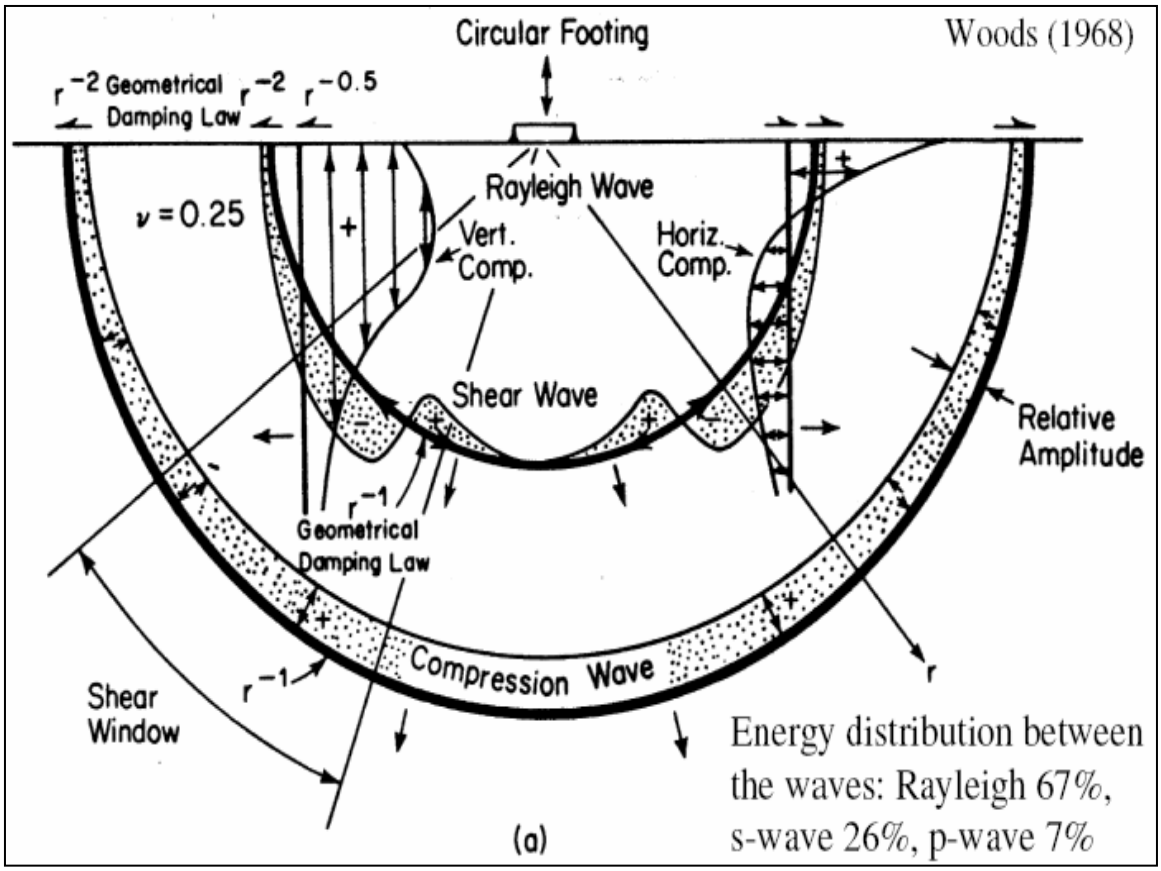

Figure 4.1: Particle motions associated with seismic waves. Unlike compressional P-waves, S-waves are confined to the upper layer of (and traveling along) the Earth's surface. The loss of energy is due to circular spreading (square root) as opposed to spherical spreading (cube root). Methods using Rayleigh Wave Analysis are said to be more robust.

The acquisition of Rayleigh wave data is relatively straightforward. Twenty-four low-frequency (4.5 Hz) vertical geophones, placed at 0.5m intervals, were configured in a streamer array and oriented perpendicular to a known tunnel or culvert. Seismic energy was generated at an offset (distance to nearest geophone) of 6m using a 100lb impact source mounted on a trailer (Figure 4.2). The generated Rayleigh wave (desired type of surface wave) data were recorded using a 24-channel engineering seismograph using the RAS-24 software. The geophone array was moved at 0.5m intervals after each shot. The seismograph recorded each consecutive shot as the streamer array crossed the location of the tunnel. At the end of the survey line, the operator processed the data and compared his selection to the field measurements of the known tunnel. Based on the comparison of interpreted to known location of the tunnel, the degree of error was determined.

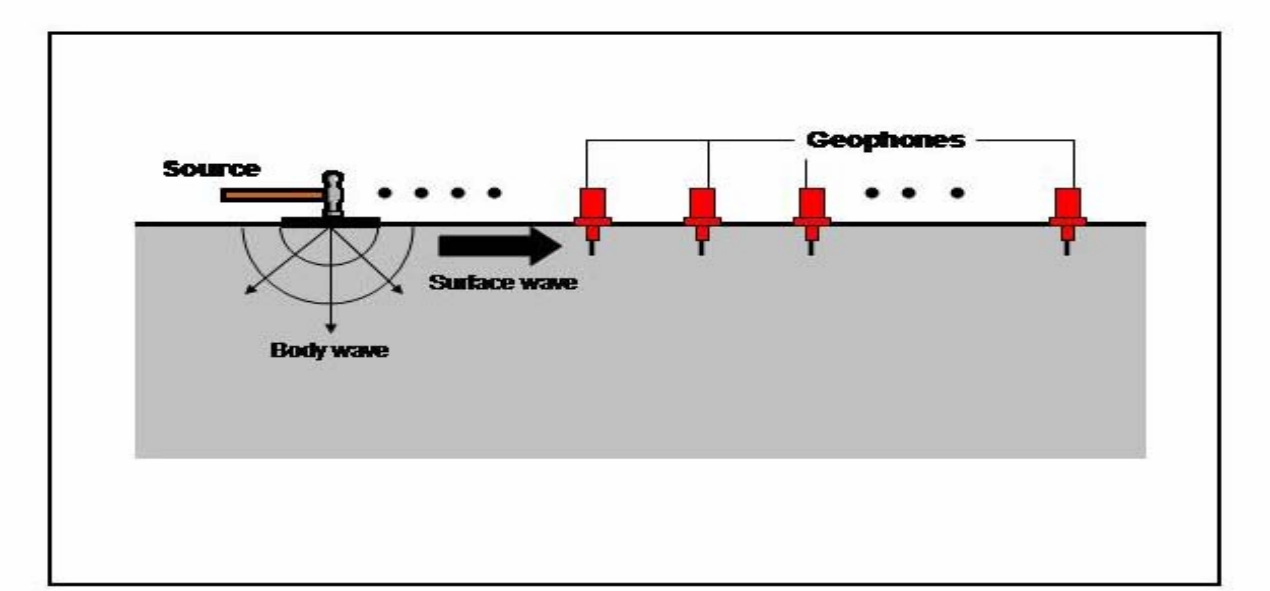

Figure 4.2: Acquisition of MASW field data.

4.2 Single Shot Gathers Using Rayleigh Waves

The standardized pre-processing RAS-24 (channel) software settings were determined during the preliminary field investigation at Ber Juan Park in the Spring of 2008. At the time, there were expectations that SWCO, SF and AARW might be able to detect tunnels down to 3m. Logic followed that if the team could confidently detect tunnels through commonly used filters applied to raw data, then post-processing algorithms (SF & AARW) could be applied in the MATLAB code to the same in an automated and rapid manner. Based on common shot an SWCO analysis of pre-processed, depth investigation limits were realized. Excursions using SF & AARW to identify the tunnel a 2 and 3m depth at Ber Juan using the seismic data were inconclusive.

Multi-channel Rayleigh wave data were acquired across a 1meter diameter spillway tunnel along three parallel traverses with surface to tunnel separation of 0.90m, 2.15m, and 3.13m depth respectively 1m. The data were acquired by placing a 24-channel array perpendicular to the center-line of the spillway tunnel and incrementally moving the array across the tunnel. The sledge hammer source offset was 6m. The 4.5 Hz geophone array spacing was at 0.5m intervals. Single shot data were analyzed to visually locate and to highlight attenuation effects associated with the tunnel. The field records were then velocity filtered in order to enhance back-scattered Rayleigh wave energy thereby allowing for visual identification of the tunnel location.

Initially, the Missouri University of Science and Technology's Department of Earth Science conducted single shot gather seismic surveying using a range of source to receiver off-sets from 10 to 3m, geophones with center frequencies from 100, 28, 14, and 4.5 Hz, and geophone spacing at 0.25 or 0.5m respectively. Raw data sets were then compared with the aid of ReflexW seismic software to select geometrical parameters. The survey team adopted a source to receiver offset of 6 m, geophone center frequency of 4.5 Hz with a spacing of 0.5m given the quality of signal response to the known tunnel as well a equipment constraint considerations. Calibration measurements of the geophones in the preliminary experiments were not conducted. Previous literature on this subject at the time of the experiment showed nominal affects when comparing the known embedment depths to the interpretation.

The ReflexW seismic software package was used for processing of the raw data depicted in figure 4.3 below. An analysis of the data indicates the onset of attenuation from the seismic source (from left to right.) This can be characterized of an expression of a void on surface wave field records. The seismic waves are expressed vertically with horizontal axis being the 0.5m distance between the geophones. The known center-line or crown of the concrete lined tunnel is at geophone 6 on the trace. We may interpret the onset of attenuation as left limit and subsequent continued weakening of amplitude of surface waves further to the right. This range (e.g. geophone 4 through 6 on the 0.90m trace as example) does not permit approximation of depth or left and right limits. However, the attenuation phenomenon is an indicative of void presence and can be used to corroborate the characterization that a void may be present.

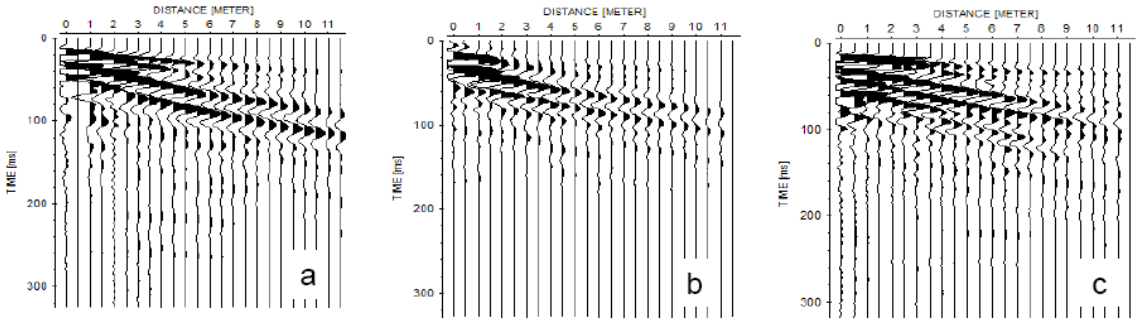

Figure 4.3: (a) 2D Rayleigh wave profile above the known Ber Juan spillway tunnel at 0.90m embedment depth; (b) at 2.15m depth; (c) at 3.13m depth.

Velocity Filter to Enhance Back-Scattered Energy Scattering of incident energy due to a sharp contrast on acoustic impedance, such as a void, is observed to produce reflection, refraction and diffraction that will result in attenuation of Rayleigh waves. The produced back-scattered energy, referred to by the geophysical practitioner as noise, can be indicative of shallow tunnels. From a common shot gather, we commonly observe negatively oriented diffraction energy, dipping from right to left, after the primary Rayleigh wave arrivals. To accentuate diffracted energy for further analysis, we can apply F-K filtering to eliminate left to right dipping primary Rayleigh waves, apply a horizontal cut filter, and discriminate against aliasing that may be interpreted by post-processing as apparent right to left dipping energy. Parameters for processing were bandpass filtering 4 – 80 Hz and F-K filtering for velocities from -150 to -400 m/s. As example, Figure 4.4 below demonstrates the application of these rules to the raw data as one technique to enhance this back-scattered energy associated with the Ber Juan tunnel. Xia et al. (2006), present a simple method in the time-space domain based a travel-time equation of surface-wave diffractions to detect voids directly from a shot gather. Similarly, using single shot Rayleigh wave records, the geometrical formulae are applied to approximate embedment depth at the end of this paper.

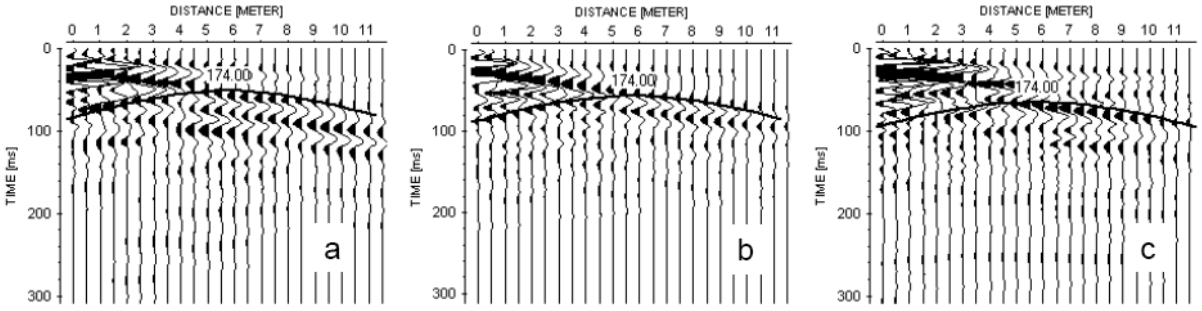

Figure 4.4: (a) 2D Rayleigh wave velocity profile above the known Ber Juan spillway tunnel using FK filter with a diffraction travel time curve for (a) tunnel at 0.90m embedment depth; (b) at 2.15m depth; (c) at 3.13m depth.

Figure 4c presents a challenge since we can calculate the two way travel time of t_o (apex of the hyperbolic curve representative of the top of the tunnel void) given the dominant phase velocity (V_R) of 158m/s and known depth of the void at 3.13m. As example, in figure c we may pick t_o = 0.065ms and t_x = 0.080ms at geophone 2 from the trace. Using these pick values and quadratic equation to solve for height (Xia, 2006), the depth is calculated to be 1.78m. Observe that the traces to the right of the apex in Figure c is challenging to interpret as it appears to form a line with slope rather than a shallow hyperbolic curve. Given we know the blueprint depth to the void as 3.13m, the combination of human subjectivity and circular shape of the tunnel may inject additional error beyond inhomogeneous field conditions. In his numerical modeling results, Giles et al. (2005) reported that cavities with circular sections generate less diffraction than rectangular sections.

4.3 Common Offset Analysis

As previously discussed in section 3.3, SWCO 2D gathers allowed for visual identification of voids down to 2 meters. However, the SWCO with the known tunnel at a depth of at 3 was indistinguishable. Combined with the increasing error versus depth using Xia's method, the inability of SF and AARW to confidently detect round tunnels at 2 and 3m depth, the team opted to focus on tunnels at about 1m depth.

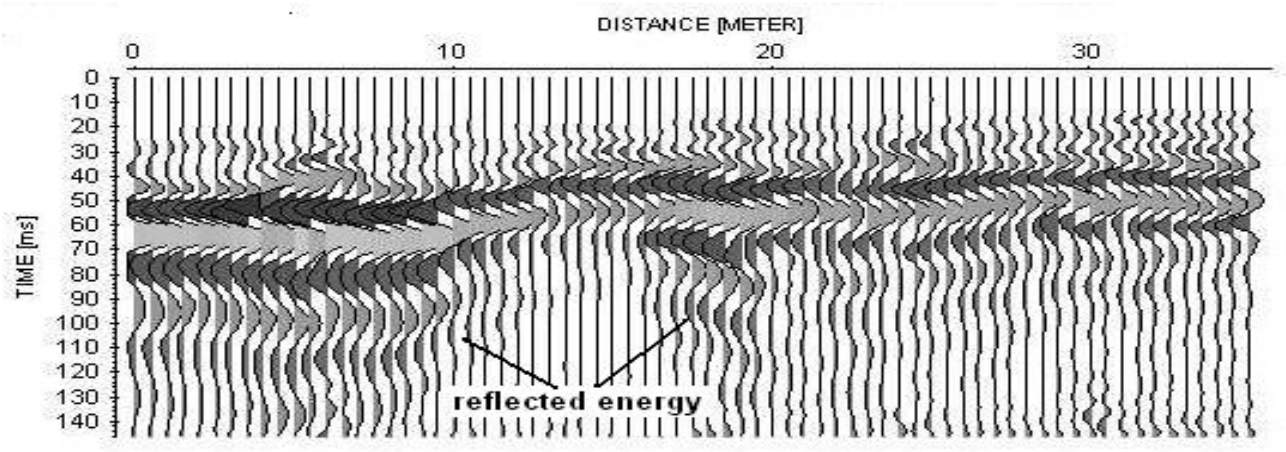

Figure 4.5: 2D Rayleigh wave profile above a known 1m embedment depth at Ber Juan Spillway Tunnel using FK filtering. Raw data allows or visual interpretation of tunnel location.

4.4 Data Acquisition Settings

The default RAS-24 setting for gain function is 12db applied to recover signal loss as a function decay over distance. The standard file format is known as SEG-2 that is also user friendly to MATLAB and a variety of other seismic and signal processing programs. Record length was reduced from the default setting of 1 to 0.5 seconds. The maximum vertical depth for the two-way travel time of a slow soil (100m/s) is 25 meters optimally. And, using theoretical vertical resolution, the maximum depth is estimated at ¼ λ equal to 12.5 meters. The Nyquist rate is the minimum sampling rate required to avoid possible aliasing of the data based on relative size of the anomaly. Using the discrete time system, the sampling rate should be twice that of the target width. At the sampling rate of 1.0 ms (or 1000 samples per second) the maximum velocity of the soil for 1m diameter tunnel is 500m/s. To avoid aliasing of a 0.5m diameter tunnel the minimum is 250 m/s. For purposes of unconsolidated soil, alluvium or fill associated with manmade activity, the sampling rate is appropriate. The overall processing time from shot to GUI display was 10 seconds. In harder limestone or sandstone, the sampling rate should be increased up to 0.025 ms. The trade off is that processing time per shot will be increased to 90 seconds per shot.

A summary of the RAS-24 settings is as follows:

- Seismic data files are SEG-2 format
- The gain function is 12 db
- The record length is 0.5 seconds
- The sampling interval is every 1.0 ms (milliseconds)

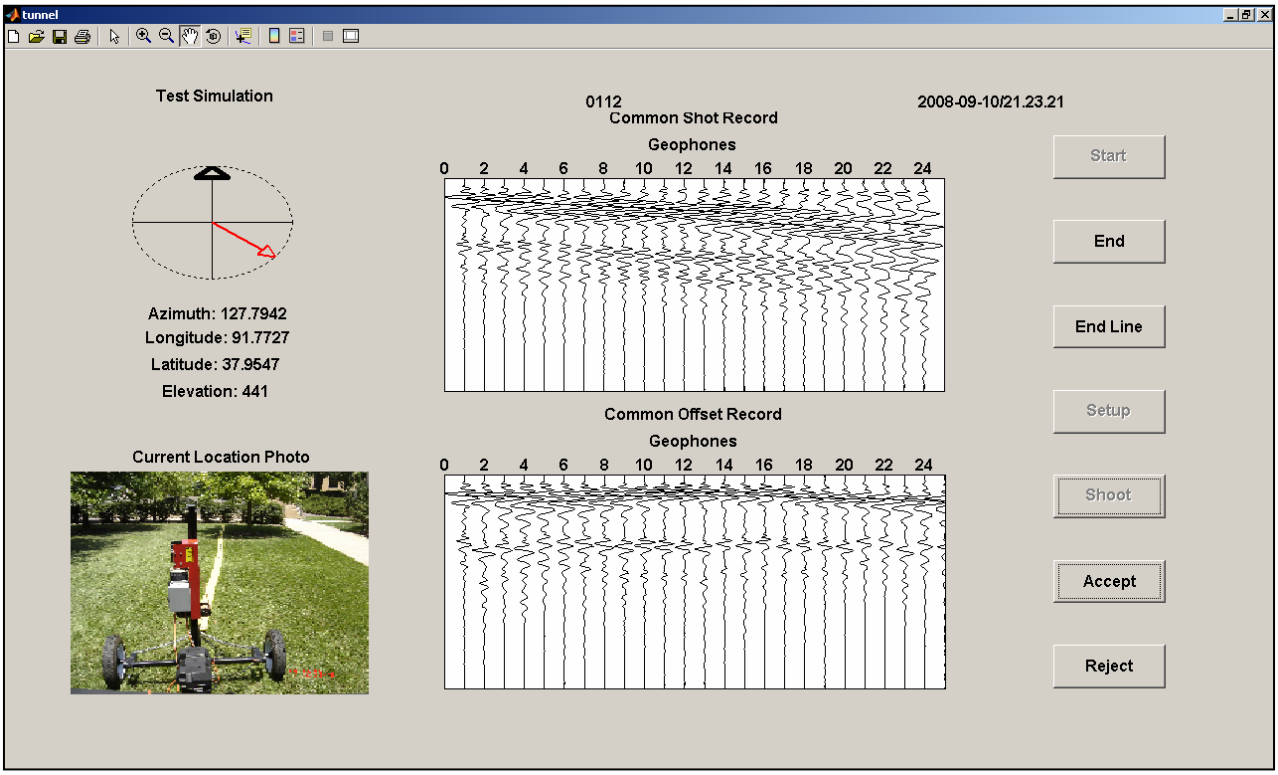

Figure 4.6: The Graphic User Interface (GUI) allows the operator to visually inspect both the common shot gather and the common offset records before further seismic data processing. Data acquisition settings results in a 10 second processing time between the actual shot and the display the data in the GUI seen above.

5. POST-PROCESSING ALGORITHM SUMMARY

Post-processing using SF and AARW algorithms within MATLAB occurs once a survey line is complete. SF and Spiking Statistic Measure (SSM) used in the 2D Mapping tool are one and the same. MATLAB pulls the individual SEG2 files from the historical RAS-24 data base. This process is not subjective but an autonomous routine. Given the DMSU is operated properly in reasonable conditions, the algorithm(s) will resolve and identify anomalies associated with voids. This does not preclude false positives. However, the output is plotted on a 2D map where the operator can apply his or her judgment in selecting which anomalies are likely tunnel locations (discussed later). The SF builds its analysis similar to the SWCO by statistically comparing the difference in each shot gather to the next. AARW uses the common shot gather exclusively to locate anomalies. An AARW sub-array technique then reduces error by essentially overlapping each common shot to validate the anomaly at a given location.

5.1 Spiking Filter (SF)

This section describes an algorithm that uses spiking filters designed from the first few geophone responses in a common shot gather to attempt to deconvolve responses of all of the geophone responses of the shot.

Spiking Filters: A spiking filter is a filter that attempts to "de-convolve" a given signal $y(n)$ into an ideal excitation "spike" $u(n)$ and an M-length filter with impulse response $h(n)$. Here, $u(n)$ consists of all zeros except at one point where it is equal to one. That is

$$u(n) = \delta(n-d) = \begin{cases} 1 & n = d \\ 0 & n \neq d \end{cases}$$

Where the delay, d, is as-yet unknown.

The objective is to design $h(n)$ such that

$$\hat{u}(n) = y(n) * h(n)$$

is as close as possible to $u(n)$. Accordingly, we define an error signal

$$e(n) = u(n) - \hat{u}(n)$$

and we wish to minimize the squared error

$$\varepsilon = \sum_{n=0}^{N+M} e^2(n)$$

Casting the above ideas in matrix form we define the following:

$$Y = \begin{bmatrix} y(0) & 0 & 0 & \cdots & 0 \\ y(1) & y(0) & 0 & \cdots & 0 \\ y(2) & y(1) & y(0) & \cdots & 0 \\ \vdots & \vdots & \vdots & & \vdots \\ y(N) & y(N-1) & y(N-2) & \cdots & y(N-M) \\ 0 & y(N) & y(N-1) & \cdots & y(N-M+1) \\ 0 & 0 & y(N) & \cdots & y(N-M+2) \\ \vdots & \vdots & \vdots & & \vdots \\ 0 & 0 & 0 & \cdots & y(N) \end{bmatrix}, \quad \mathbf{h} = \begin{bmatrix} h(0) \\ h(1) \\ \vdots \\ h(M) \end{bmatrix}, \quad \mathbf{u} = \begin{bmatrix} u(0) \\ u(1) \\ \vdots \\ u(M) \end{bmatrix}$$

So the above equations become,

$$\hat{\mathbf{u}} = \mathbf{Y}\mathbf{h}, \quad \mathbf{e} = \mathbf{u} - \hat{\mathbf{u}}, \quad \varepsilon = \mathbf{e}^T\mathbf{e}$$

Minimizing ε with respect to the weight vector $\mathbf{h}$ results in the orthogonality equations:

$$\mathbf{Y}^T\mathbf{e} = \mathbf{Y}^T\left(\mathbf{u} - \mathbf{Y}\mathbf{h}\right) = \mathbf{0}$$

And solving for $\mathbf{h}$ yields

$$\mathbf{h} = \left(\mathbf{Y}^T\mathbf{Y}\right)^{-1}\mathbf{Y}^T\mathbf{u}$$

The error signal is then

$$\mathbf{e} = \mathbf{u} - \mathbf{Y}\mathbf{h} = \mathbf{u} - \mathbf{Y}\left(\mathbf{Y}^T\mathbf{Y}\right)^{-1}\mathbf{Y}^T\mathbf{u} = \left(\mathbf{I} - \mathbf{P}\right)\mathbf{u}$$

Where

$$\mathbf{P} = \mathbf{Y}\left(\mathbf{Y}^T\mathbf{Y}\right)^{-1}\mathbf{Y}^T$$

Thus,

$$\varepsilon = \mathbf{u}^T\left(\mathbf{I} - \mathbf{P}\right)^2\mathbf{u} = \mathbf{u}^T\left(\mathbf{I} - \mathbf{P}\right)\mathbf{u}$$

Since

$$\mathbf{u} = \begin{bmatrix} 0 \\ \vdots \\ 0 \\ 1 \\ 0 \\ \vdots \\ 0 \end{bmatrix} \leftarrow d^{th} \text{ element}$$

So, the squared error is

$$\varepsilon = 1 - \mathbf{P}_{d,d}$$

Thus, we can minimize ε by picking the largest diagonal element of $\mathbf{P}$. That element also determines the best value of d.

Application of Spiking Filters to Tunnel Location: If there is no anomaly within the region between the source pulse and the last geophone, the spiking filters designed from the signals of the first few geophones should do a good job of deconvolving the responses from all the geophones. However, if an anomaly, such as a void exists, the resulting reflections and diffractions will disturb the geophone responses such that a spiking filter designed from one response will do a poor job of deconvolving the others.

This observation suggests the following algorithm:

1. For i=1:N
    a. Design a spiking filter $\mathbf{h}_i$ from the response signal of geophone i
    b. Use the spiking filter to deconvolve the responses of all the geophones responses of the shot
    c. Calculate the ratio of the deconvolved shot energy over the original shot energy
2. Find the minimum of the above N ratios
3. If the resulting statistic is above a threshold, declare an anomaly present

Applying this algorithm to the BerJuan site data yielded encouraging results. Figure 5.1 shows the results of the algorithm applied to data collected on June 27, 2008 where the offset was 3m and the spacing between geophones was 0.5m. The initial shot was 3m to the left of the tunnel and the shots were taken every 0.5m. Thus, the excitation was over the tunnel at the 7th shot, the first array geophone was over the tunnel on the 13th shot and the last array geophone was over the tunnel on the 37th shot. The largest statistic response was just after the excitation passed over the tunnel. Then it diminishes quickly.

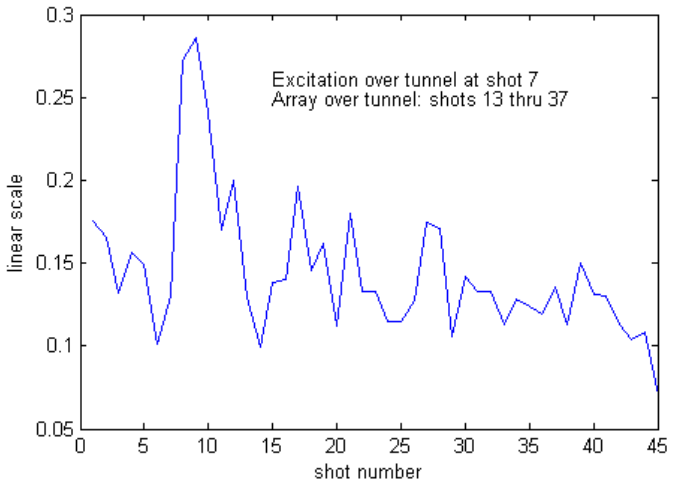

Figure 5.1: Spiking statistic: the statistic peaks just after the excitation passes over the tunnel at shot 7. The 24 geophone array passes over the tunnel from shot 13 through 37. The array spacing was 0.5m and the excitation offset from the array was 3m.

Figure 5.2 shows the results of the algorithm applied to data collected on July 11, 2008 where the offset was 6m and the spacing between geophones was 0.25m. The initial shot was 3m to the left of the tunnel and the shots were taken every 0.5m. Thus, the excitation was over the tunnel at the 7th shot, the first array geophone was over the tunnel on the 19th shot and the last array geophone was over the tunnel on the 31th shot. Just as with the previous data, the largest response of the statistic was just after the excitation passed over the tunnel. Then it diminished quickly.

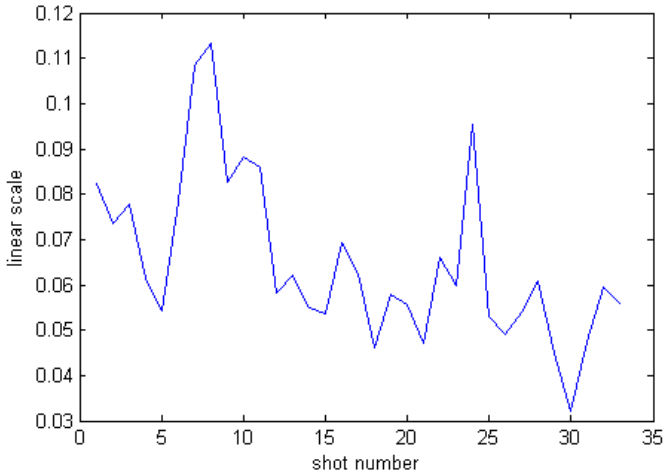

Figure 5.2: Spiking statistic: the statistic peaks just after the excitation passes over the tunnel at shot 7. The 24 geophone array passes over the tunnel from shot 19 through 31. The array spacing was 0.25m and the excitation offset from the array was 6 meters.

Another data set was taken on June 3 and the results are shown in Figure 5.3. There, the offset was 6m and the spacing between geophones was 1m. The initial shot was 6m to the left of the tunnel and the shots were taken every meter. Thus, the excitation was over the tunnel at the 7th shot, the first array geophone was over the tunnel on the 13th shot and the last array geophone was over the tunnel on the 37th shot. As with the first two data sets, the largest response of the statistic was just after the excitation passed over the tunnel. Then it diminished quickly.

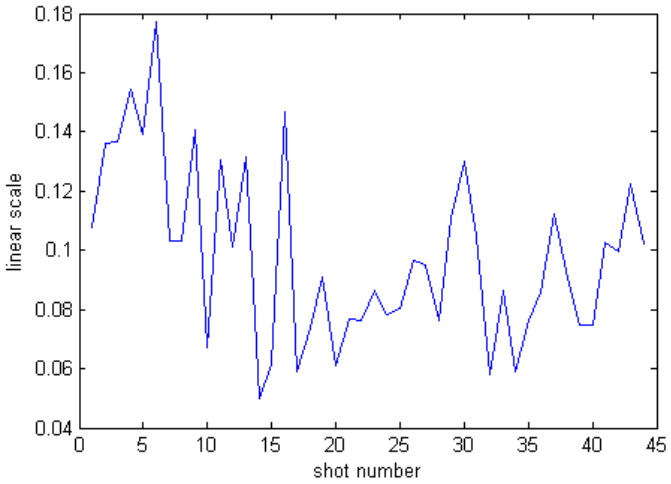

Figure 5.3: Spiking statistic: the statistic peaks just before the excitation passes over the tunnel at shot 7. The 24 geophone array passes over the tunnel from shot 13 through 37. The array spacing was 1m and the excitation offset from the array was 6m.

5.2 Attenuation Analysis of Rayleigh Waves (AARW)

A technique known as Attenuation Analysis of Rayleigh Waves (AARW) was proposed (Nasseri, 2006). This technique is based on investigating the effect of lateral inhomogeneities, i.e., cavities, on the propagation of Rayleigh waves, which are a type of surface waves (Figure 5.4). This technique quantitatively determines the location of an underground void, specifically detecting and locating a tunnel. However, it does have a rather high false alarm rate and also suffers from the so-called coupling problem (described below). Thus, further analytical and experimental investigations are required.

This contribution examines the AARW algorithm using seismic data sets of single-shot-gather Rayleigh waves and quantitatively measures the geospatial location of the tunnel in the earth's subsurface. The objective is to employ array signal processing techniques on the AARW algorithm to enhance its performance. The proposed method can also be applied to other tunnel detection methods.

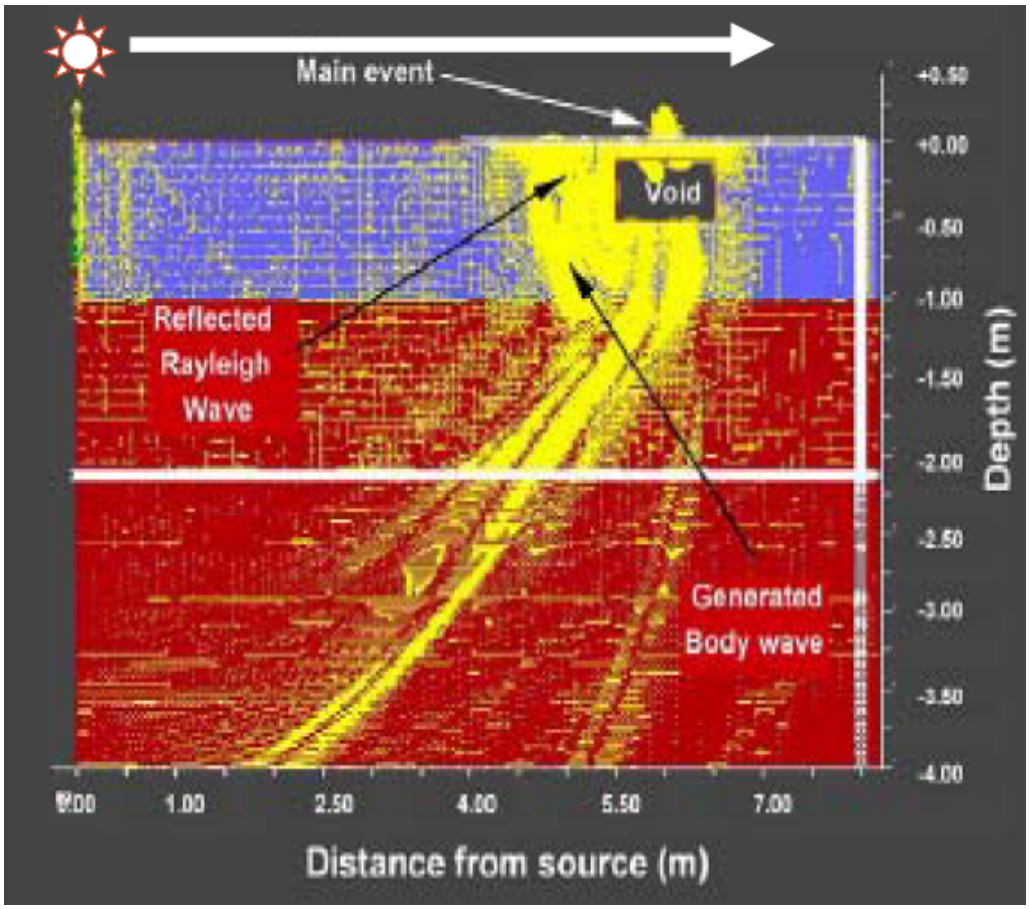

Figure 5.4: FLAC 2D Model simulating a seismic wave encountering a void: Wave attenuation accounts for reflections, scattering, and mode conversions at wave front boundaries. At the leading edge of the void the waves are magnified then attenuated, and the back edge attenuation is followed by magnification (Nasseri-Moghaddam, 2006).

The energy levels across the sensor array are not only affected by the underground voids, but also by the so called geometrical damping phenomena. The geometrical damping is a decrease in the amplitude of a spherical or a cylindrical wave, both in time and space. As the wave moves forward the density of the energy at the wave front decreases. Figure 5.5 shows the Rayleigh wave responses recorded by a 24-element 0.5m spaced geophone array. The red dashed line indicates the actual location of the underground tunnel. It can be noticed that the energy degradation due to geometrical damping is significant at the far end of the array.

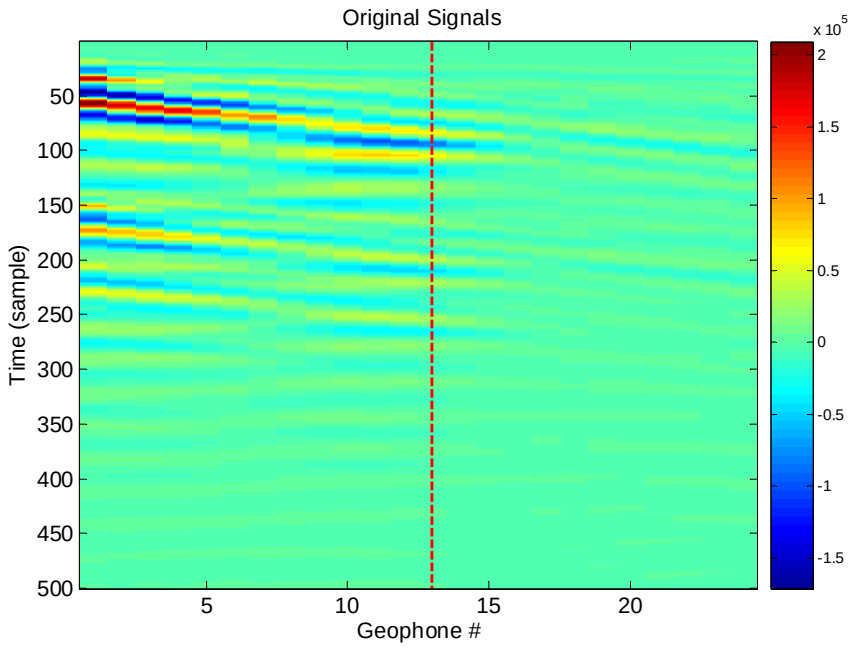

Figure 5.5: The Recorded Wave Responses

In the AARW method, only energy variations caused by the voids are considered. Thus, before calculating the energy on each sensor, a set of gain coefficients must be applied across the array elements to compensate for the effect of geometrical damping. These coefficients can be calculated using the following function (Nasseri, 2006):

$$g_i = \left(\frac{d_i}{d_1} \right)^{\alpha}$$

where g_i represents the gain coefficient of sensor i and α denotes the gain factor. The terms d_i and d_1 are the distances from the excitation source to sensor i and sensor 1, respectively. The amplified sensory signals x'_i can be obtained by:

$$x'_i(k) = g_i x_i(k)$$

where $x_i(k)$ denotes the i^{th} geophone signal at time index k. The amplified signals are displayed in Figure 5.6.

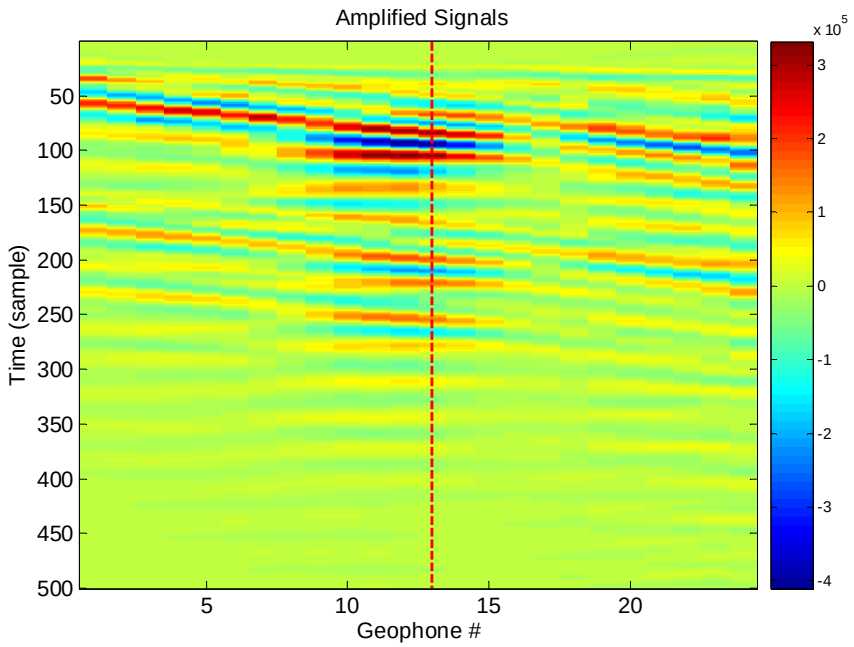

Figure 5.6: The Amplified Wave Responses

Since the effect of attenuation and amplification is more observable in the frequency domain, the time domain signals are transformed into the frequency domain where the energy calculations are performed. Figure 5.7 displays the recorded wave responses in the frequency domain. It shows that most of the signal energy is concentrated in the frequency band below 200Hz. Therefore, an optimum frequency range can be selected. This range may vary with the geometry of the recording array, background noise, etc.

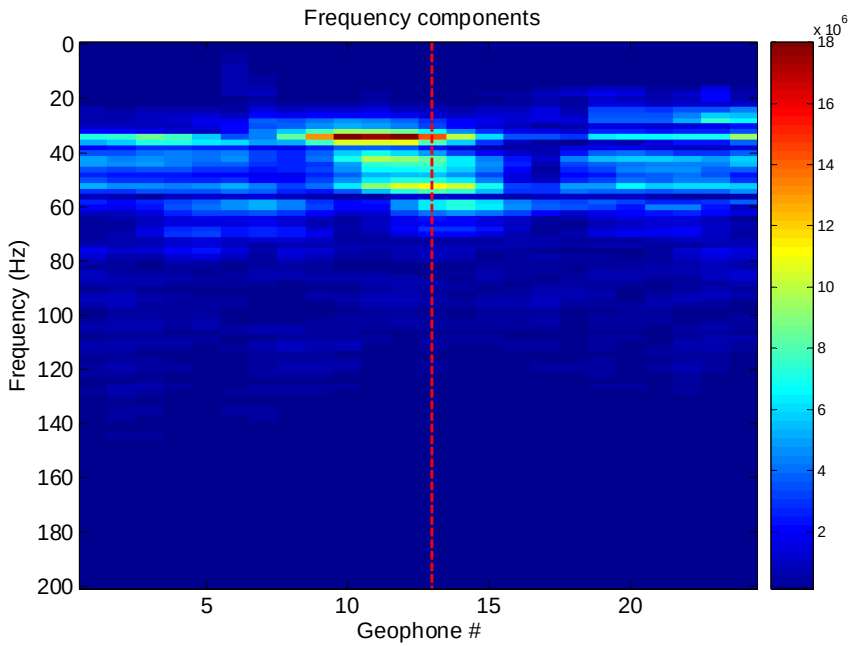

Figure 5.7: The Amplified Wave Responses in Frequency Domain

Over the reliable frequency range *B*, the cumulative spectrum energy at each receiver location is estimated as follows:

$$E_i = \sum_{f \in B} \left| \mathrm{X}_i(f) \right|^2$$

where X_i stands for corresponding frequency components of the amplified signals x'_i and f denotes the frequency. Normalizing the cumulative energy with the maximum energy across the array yields a new set of parameters called the normalized energy-distance parameters (*NED*):

$$NED_i = \frac{E_i}{\max(\mathrm{E})}, \quad \mathrm{E} = [E_1, \cdots, E_i, \cdots, E_N]$$

The above equation indicates that the value of *NED* is within [0, 1], and its variation with distance shows the location of the void. To locate the tunnel, the *NED* parameters are plotted versus distance. Due to the existence of energy concentrations, high values of this curve appear before and after the void location. The *NED* increases to its maximum value of 1 and then drops, and again rises to another high. The maximum value occurs in the vicinity of the near boundary of the tunnel. The second high value occurs in proximity of the far boundary of the tunnel. A successful detection case is shown in Figure 5.8. The center of the tunnel is indicated with vertical dashed arrow. The plots show that the *NED* values clearly reveal the location of the void. When the width of the tunnel is small compared to the array spacing, the highs and lows might not be distinguishable. In such cases, the location of near and far boundaries of the tunnel can not be estimated. However, the peak in the curve can always be seen at the sensor close to

the near boundary of the tunnel, and high values can be expected at those sensors above the tunnel. So practically, we take the peak of the curve and consider it as an indication of the tunnel location.

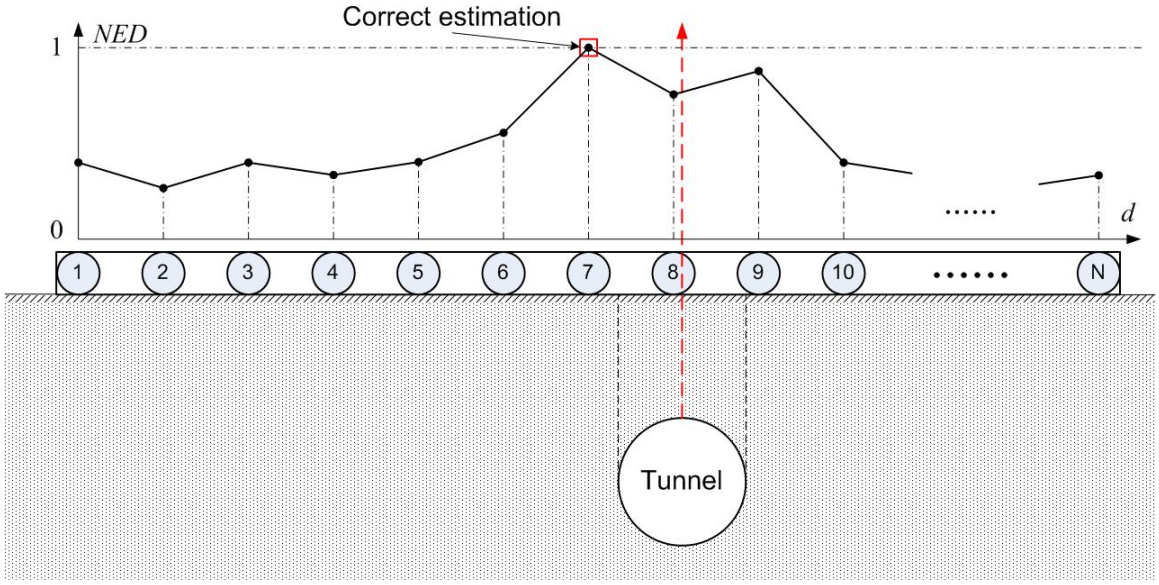

Figure 5.8: The NED Parameters versus Distance

AARW Methodology. Although AARW is a promising tool for tunnel detection, it exhibits several limitations. First, the AARW method is a multi-sensor approach, and a set of seismic sensors is placed on the ground surface to acquire data. It requires that all sensors have the same sensitivity to the active surface (Rayleigh) waves. However, unlike other types of sensors working in one single media, such as optical and acoustic sensors, these seismic sensors work on the interface between different media. Therefore, they suffer from the so called coupling problem. Different seismic sensors couple to the ground at different sensitivities. This coupling problem greatly affects the amplitude of the cumulative signal energy at each sensor. Second, this method basically detects underground inhomogeneities, that is, it not only detects tunnels, it detects other types of voids, as well. Since the AARW method has no capacity to discriminate voids and tunnels, those unwanted detections generate false alarms. These problems significantly degrade the performance of the AARW method. To address them, a post-processing method employing array processing techniques is proposed. This method contains three units: a sub-array processing unit, a confidence level unit, and a clustering unit.

Sub-Array Processing. According to the principle of Rayleigh wave propagation, underground inhomogeneities other than tunnels, such as small voids, can also generate a local maximum on the *NED* curve. In some cases, this type of local peak is even higher than that generated by a tunnel. When the tunnel is present, an incorrect estimation will be given. When the tunnel does not exist, a false alarm will be generated. This is shown in Figure 5.9.

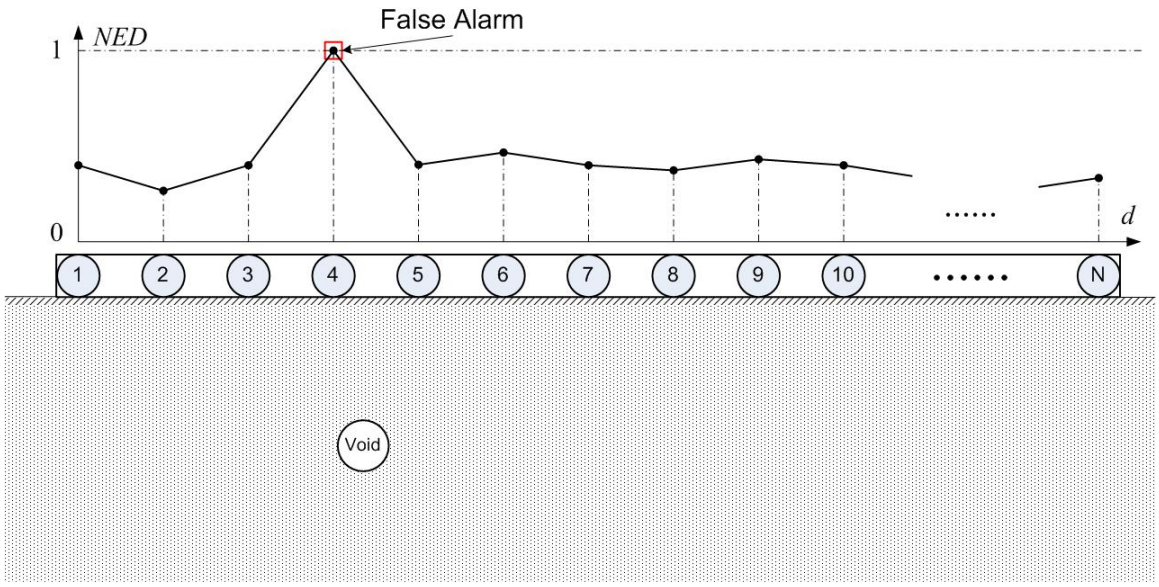

Figure 5.9: False Alarm Generated by Small Voids

To solve this problem, we note that in most cases inhomogeneities have a smaller width than that of underground tunnels. Also their size is small compared to the spacing of the sensor array. Thus, a sharp peak can be expected near the location of the inhomogeneity. On the other hand, *NED* values caused by a tunnel form a ridge in the *NED* curve which is much wider than that generated by a smaller void. Accordingly, we propose using a sub-array processing unit. The basic idea is to divide the original sensor array into a few sub-arrays. An example is illustrated in Figure 5.10.

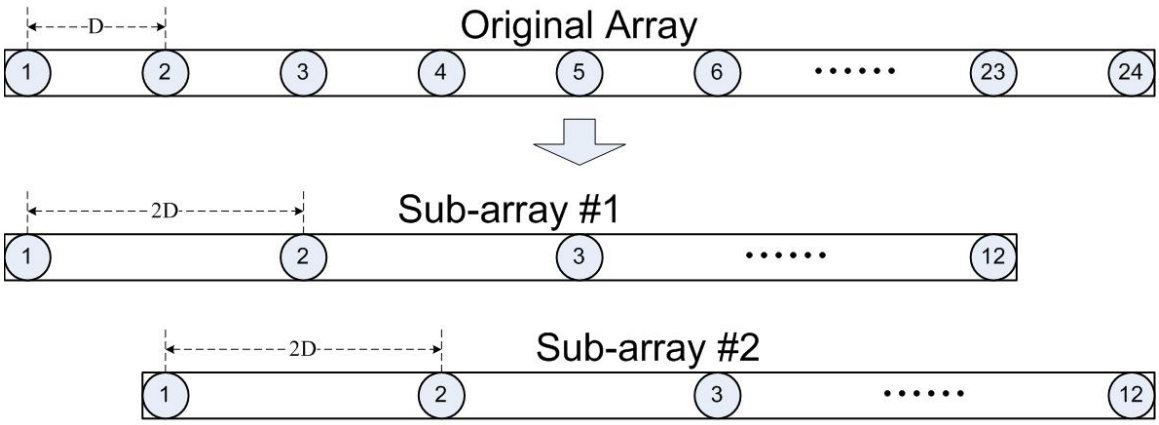

Figure 5.10: Schematic of Sub-Array Processing

In Figure 5.10, the 24 sensors in the original array are regrouped into two 12-element arrays. Sub-array 1 takes the odd-numbered sensors and sub-array 2 takes the even-numbered sensors,

without overlapping. The new arrays are spaced at 2*D* apart. Any sharp peak generated by the small voids can only appear in one sub-array. For example, if a sharp *NED* peak appears at geophone 5 in the original array, this peak will only exit at geophone 3 of sub-array 1. Meanwhile, if we do not find any peak at any geophone in sub-array 2 at nearby locations, we may consider it as a false peak or at least reduce the confidence level of this estimation. This process is illustrated as follows:

$$D_p = |p_1 - p_2|$$

where p_1 and p_2 represents locations of the two *NED* peaks in sub-array 1 and 2, respectively. The term D_p is the distance between these two peaks. A threshold ε is introduced to determine whether it is a valid detection:

$$\begin{cases} D_p < \varepsilon & \Rightarrow \text{ Valid detection} \\ D_p > \varepsilon & \Rightarrow \text{ Invalid detection} \end{cases}$$

This threshold must be carefully adjusted. A high threshold could cause some false alarms to be missed, and a low threshold could eliminate some correct estimations. Setting it equal to the width of a normal manmade tunnel is a good option. If a tunnel exists under the array, *NED* peaks forms a wide ridge and they can be detected on both sub-arrays at nearby locations. An example of valid detection is shown in Figure 5.11. In this figure, the solid line is the *NED* curve for the original array; the dashed line with circles represents the *NED* curve for sub-array 1; the other dashed line with pentagrams represents the *NED* curve for sub-array 2; the vertical dashed arrow shows that the tunnel is located under geophone 13; the estimated location is represented by the solid square, which is at geophone 12. In this case, the *NED* peaks on both sub-arrays are located close together.

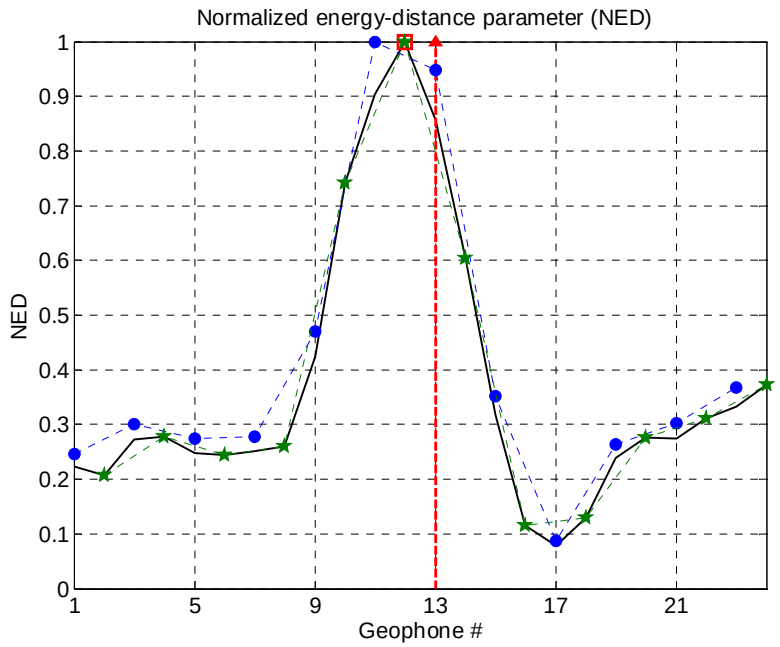

Figure 5.11: A Valid Detection

Figure 5.12 shows an example of an invalid detection. In this case, no tunnel exists under the array. However, the *NED* curve has a peak at geophone 6. After sub-array processing, one peak is found at geophone 17 (geophone 8 in sun-array 1), and the other is found at geophone 6 (geophone 3 in sub-array 2), respectively. Since distance between the two peaks, D_p, is much bigger than the threshold, the detection at geophone 6 is considered as a false alarm.

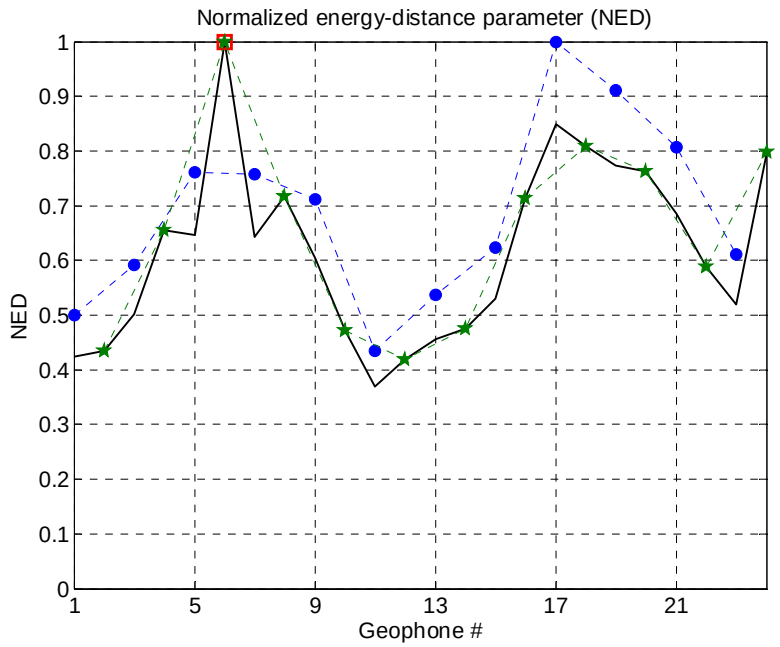

Figure 5.12: An Invalid Detection

Confidence Level. The survey procedure of the proposed method is conducted as follows (shown in Figure 5.13). Firstly, the detection system is placed in the area of interest, and a straight survey line with a few observation points across the area is selected. The distance between adjacent observation points, A, is set as an integral multiple of D. Then, the system moves forward along the survey line. At each point, the system is halted; the sensor array is attached to the ground; the impact source performs one shot and generates high-amplitude surface waves. The wave responses are recorded by the sensors. Then the data is processed instantly by the computer, and the *NED* values are calculated. After each shot the system moves to the next recording point until the entire area is inspected. At the completion of the survey line, the seismic data from all shots is analyzed. Normally, one survey line is sufficient. In some highly interested area, multiple survey lines can be performed, which could increase the accuracy even more.

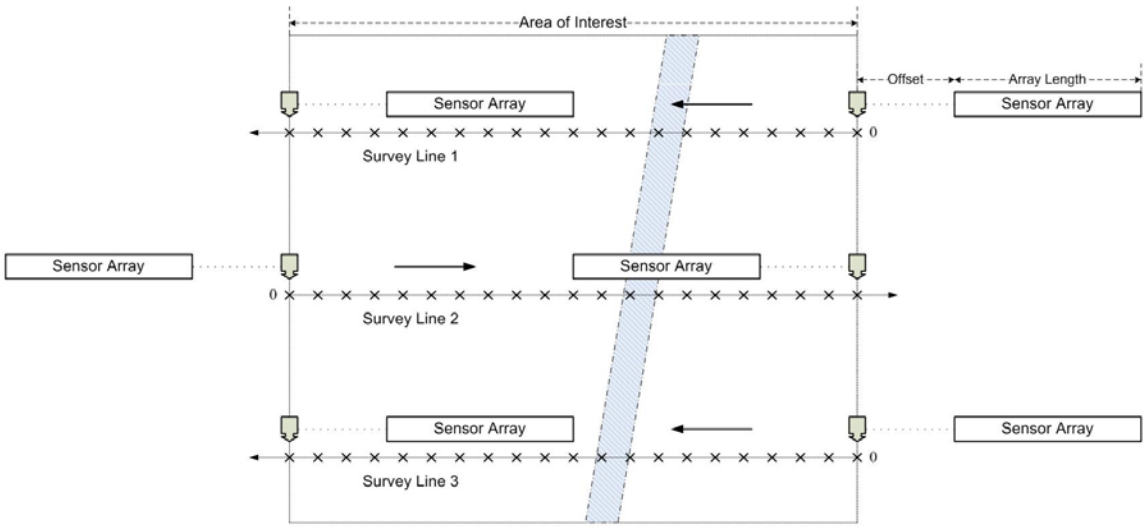

Figure 5.13: The Survey Procedure

The proposed method is a multi-channel and multi-shot method. Therefore, when the sensor array is passing over the tunnel, there are multiple chances to locate the tunnel. At each shot, a peak can be found in the *NED* curve, which is considered an estimation of the tunnel location. If the estimations are all correct, looking on the moving sensor array, each estimation is shifted by an array advance, A. If looking on the ground, however, the estimations do not vary. Therefore, by comparing the previous K estimations, a confidence level $\zeta(n)$ for the current estimation can be computed:

$$\zeta(n) = 1 - \frac{u(n) - v(n-1)}{L}$$

where $u(n)$ denotes the current estimation, and L represents the array length. The term $v(n\text{-}1)$ is the estimated tunnel location for the previous K shots. It can be calculated using:

$$v(n-1) = \frac{\sum_{k=1}^{K} u(n-k)}{K}$$

The confidence level $\zeta(n)$ ranges from 0 to 1. When $u(n)$ equals $v(n\text{-}1)$, $\zeta(n)$ equals 1. The biggest distance between $u(n)$ and $v(n\text{-}1)$ is the array length L. In this case, $\zeta(n)$ equals 0.

Clustering. As noted before, a sensor array with N elements can provide N opportunities to locate a tunnel. Thus when the array is over the tunnel, the confidence levels of those detections will be relatively higher than that of the other detections. A cluster of shots, which has the highest cumulative confidence levels, can be found using:

$$C(n) = \max_{n} \left\{ \sum_{k=0}^{N-K-1} \zeta(n+k) \right\}, \; n = 1, \cdots, M - (N - K - 1)$$

where $C(n)$ is the desired cluster and M is the total number of shots in the interested area. Normally, a cluster of N-K consecutive shots is considered, and most of the shots generate a correct estimation and have a high confidence level. Taking the average value of the estimated locations within the cluster generates an accurate result.

Experimental Results. In this section we present the results of experiments carried out to test the performance of the proposed method. The experiments were conducted using a specially designed tunnel detection system for the DMSU. The surface of the ground at the recording site was dry pavement. The survey was set-up such that the streamer array was oriented perpendicular to the known tunnel. The experimental setup parameters are shown in Table 5.1.

Data set	MST campus, Aug 15, 2008, reverse line
Length of the survey line	35.0 meters, 71 shots
Number of geophones, *N*	24
Geophone spacing, *D*	0.5 meter
Array length, *L*	11.5 meters
Distance between source and geophone 1	6.0 meters
Advancing, *A*	0.5 meter
Depth of the tunnel	1.0 meter
Sample rate, *fs*	1 ms (1000 Hz)
Record length	0.5 second (500 samples)
Reliable frequency range, *B*	0 Hz ~ 200 Hz
The factor of the gain function, α	2.3
Number of previous shots considered, *K*	8
The distance between the tunnel center and the first survey point	11.5 meters

Table 5.1: AARW Experimental Setup.

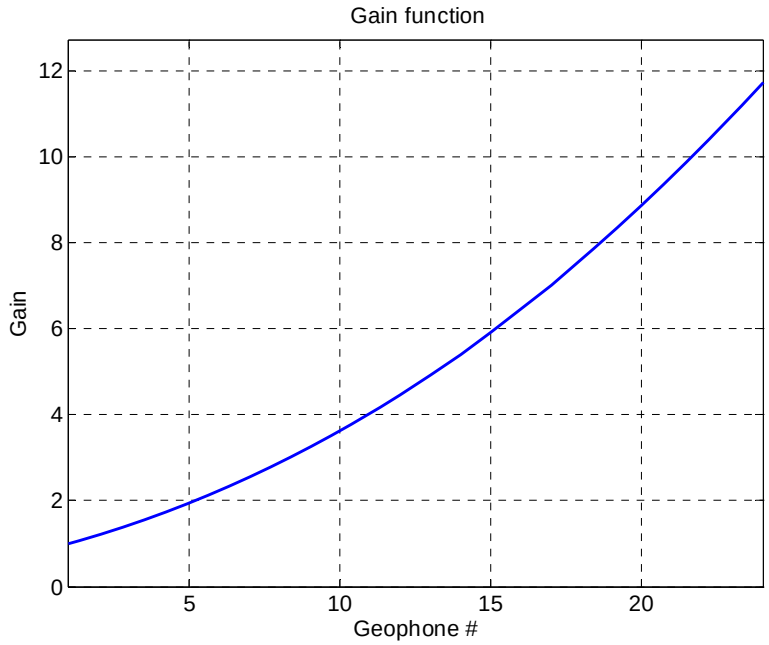

Figure 5.14: The Gain Function

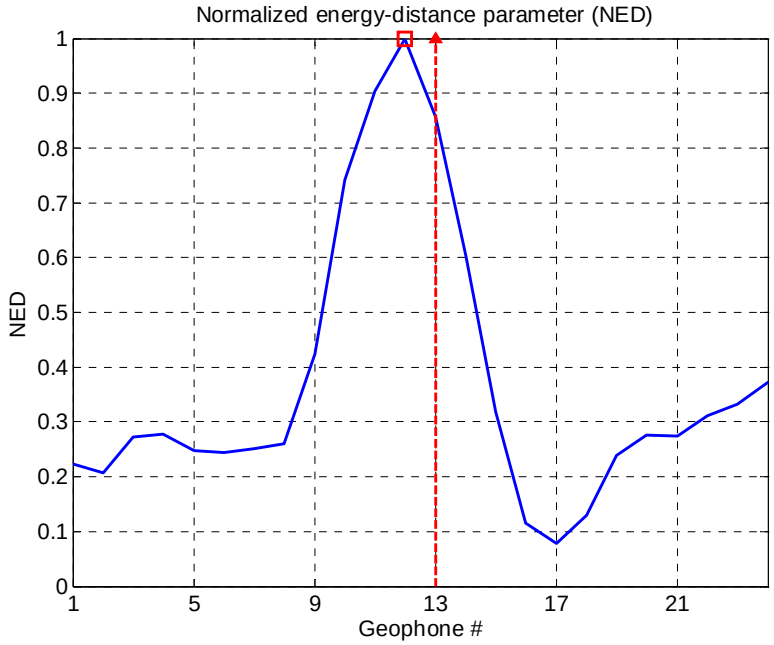

Figure 5.15: The NED Curve for One Given Shot

The *NED* values for all 71 shots are shown in Figure 5.16. In this figure, each of the 71 rows represents one shot and each of the 24 elements in a row denotes the *NED* value for that shot. In the 24 shots from #36 to #59 (the region between the two white dashed lines), the tunnel was within the range of the geophone array. The locations of the tunnel within this range are represented with 24 white pentagrams. Each of the 71 green circles in the figure shows the location of the *NED* peak in one shot. For example, in shot #50, the tunnel was right below geophone #15 and the *NED* peak appeared at geophone #13.

Within the range between shot #36 and shot #59, if the green circle is close to or overlaps the white pentagram in each row, a correct estimation of the tunnel location can be generated. In this case, 21 correct estimations were obtained. If the green circle is far away from the white pentagram, the estimation is incorrect. Beyond that range, any green circle is a possible false alarm. In this case, 47 false alarms and 3 incorrect estimations were found, which are circled by black dashed lines in Figure 5.16.

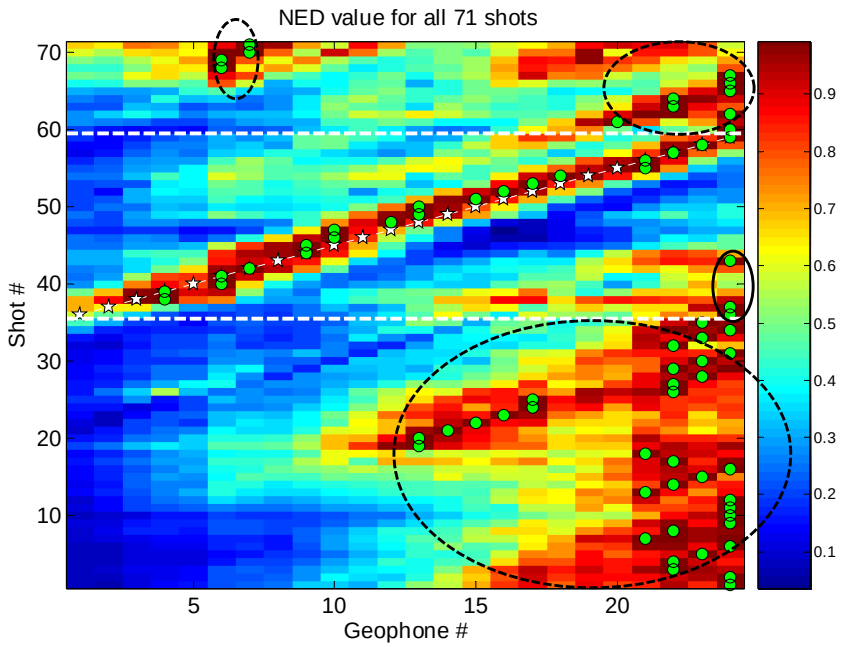

Figure 5.16: NED Curves for All Shots

The confidence level for each estimation was calculated, as shown in Figure 5.17. The recorded data was processed in sub-arrays. When the distance between the two *NED* peaks in the two sub-arrays is over 1.5 meters, the estimation was considered as a false alarm and removed. Then, the clustering unit scanned the rest of the estimations and found the cluster with the highest cumulative confidence level. Figure 5.18 shows that the cluster was between shot #43 and #58. There were 16 estimations within this cluster, and 15 of them were valid estimations.

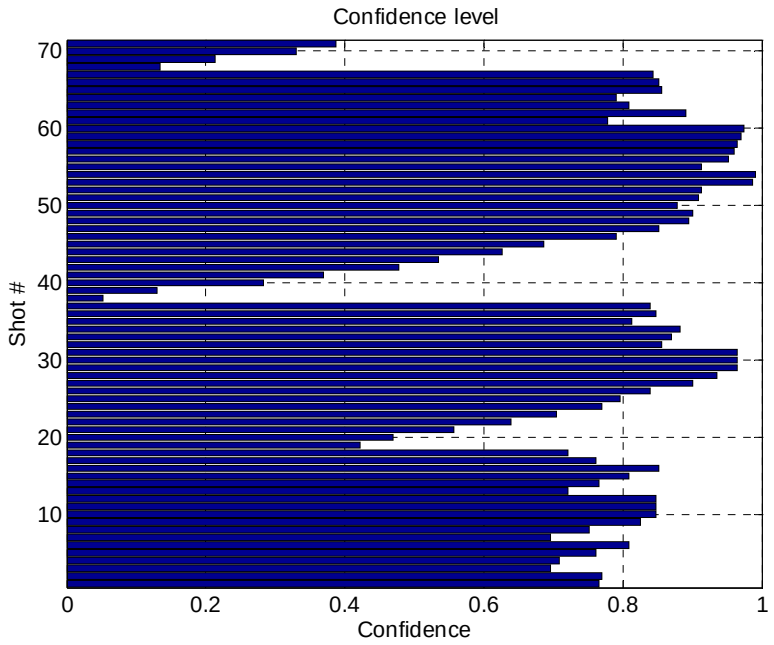

Figure 5.17: Confidence Levels for All Shots

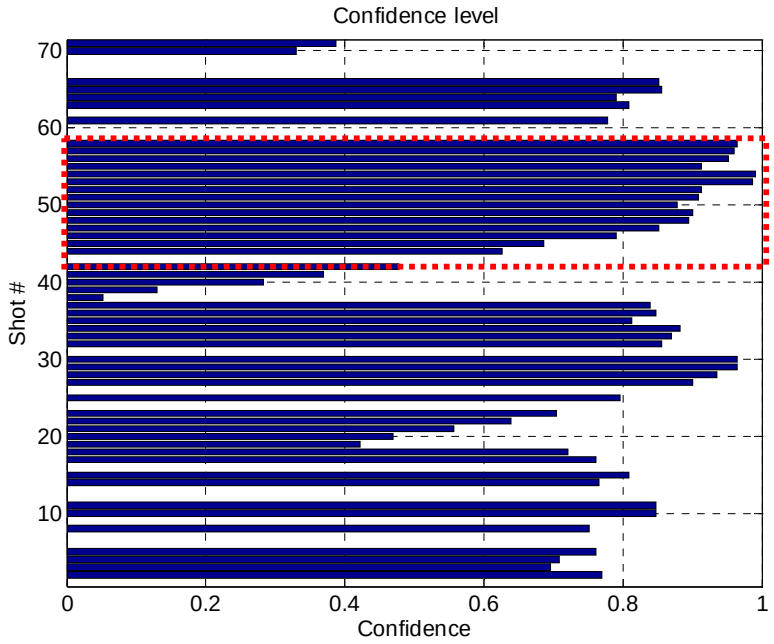

Figure 5.18: The Cluster of Shots with the Highest Cumulative Confidence Level

Figure 5.19 shows the 15 correct estimations within the cluster. Taking the average value of them provided the estimated location of the tunnel, which was 11.9 meters from the first survey point. Comparing with the actual distance, there was a 0.4 meters error. Since this method actually estimates the near boundary of the tunnel, this error is within a reasonable range.

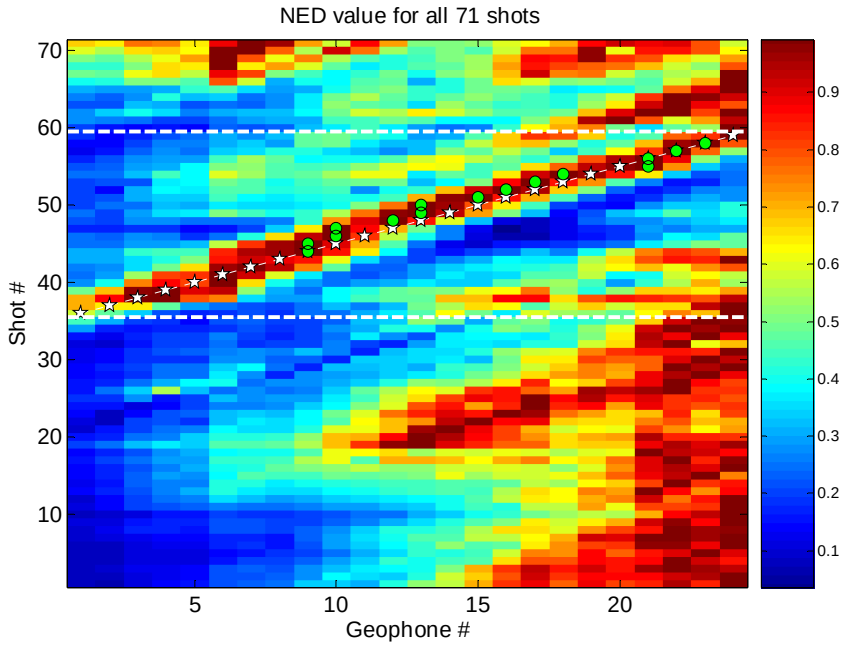

Figure 5.19: The Correct Detections

This approach is based on the well known AARW method and a proposed post-processing method. This post-processing method exploits array processing techniques and contains three steps. The first step processes the recorded data in sub-arrays, acting as a filter which removes some false alarms or incorrect estimations. The second step estimates the confidence level of each detection result. The last step scans all detections and searches the cluster with the highest cumulative confidence level. Experiments using real-world data demonstrate that this new approach significantly improves accuracy and reduces false alarms.

6. FIELD MEASUREMENTS AND COMPLEMENTARY TESTS

Field measurements of test site tunnel structure and the surrounding host material is the basis by which to compare accuracy of the DMSU software output. The caveat being that the software and subsequent operator interpretation show general agreement to the geospatial 'ground truth' of the tunnel(s) location and is not a false positive. The objectives of complementary geophysical tests were to provide a means to corroborate subsurface material properties where records or direct observation was not available.

6.1 Overview

Direct measurements were made by tape measure in metric units. A leveling rod was used to determine slope of the ground surface. USGS on-line Mapserver was used to determine the general latitudes and longitudes of the sites. Liner thickness & material properties were estimated by direct observation. Plugs from soil surfaces were logged from 5 to 8cm. Pavements were assumed to be underlain by compacted gravel. Boring logs were not available. Ground Penetrating Radar (GPR) was used as the complementary geophysical survey method for pavements and Electrical Resistivity method for soil. Additional control analysis (material to the left and right of the tunnel with no voids) was conducted using shear wave dispersion profiling.

Figure 6.1: Missouri S&T Graduate Students conducting geophysical tests; (a) GPR with a 400 Hz antenna was used on asphalt and concrete, and (b) electrical resistivity was used for soil as the respective complementary geophysical methods.

6.2 Direct Measurements

Asphalt and concrete pavements surfaces provide excellent coupling for both the impact source and the surface laid geophone receivers for the DMSU. Hence, seismic signals do not attenuate significantly due to surface conditions as do soils with undulating vegetated topography. Conversely, it is problematic to directly observe the stratigraphy directly below the surface of the pavement in urban environments where as build plans are not available. Therefore, we rely heavily on redundant non-destructive geophysical methods to more accurately characterize the subsurface.

For the pavement cases we have selected the Missouri University of Science & Technology Physics Building (Pavement) site as example to outline the methodology used to directly measure the tunnel.

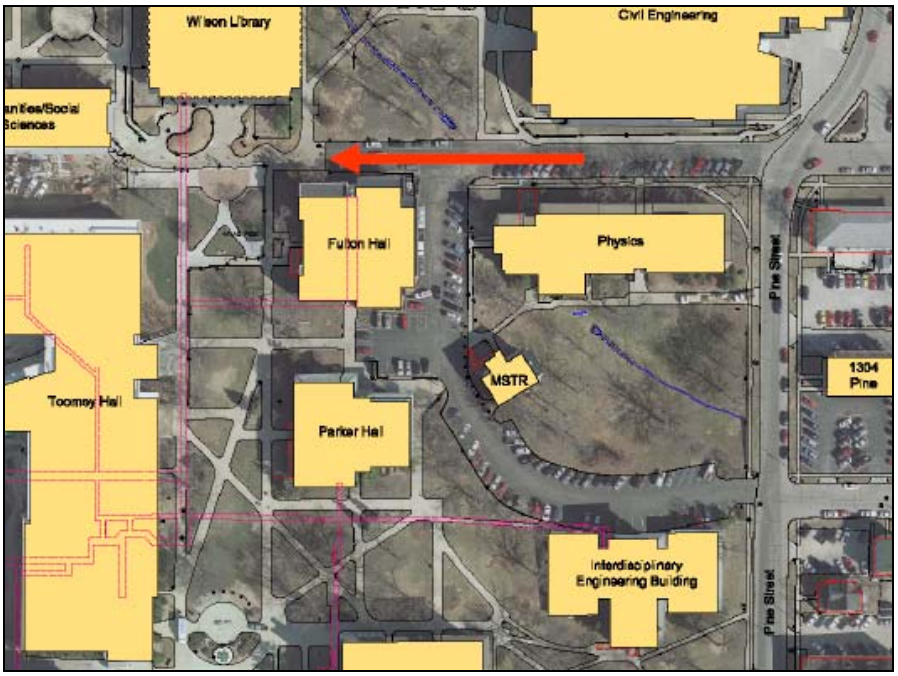

Figure 6.2: Plan view of 14th Street parallel to the Physics Building was the 2nd survey site. The approximate survey line is depicted as the red line (direction of advance from right to left). No boring log or construction drawings were available.

Figure 6.3: Measurements were conducted to within 1cm but were rounded to the 0.1m for simplicity. Here we see the measurements superposed on a picture of the concrete lined 'physics building tunnel' running underneath 14th Street.

Figure 6.4: Measurements taken from the northern embankment as the drainage tunnel submerged under the campus.

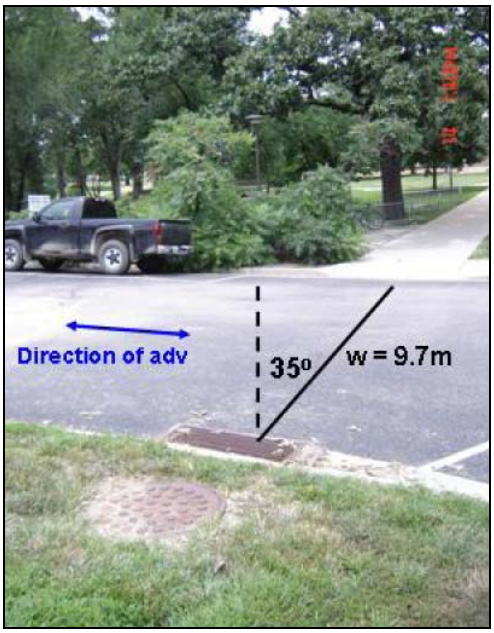

Figure 6.5: A tape dropped from the grate (lower part of the picture) confirmed that the embedment depth of the tunnel remained at a depth of 1.0m. Note a 35° deviation from the perpendicular DMSU survey line.

For soil cases we include direct examination of soil sample plugs to determine the depth of root systems as well as moisture content. In the case of the Ber Juan Park Spillway Tunnel, 'as build drawings were available to further estimate subsurface material properties.

Figure 6.6: University of Missouri Tech Park - Soil Field Test. (a) Roll & Thread Test was medium plastic soil with no odor and gritty taste; (b) embankment with a mix of fine gravel.

For example, soil samples were taken at a the approximate center point along both the control arrays at the University of Missouri Technical Park. The purpose was to determine the depth of anomalous organic or other materials not representative of the clayey fill. Soil plugs were taken to a depth of about 12cm and a diameter of 5cm. The grass and root systems were observed to be confined to the upper 3cm. The soil was described as 80% clay, 10% fines, and 10% cobbles respectively. Two cobbles measure between 3.5 and 4.5cm length, 3.5 and 2.5 width, and 1.5cm height. According to *Military Soils Engineering Field Manual 5-410*, a roll & Thread, Ribbon, and Taste test categorized the sample as medium plastic clay that could be rolled and did not crumble. The mixed soil sample had a slightly gritty taste and did not exhibit organic characteristics.

6.3 Complementary Geophysical Methods:

GPR. A GSSI 3000 Utilityscan GPR system with 400 Hz antenna was used to scan the asphalt / pavement and soils containing tunnels at the Physics Building, University of Missouri Technical Park (Pavement), and Bishop Street Tunnel sites. GPR utilizes a high frequency electromagnetic pulse to detect changes in dielectric constants evaluated for reflecting boundary depth and type of material. The dielectric constants in the subsurface change at boundaries where the electric properties alter such as encountering metal or a soil of different types. Using the GPR data and ReflexW software, an approximate velocity of 70 mm/ns was defined for the material below the pavement that is consistent with average soil parameters (Reynolds, 2000, p. 704). The interpretation of the GPR data corroborates the locations of the respective voids. Embedment depth and width were approximated directly from the profiles below (Figures 6.7 to 6.9).

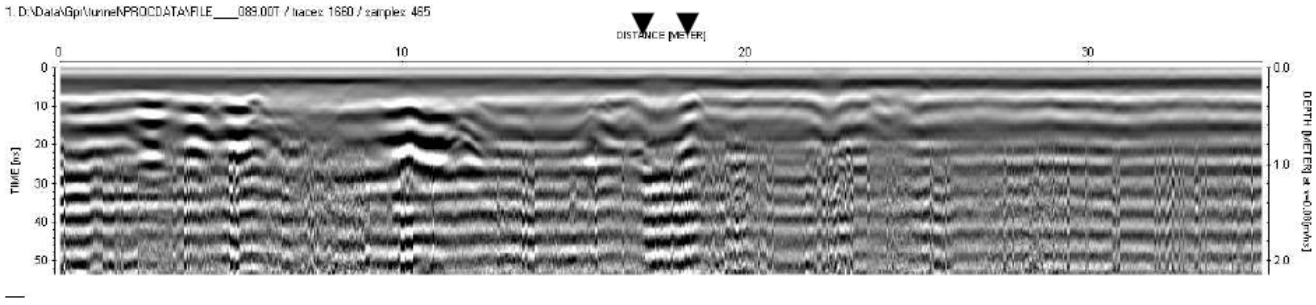

Figure 6.7: Physics Building asphalt road GPR survey where the triangles signify the edges of the box tunnel. The tape measured depth was 1m and the width at cos35^{o} was 0.73m (true void width at the angle perpendicular to the survey line).

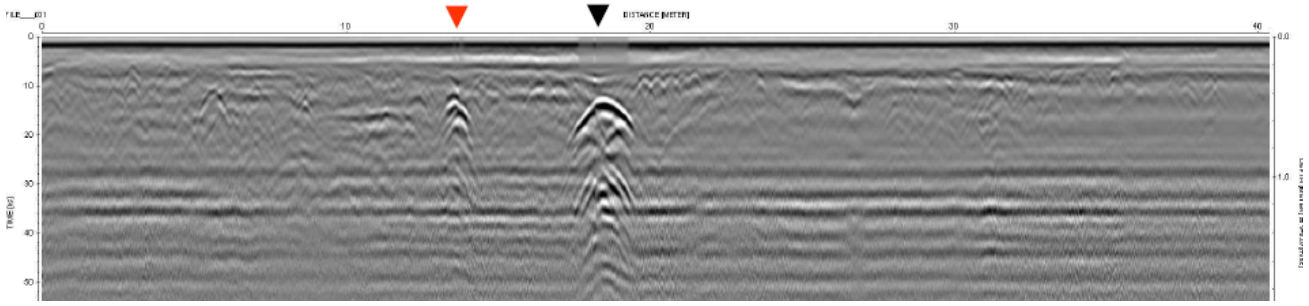

Figure 6.8: Tech Park concrete road GPR survey where the triangle corresponds to the center- line of the corrugated metal culvert. The tape measured depth was 0.42m. The red triangle appears to be a utility cable or pipe.

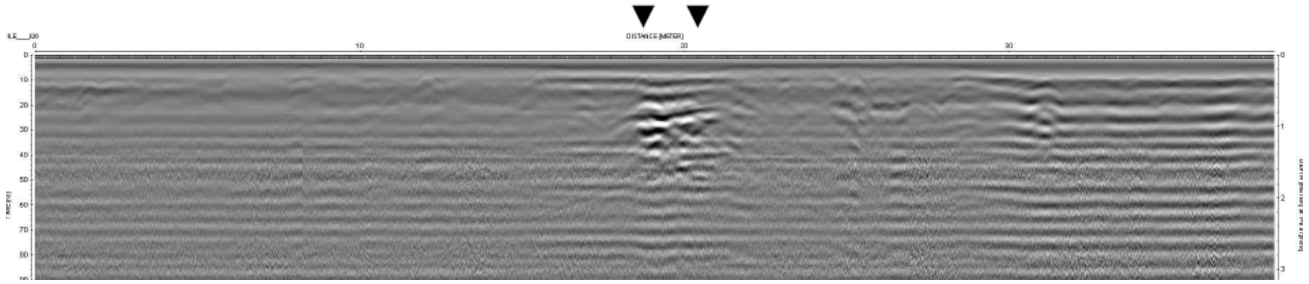

Figure 6.9: Bishop Street concrete sidewalk GPR survey where the two triangles signify the interpreted edges of the box tunnel. The tape measured depth was 1.23m and the width was 3.15m.

Resistivity. An AGI SuperSting automated resistivity system was used with to measure the resistivity of soils containing tunnels at Ber Juan, University of Missouri Technical Park (Soil), and Wilson Library sites. The measurements were taken using automated array scanning resistivity in Dipole Dipole configuration producing an inverted true-resistivity depth model. Electrodes were placed at 1m intervals respectively. The imaging pseudo-section perpendicular to the spillway tunnel in profile yields the existence of a resistive circular area assumed to be the void. Moreover, the cross-sections as a whole exhibits relative measure of homogeneity below the immediate thin capping surface. A nominal resistivity range of 15 to 20 Ωm is consistent with clayey and 30 to 50 Ωm of compacted fill (Reynolds, 2000 p. 442). The interpretation of the resistivity data corroborates the locations of the respective voids. Embedment depth and width were approximated directly from the profiles below (Figures 6.10 to 6.12).

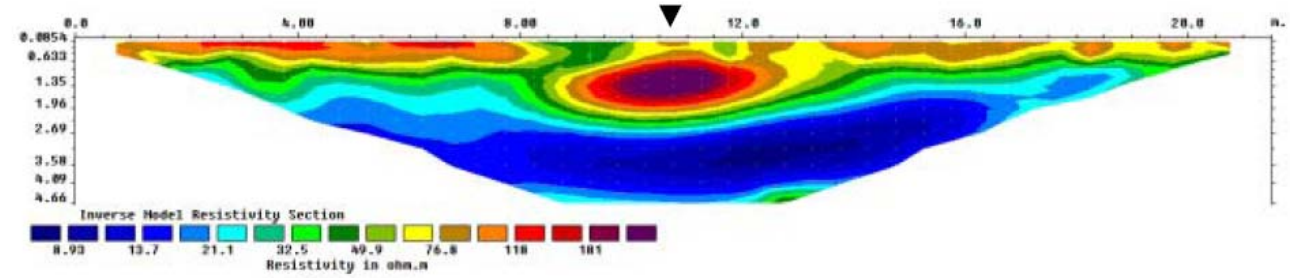

Figure 6.10: Ber Juan Park spillway tunnel electrical resistivity survey. City of Rolla - Ber Juan Dam Details and direct measurements were used as a basis to determine tunnel geometry and material properties.

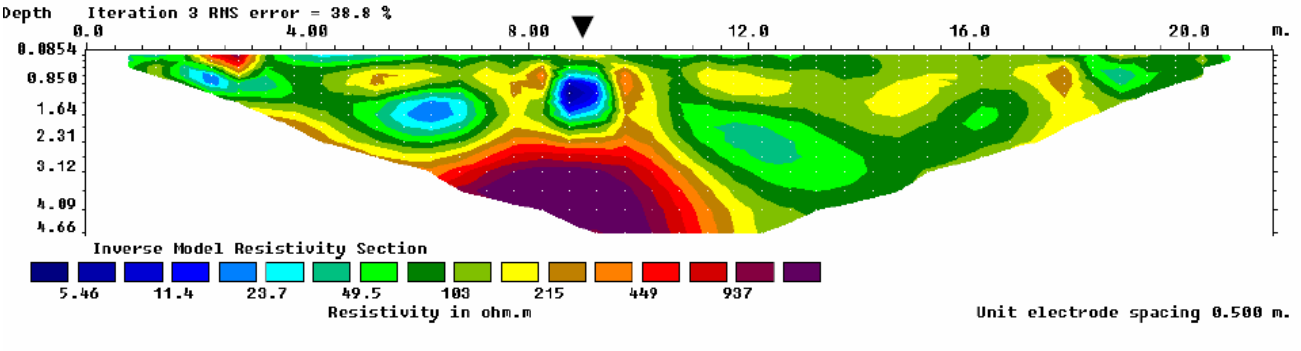

Figure 6.11: Tech Park Soil electrical resistivity survey. The downward arrow is the location of the center-line of the culvert on the surface. For this pseudo-section we have a low resistivity anomaly because of the corrugated metal culvert liner.

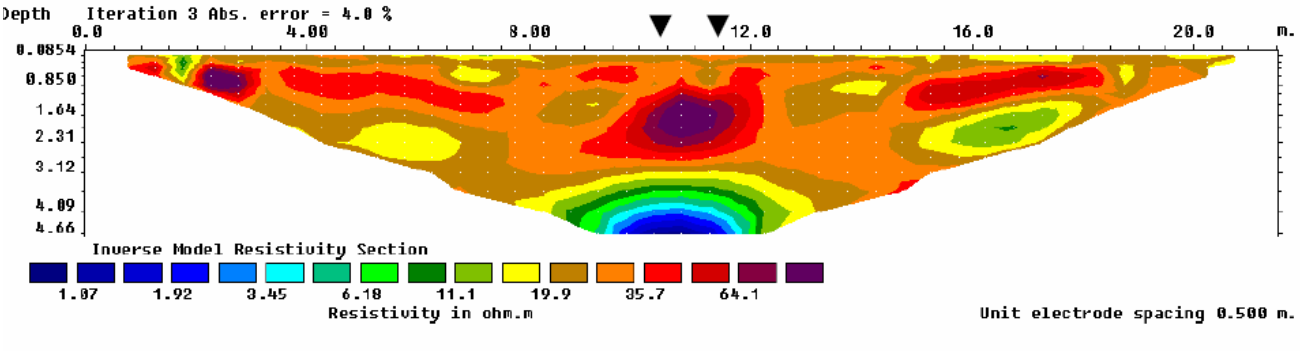

Figure 6.12: Wilson Library Utility Tunnel resistivity survey. The two downward arrows represent the approximate surface location of the two edges of the box tunnel.

6.4 Lithological Interpretation of Surface Wave Vertical Profiling

Seismic shear wave data can be used to construct a pseudo boring log. For example, a lithological interpretation using surface wave profiling was conducted on the Ber Juan Earthen Dam to ensure reasonable agreement to corresponding blue prints and field observations. The analysis is conducted on an area of the Dam where a tunnel of interest has a separation of at least 10m to any geophone. Therefore, we would not expect to see anomalous energy in what is otherwise a homogeneous clayey soil. The shear wave velocity (v_s) is approximated by dividing the P-wave velocity by 1.7 v_s. The approximated values for the given material properties are used to construct the pseudo boring log from the calculated shear wave velocities of the seismic survey.

Again, we can derive boring log shear wave velocities of geologic materials are from P-wave velocities from Reynolds, 1997. The approximate shear wave velocities of materials associated with the Earthen Dam are summarized below:

Material	Vp (m/s)	Vs (m/s)
Soil	100-500	59-294
Landfill	400-750	235-442
Clay	1000-2500	588-1470
Sandstone	1400-4500	824-2647
Limestone (Soft)	1700-4200	1000-2470

Table 6.1: Associated material velocities representative of Ber Juan Earthen Dam

Using the Ber Juan site, reading directly from profile blueprints provided by the City of Rolla, Missouri the (minimum) depth of the emplaced clayey fill is 3.9m corresponding to the seismic survey control lines (that contain no tunnel). Note that in the blueprint profile figure below the tunnel would be absent.

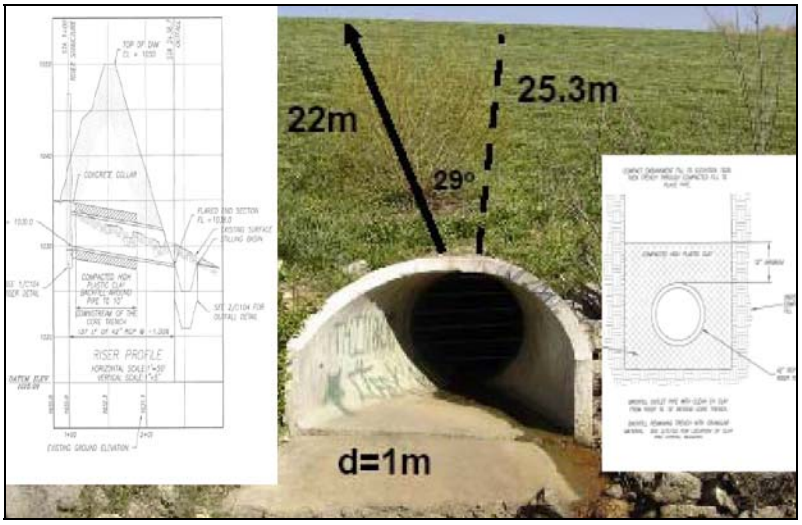

Figure 6.13: City of Rolla - Ber Juan Dam Blueprints and direct measurements were used as a bass to determine tunnel geometry and material properties. The Blueprint(s) were used to compare shear wave profile.

Shear Wave to Pseudo Boring Log. A Seismic survey was conducted over Ber Juan Earthen Dam approximately half way up the slope and on either side (left and right) of the spillway tunnel. This was a survey control measure used later as comparison for the survey taken in the vicinity of and over the spillway tunnel. The geometry was the same as used with obtaining tunnel data: 0.5m geophone spacing, 3m source to receiver offset. It is important to note that the profile was calculated for the control where a source as placed both on the left (3m) and the right (3m) of the first geophone in the event the profile was inconsistent. As example, tilted or sloping layers of different soil materials would manifest itself as change in velocity at different depths. In this case, no significant inconsistencies were noted on either the left or right vertical shear wave profiles.

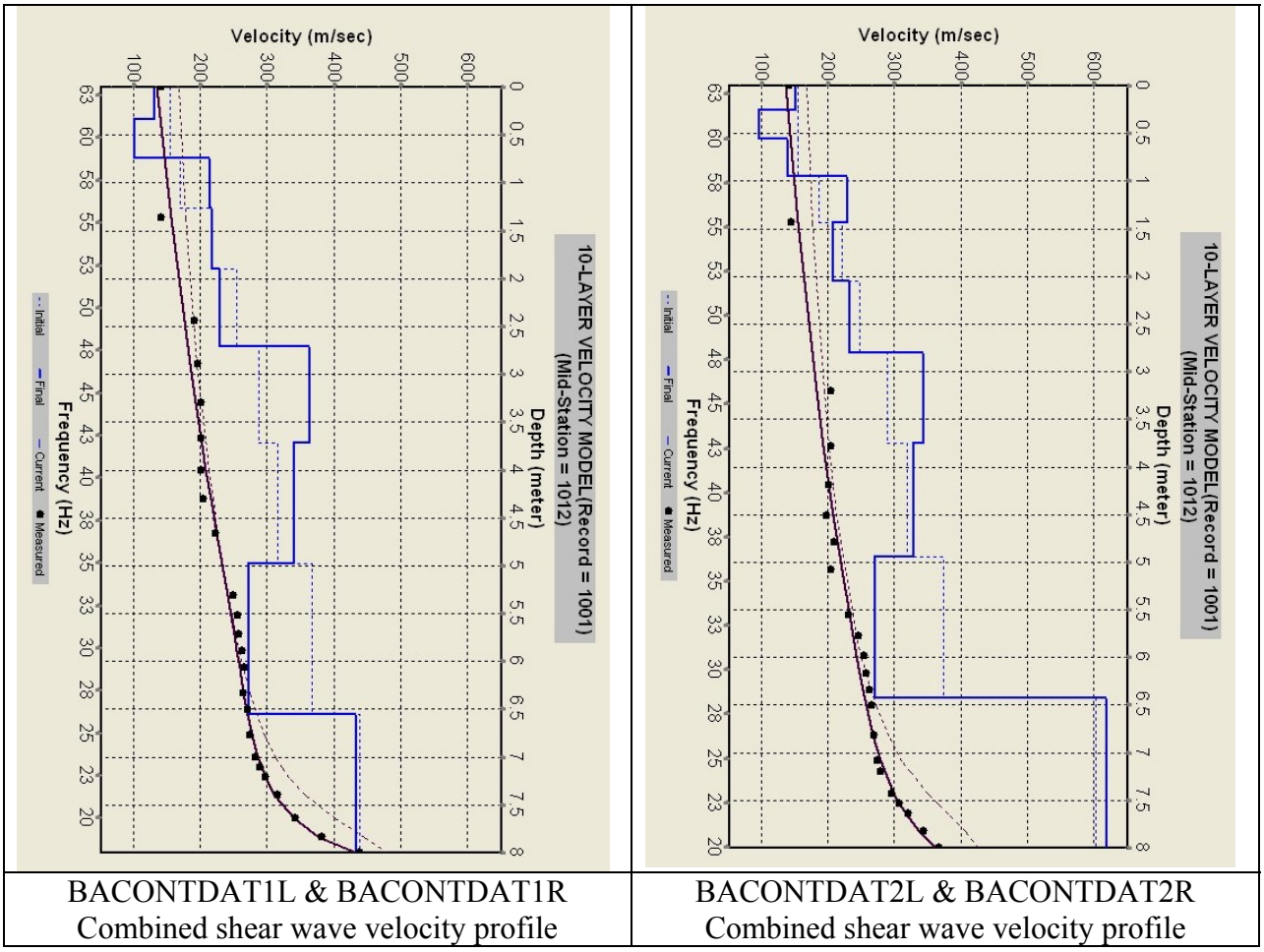

BACONTDAT1L & BACONTDAT1R Combined shear wave velocity profile	BACONTDAT2L & BACONTDAT2R Combined shear wave velocity profile

Figure 6.14: Vertical Seismic Shear Wave Profile from left and right survey lines respectively (Dr. Nasseri-Moghaddam, 2008).

The shear wave velocity profile (above) is transformed in tabular form to a pseudo boring log (depth versus shear wave velocity). The shear wave velocities are matched to observed / documented materials. The velocities were transcribed visually from the shear wave profile to the pseudo boring log (below.) For analysis, velocities were averaged over a segment based on grouping of similar velocities with the rationale explained at the conclusion of this work.

Depth (m)	Thickness (m)	Shear Wave Velocity (m/s)	Corresponding Material
0 - 0.75	0.75	150	Soil
0.75 - 2.25	1.5	225	Clayey Soil
2.25 - 5	2.75	340	Clayey Soil
5 - 6.5	1.5	275	Soil
6.5 - 8 left	1.5	425	Clayey Soil
6.5 - 8 right	1.5	610	Interbeded Soil with Limestone

Table 6.2: Pseudo boring log of Ber Juan Earthen Dam

Interpretation The shear wave velocity profile is consistent with blueprints and field observations to the depth of interest of 4 meters. The upper 0.75m may be associated with a cap of loamy clay used to support the growth of grasses covering the slope of the dam. The clayey soil or core of the dam was a minimum of 3.96m deep half way up the slope between the crest and the base. The rationale for average the associated 'final' velocities from the shear wave profile was due to 1) highly pristine clayey soil was transported into the job site and compacted in lifts according to Mr. Bryan Parker (the Professional Engineer who supervised the Dam's construction), and 2) loading of overlying clayey soil will contribute to increased compaction at greater depth. It appears that at a depth of 5m, local soil was used as a base course more indicative of a common soil or orthent. I interpret that at 6.5m we see the manifestation of the undisturbed base of which the left survey line is indicative of pediments from area of drainage and the right survey line inter-bedded soil and limestone. This interpretation was made based on air photograph before construction of the dam. The shear wave seismic profile is consistent with the blueprints, field observations, and common construction practices.

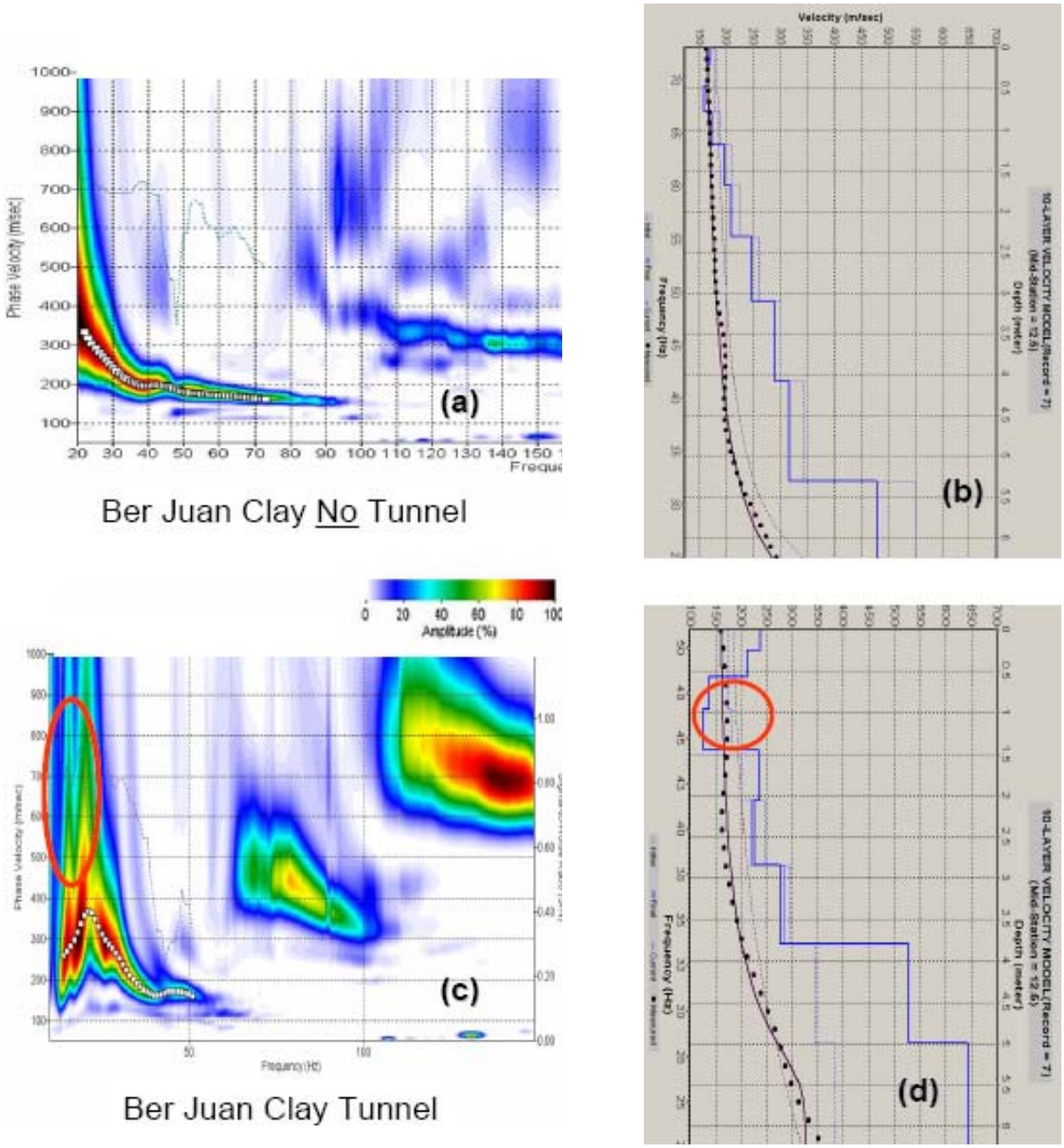

Figure 6.15: Dispersion images and inverted models of Ber Juan surface-wave line after the preliminary analysis. (a) Top Left dispersion image of control, although the frequency begins at 20Hz, there is an inferred coherent slope increasing at lower frequencies toward higher velocities; (b) steady increasing velocity at depth; (c) the dispersion image containing the tunnel shows lack of coherent energy compared to the control; (d) decrease of velocity using the surface wave inversion model typical to abandoned mine and sinkhole features (O'Neill, 2008).

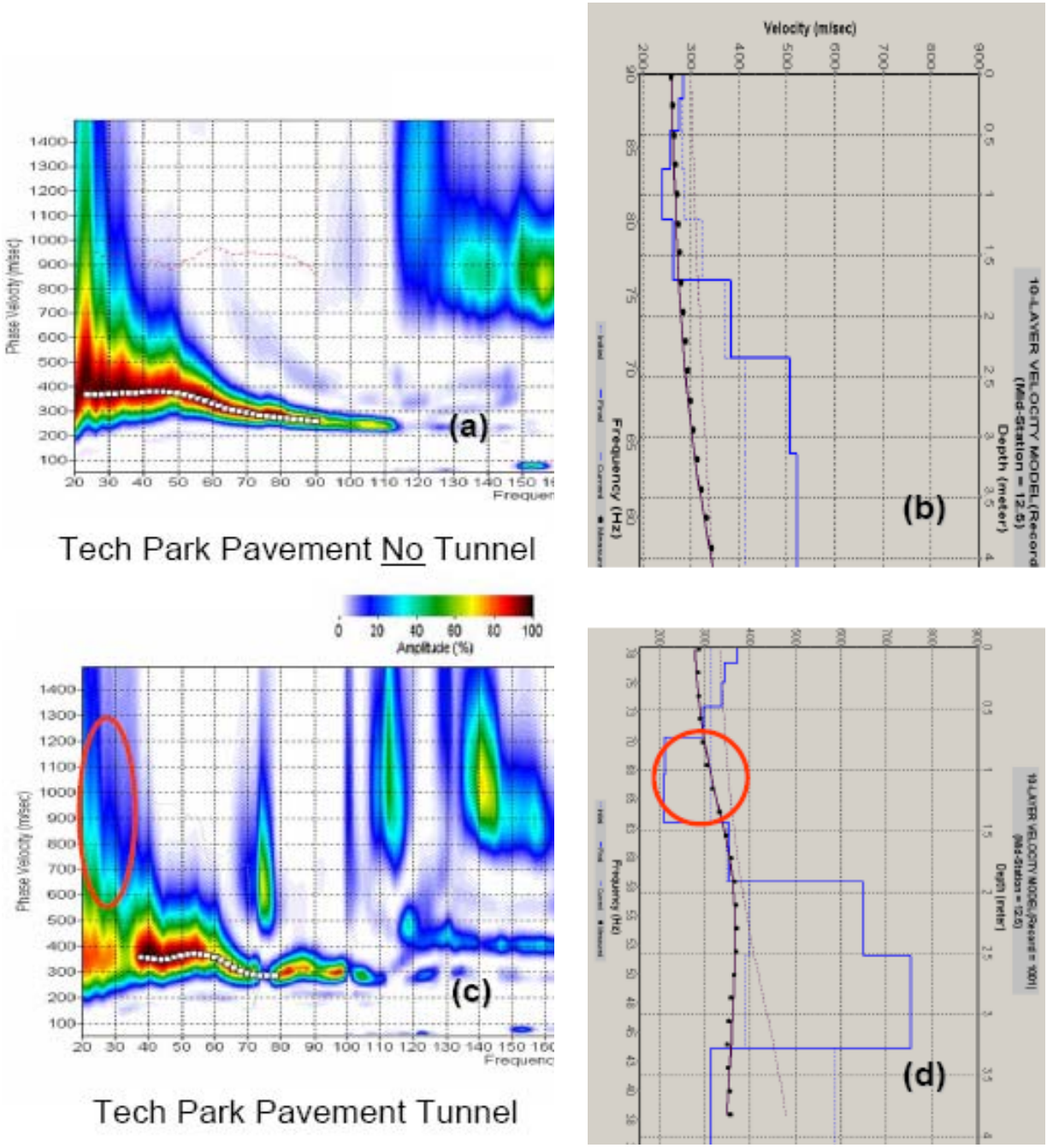

Figure 6.16: Dispersion images and inverted models of Tech Park surface-wave line. (a) Top left dispersion image of control; (b) steady increasing velocity at depth; (c) the dispersion image containing the tunnel shows lack of coherent energy compared to the control; (d) decrease of velocity using the surface wave inversion. The pavement cases have a more pronounced break in coherent energy over a tunnel as compared to soils.

6.5 Tabularized Site Measurements Summary

SITE SUMMARY	
Date of Survey	**June 2008**
Location	**Ber Juan Park (Clay), Spillway Tunnel, Longitude -91° 45' 26" W Latitude 37° 57' 07" N**
Field crew	**Site Forman / DMSU Driver: Evginey Torgashov** **Software Operator: Pretam Modur; Safety: Nik Putnam**
Tunnel Tape Measurements	**Embedment Depth: 0.90m** **Dimensions: 0.96m diameter**
Tunnel Liner	**Circular Concrete Liner 0.05m thick**
Tunnel Orientation	**Perpendicular to array. DMSU at 8% Grade causing streamer to slide on grass. Pickets were used to guide streamer along survey line.**
Topography & Streamer Drift Error	**Grass causing some coupling attenuation.**
Site Conditions / Weather	**Soil was moist but not wet. Grass wet in early morning.**
Lithology	**CAP: Visual; Grass & Loam; Alt. 100 Ωm** **HOST: Blueprints; Clay; Alt. 30 Ωm**
Structures or Buried Utilities	**None**
Source Configuration	**Rubberized Foot**
Line Length	**23.5m**
Background Noise	**Moderate Traffic, took shots between semi-tucks.**
Notification Requirements	**Permission by City of Rolla Parks Department**
Portal Picture	

SITE SUMMARY	
Date of Survey	**September 2008**
Location	**Adjacent to the Physics Building on 14th (asphalt pavement) Street; Longitude - 91° 46' 25" W Latitude 37° 57' 19" N**
Field crew	**Site Forman / DMSU Driver: Evginey Torgashov** **Software Operator: Pretam Modur; Safety: Nik Putnam**
Tunnel Tape Measurements	**Embedment Depth: 1.00m** **Dimensions: 0.80m height x 0.73m width**
Tunnel Liner	**0.2m**
Tunnel Orientation	**55° angle from survey line**
Topography & Streamer Drift Error	**3% slope downhill to south east causing drift 0.5m from marked center-line.**
Site Conditions / Weather	**Dry**
Lithology	**CAP: Visual; Pavement** **HOST: Assume Compact Gravel Layer & Mixed; Alt. V=70 mm/ns**
Structures or Buried Utilities	**Not Apparent**
Source Configuration	**Rubberized Foot**
Line Length	**40.5m**
Background Noise	**Waited for Traffic**
Notification Requirements	**University Police**
Portal Picture	

SITE SUMMARY	
Date of Survey	October 2008
Location	Technical Park (Mixed Soil) south side of the office building; Longitude -92° 06' 25" W Latitude 37° 45' 37" N
Field crew	Site Forman / DMSU Driver: Evginey Torgashov Software Operator: Colin Stagner; Safety: Nik Putnam
Tunnel Tape Measurements	Embedment Depth: 0.30m Dimensions: 0.60m diameter
Tunnel Liner	Corrugated Metal
Tunnel Orientation	Perpendicular to survey line
Topography & Streamer Drift Error	Sloping terrace (not perfect straight survey line) causing 0.5m drift from marked center-line
Site Conditions / Weather	Dry
Lithology	CAP: Visual; Grass & Hard Loam; Alt. 50 Ωm HOST: Embankment; Mixed Soil; Alt. 20 - 200 Ωm
Structures or Buried Utilities	Sidewalk 5 meters North; Drainage tunnel 25 meters south
Source Configuration	Plate and Hammer Head
Line Length	29.5m (Constrained by Building, last geophone 3m past center-line)
Background Noise	Lawn Mower, Waited until finished
Notification Requirements	Alternate to CBRN / MOUT Facility. Permission by LWI.
Portal Picture	

SITE SUMMARY	
Date of Survey	October 2008
Location	Technical Park (Pavement) west side of the office building; Longitude -92° 06' 26" W Latitude 37° 45' 38" N
Field crew	Site Forman / DMSU Driver: Evginey Torgashov Software Operator: Pretam Modur; Safety: Nik Putnam
Tunnel Tape Measurements	Embedment Depth: 0.43m Dimensions: 0.84m ovate diameter (maximum side to side)
Tunnel Liner	Corrugated Metal
Tunnel Orientation	Perpendicular to survey line
Topography & Streamer Drift Error	None observed
Site Conditions / Weather	Dry
Lithology	CAP: Visual; Pavement HOST: Assume Compact Gravel Layer & Mixed; Alt. V=70 mm/ns
Structures or Buried Utilities	Utility cable or pipe 10 meters north
Source Configuration	Plate and Hammer Head
Line Length	29.5m (Constrained by Building, last geophone 3m past center-line)
Background Noise	Waited for Traffic
Notification Requirements	Alternate to CBRN / MOUT Facility. Permission by LWI.
Portal Picture	

SITE SUMMARY	
Date of Survey	**November 2008**
Location	**Utility Tunnel (Mixed Soil) below the University Quadrangle; Longitude -91° 45' 25" W Latitude 37° 57' 16" N**
Field crew	**Site Forman / DMSU Driver: Evginey Torgashov** **Software Operator: Pretam Modur; Safety: Oleg Kovin**
Tunnel Tape Measurements	**Embedment Depth: 1.00m** **Dimensions: 1.93m height x 1.20m width**
Tunnel Liner	**0.15m**
Tunnel Orientation	**Perpendicular to survey line**
Topography & Streamer Drift Error	**None observed**
Site Conditions / Weather	**Dry**
Lithology	**CAP: Visual; Grass & Loam; Alt. 50 Ωm** **HOST: Unknown; Assumed Mixed Soil; Alt. 20 - 50 Ωm**
Structures or Buried Utilities	**Sidewalks 20 meters North and South**
Source Configuration	**Plate and Hammer Head**
Line Length	**26.5m (Constrained by sidewalk, last geophone 3m past center-line)**
Background Noise	**None**
Notification Requirements	**University Police**
Portal Picture	

SITE SUMMARY	
Date of Survey	**November 2008**
Location	**Bishop Street Student Access Tunnel (Pavement) near McNutt Hall Longitude - 91° 46' 37" W Latitude 37° 57' 19" N**
Field crew	**Site Forman / DMSU Driver: Evginey Torgashov** **Software Operator / Safety: Nik Putnam**
Tunnel Tape Measurements	**Embedment Depth: 1.23m** **Dimensions: 2.80m height x 3.15m width**
Tunnel Liner	**0.1m**
Tunnel Orientation	**Perpendicular to survey line**
Topography & Streamer Drift Error	**3% grade to North in parallel with survey line, No drift observed**
Site Conditions / Weather	**Dry**
Lithology	**CAP: Visual; Pavement** **HOST: Assume Compact Gravel Layer & Mixed; Alt. V=70 mm/ns**
Structures or Buried Utilities	**Unknown.**
Source Configuration	**Rubberized Foot**
Line Length	**36.0m**
Background Noise	**Moderate Traffic, took shots between semi-tucks.**
Notification Requirements	**University Police**
Portal Picture	

7. DEMONSTRATION MOBILE SEISMIC UNIT (DMSU) TESTS

7.1 Overview

The set-up and operation of the DMSU to include software instructions is presented in Appendix A: DMSU Operations Manual of this report. Although the DMSU is automated, it is recommended field notes be used to document observations and discrepancies. As standing procedure for the DMSU, the forward advance of the unit was 0.5m per shot or station. The DigiRoller PlusII was used by the driver to approximate the advance. However, the ATV was not always accurate in moving the precise 0.5m interval: Any deviations in the advance were noted and compensated for. In addition, current software catalogues seismic records in positive sequence. Therefore, when reverse survey lines are taken, the software interpreter must orient geophone numbers in reverse on the GUI for SWCO. This is important for visual interpretation of SWCO due to the reflected energy 'pull-up' phenomenon on the near side. That is to say, the 'pull-up' (reflected wave) followed by Attenuation (flat wavelets that follow) appears more pronounced approaching the void than after passing the void with the DMSU. The common shot gather is used primarily for quality control to ensure the geophones are functioning properly.

Configuration times for the DMSU are on the order of one hour using a two person crew. After the DMSU is configured and the systems are functioning properly (e.g. GPS, Camera, test shots), the software operator uses the DMSU GUI (Figure 7.1) to collect each shot along the survey line. It is the responsibility of the driver to ensure the ATV is advanced a the proper interval and operates the seismic impact source from the cable extension. Before accepting a shot, the operator typically ensures that the common shot (upper inset) is acceptable. Acceptability criteria are outlined in the Appendix A: DMSU Operations Manual. It is noteworthy that Figure 7.1 shows a second seismic pulse due to the source pushing up the trailer chassis of the ground. This was remedied by weighing the trailer chassis with sandbags.

In order to simulate the capability of the software to be understood by lay persons, a non-geotechnical person was selected to operate the 2D mapping tool and interpret the results of the respective field tests (Figure 7.3). The anomalies identified by the software was plotted into a 2D Mapping Tool at the end of a given survey line. The operator adjusted the confidence level slider until several clusters of high-confidence anomalies are visible, ordered these clusters from strongest to weakest, and designate probable tunnel locations. The survey team can then mark the locations to the corresponding point on the survey line in the field for further investigation.

The survey lines were set-up consistently with a metric drop tape where 0m was directly over the center-line of the tunnel. Given any direction of advance, the DMSU would start at a minimum distance of -9m between the first geophone and the center-line of the tunnel. Using this system, if the software anomaly corresponded to +1m then the error is 1m past the center-line of the tunnel. Typically, the reverse survey line (of the pair used in the SOP) was used as the team established a rhythm more realistic of a practiced field crew. Optimally, a crew can survey 500 liner meters per day at a forward advance of 1m per shot.

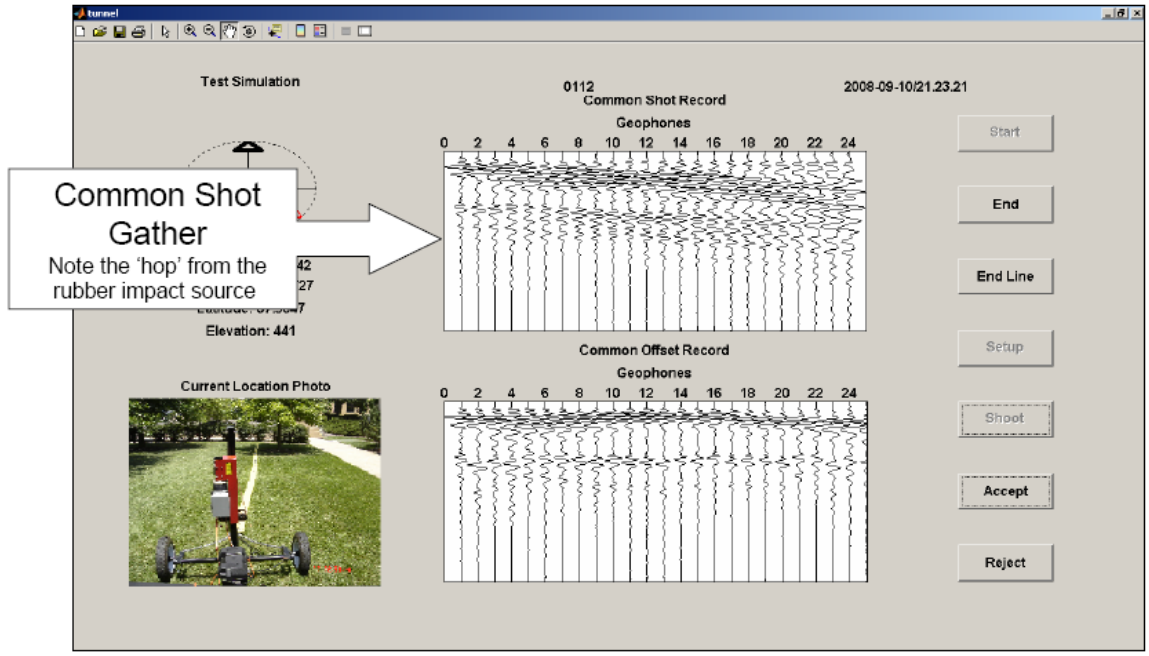

Figure 7.1: A screen capture of the Graphic User Interface (GUI) of the DMSU depicted above. The GUI is used by the software operator to accept or reject the seismic shot before advancing to the next shot location.

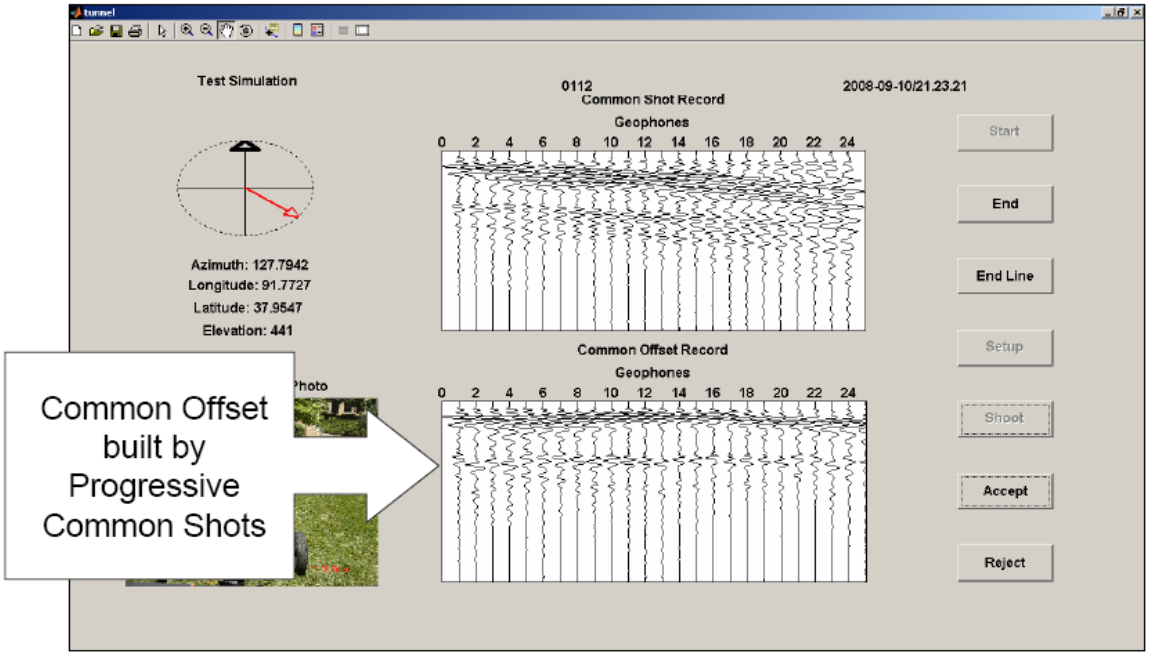

Figure 7.2: Surface Wave Common Off-set Graphic is constructed by adding a trace from each consecutive shot. This screen will be blank at the beginning of a survey line.

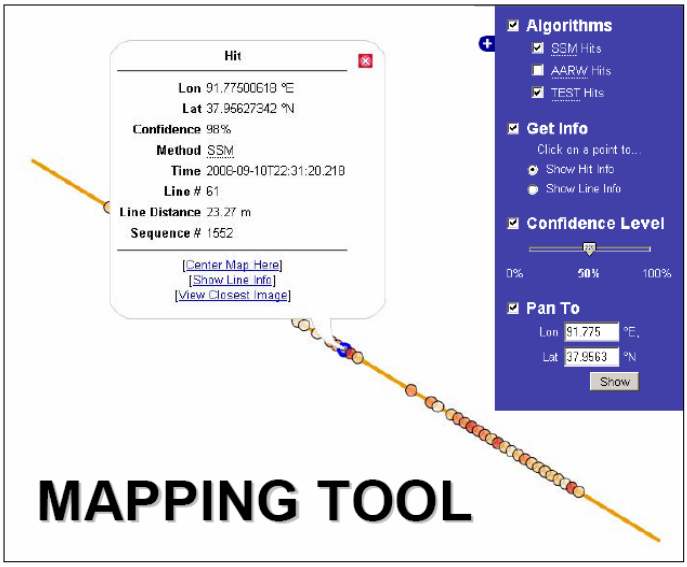

Figure 7.3: The 2D Plan View Mapping Tool depicts one interpreted location of the void among a number of anomaly detections along the streamer. The confidence level bar on the right can be used to reduce anomalies with less statistical strength.

7.2 Ber Juan Park (Clay)

The Ber Juan Park spillway tunnel was used extensively as the test site to configure DMSU hardware and validate software / algorithm capabilities in nearly pristine conditions for a realistically achievable tunnel detection depth. Given performance time constraints, the DMSU Team opted to test the system in other environments in lieu of dwelling on perfecting the output from Ber Juan Park. Therefore, the Ber Juan seismic data and interpretation is presented herein alternatively to the finalized standing operating procedure used for the DMSU as a norm. By September 2008, the system was deemed finalized and acceptable to perform tests on the Campus of MS&T and Fort Leonard Wood, Missouri.

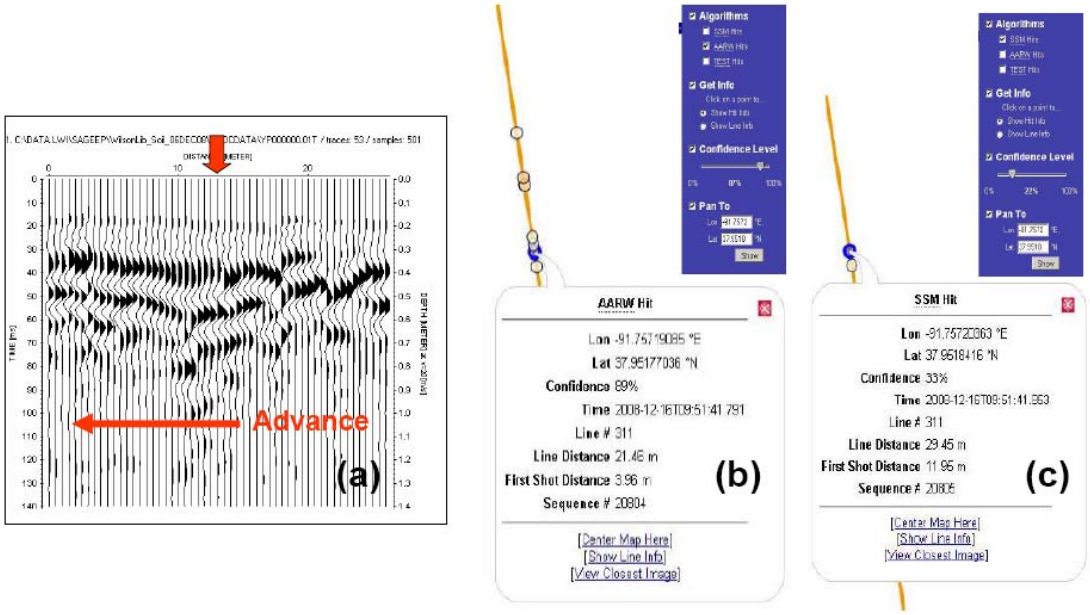

Figure 7.4: (a) SWCO with red arrow over the field measured center-line of tunnel; Note the direction of advance, (b) AARW anomaly pick located 3.96m from the seismic source first shot; (c) SF pick at 11.95m.

7.3 MS&T Physics Building (Pavement)

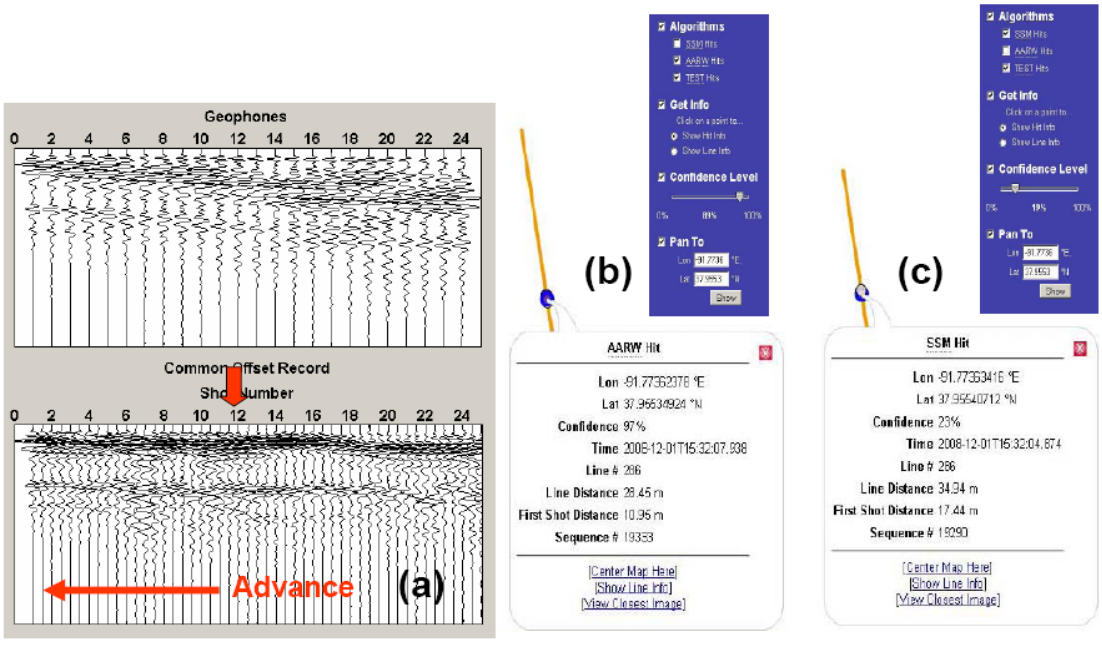

Figure 7.5: (a) SWCO with red arrow over the field measured center-line of tunnel, (b) AARW anomaly pick located 10.95m from the seismic source first shot; (c) SF pick at 17.44m.

7.4 University of Missouri Technical Park (Soil)

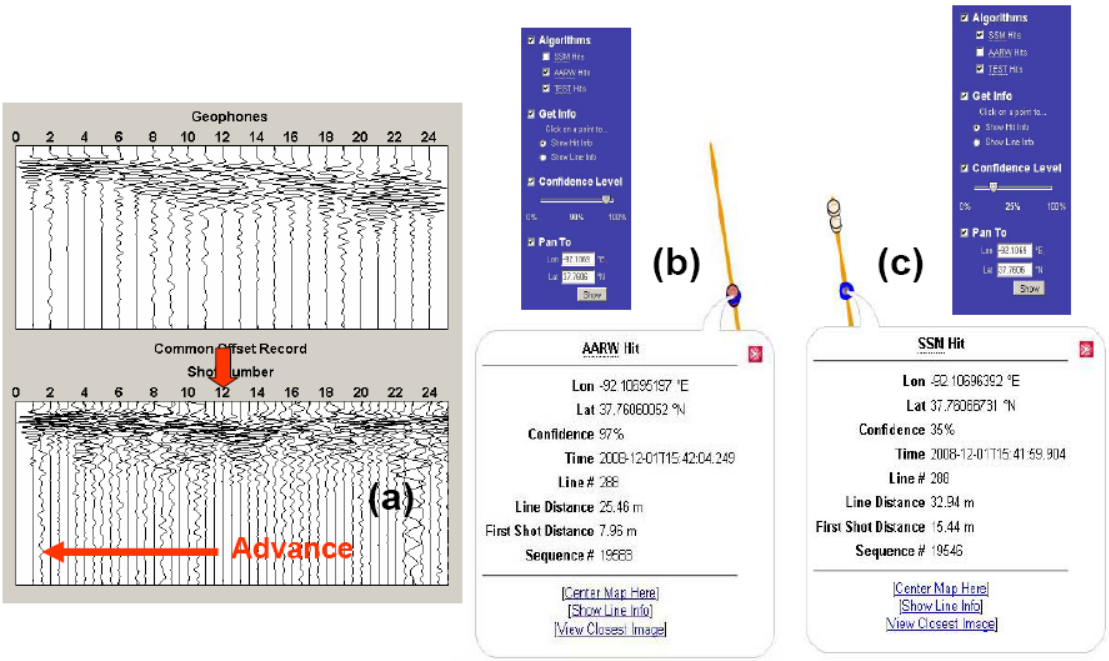

Figure 7.6: (a) SWCO with red arrow over the center-line of tunnel, (b) AARW anomaly pick located 7.96m from the seismic source first shot; (c) SF pick at 15.44m.

7.5 University of Missouri Technical Park (Pavement)

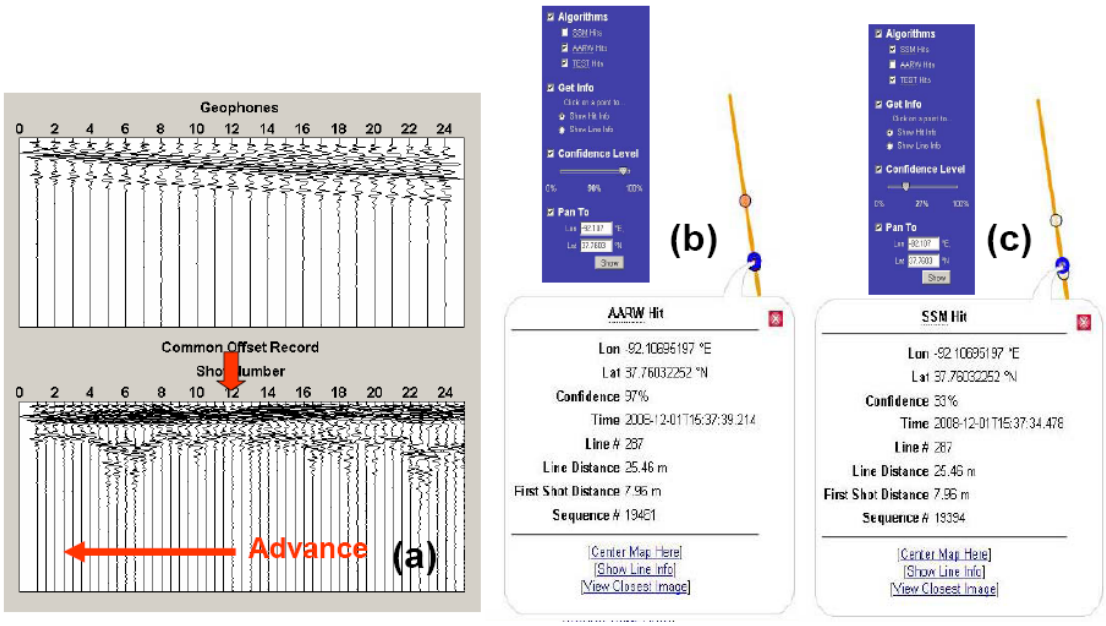

Figure 7.7: (a) SWCO with red arrow over the center-line of tunnel, (b) AARW anomaly pick located 7.96m from the seismic source first shot; (c) SF pick at 7.96m.

7.6 Missouri S&T Bishop Street Student Tunnel (Pavement)

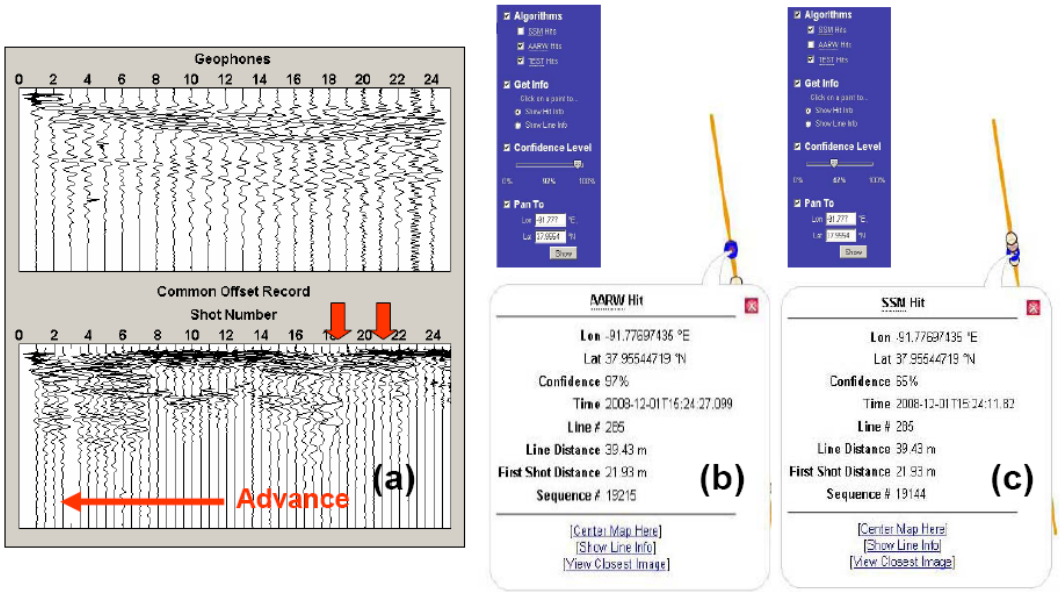

Figure 7.8: (a) SWCO with red arrow over the center-line of tunnel, (b) AARW anomaly pick located 21.93m from the seismic source first shot; (c) SF pick at 21.93m.

7.7 Missouri S&T Wilson Library Utility Tunnel (Soil)

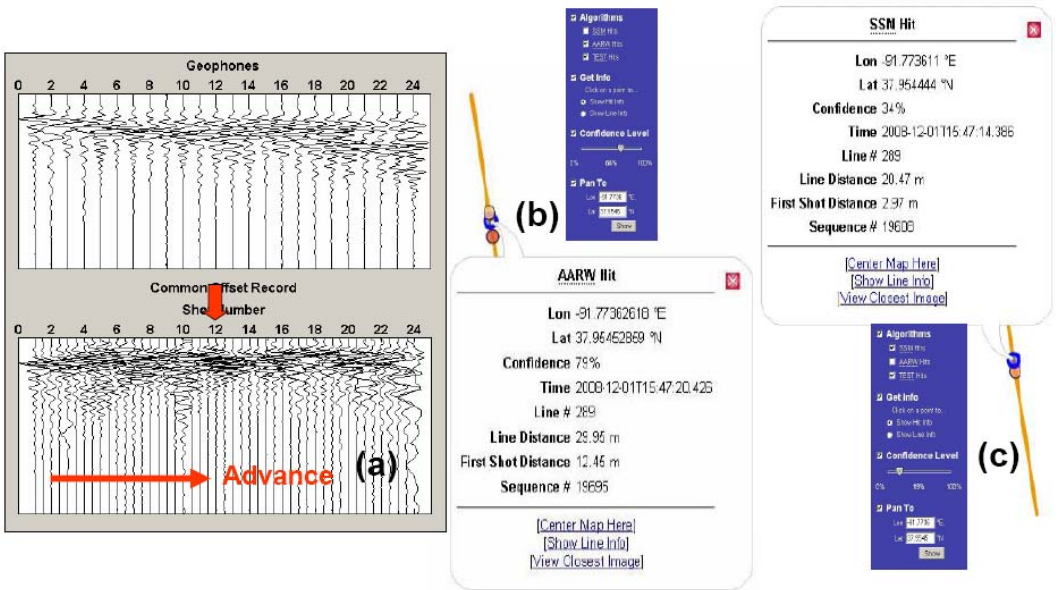

Figure 7.9: (a) SWCO with red arrow over the center-line of tunnel, (b) AARW anomaly pick located 12.45m from the seismic source first shot; (c) SF pick at 2.97m.

7.8 Global Positioning System (GPS) and Straight Line Error

The Trimble GPS Pathfinder ProXT was used to for geospatial positioning at the start and end points of the survey lines. This GPS system appears not to provide a dependable azimuth or accurate enough for DMSU purposes. The MATLAB GPS drivers also have some technical deficiencies that need to be addressed, mostly related to system sleep issues. Future recommendation is to use a real-time kinematic (RTK) GPS. An RTK GPS would be accurate enough that one could image curved areas without difficulty. The workaround was to assume a straight line and rely on the wheel counter for proper intervals. The 'straight line approximation' contributed to positioning error as observed at the LWI demonstration at the UM Research. Remarkably, that error between the tape measured center-line of the culvert and the interpreted anomaly was an error of 0.5 meters. This was visually confirmed as the array drifted 0.5 meters laterally from the marked centerline.

In figure 7.10(b) note the survey flag to the right of the streamer the marks the culvert opening. The culvert was oriented perpendicular to the array. One can discern the first geophone in the array approximately at the center-line (orange survey flaglette at opening & faint orange center-line marking paint). The camera feature is one of the visual back-up methods that takes a picture at each accepted shot an can be recalled for comparison at a later time.

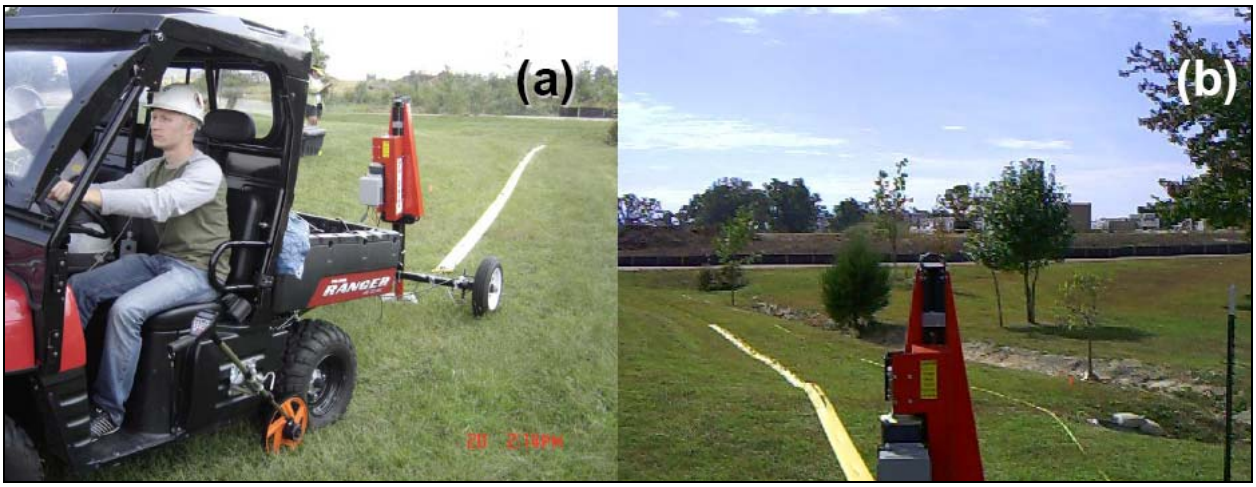

Figure 7.10: Missouri S&T Graduate Student Evginey Torgashov drives the DMSU in at the University of Missouri Technical Park on Soil. (a) Topography and grassy surface caused lateral sliding of the array, (b) recalled rearward camera photograph at the location of the anomaly where the first geophone was interpreted to be over the center-line of the tunnel.

8. COMPARATIVE ANALYSIS OF FIELD MEASUREMENTS

This section compares the field location of the tunnel center-line on the Earth's surface to the software interpreted corresponding location of anomalies associated with voids. In more complex (urban) environments, more than one void may exist. In addition, changes on the surface (moving from sidewalks to soil) and/or subsurface structures (heterogeneity) may be interpreted by the software as a void (false positive). In such environments a limited set (typically 5 or less) of anomalies identified by the software can be rank ordered for further investigation. Figure 8.1 depicts the stages of the DMSU project that leads to comparison of the tunnel anomaly to the known location of the tunnel respectively.

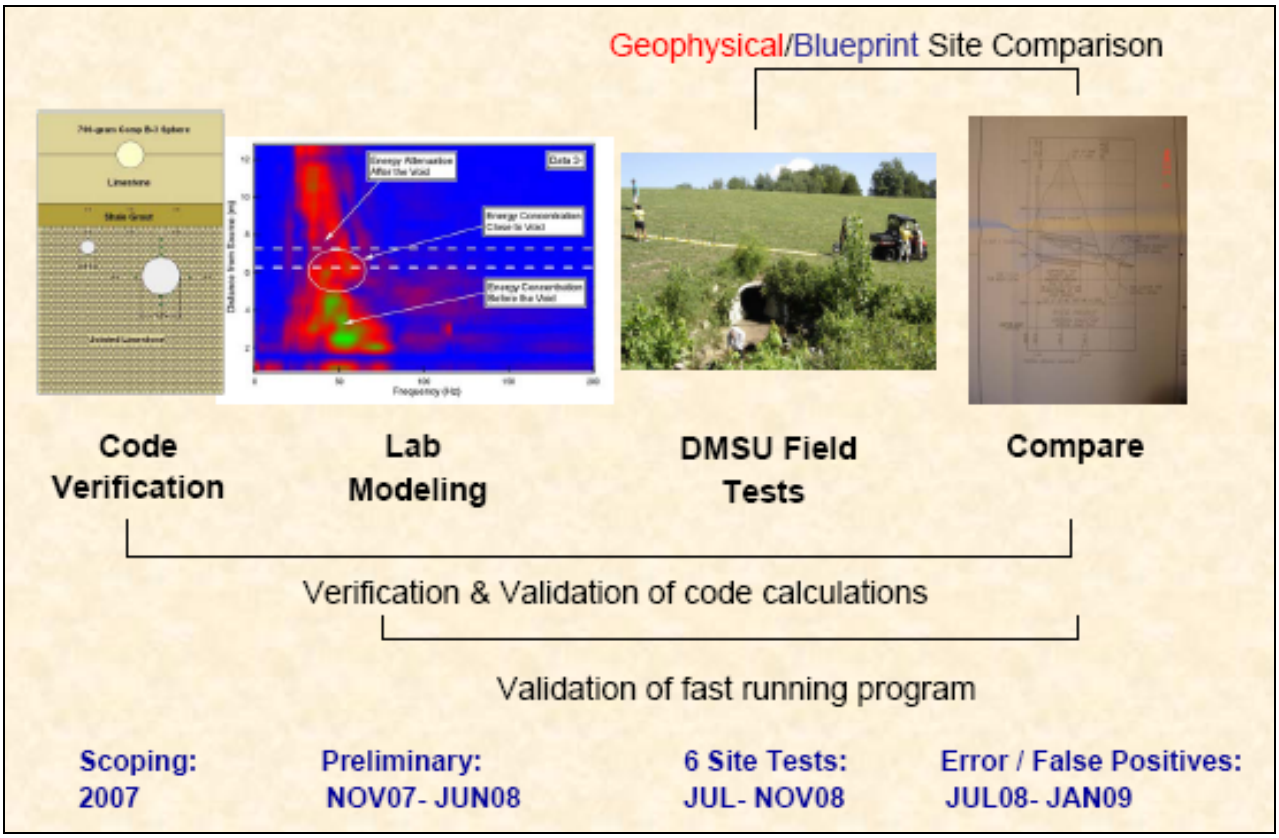

Figure 8.1: Validation of the DMSU capabilities to detect shallow tunnels involves comparing the known center-line location of the tunnel at the surface to the interpreted location of the automated software: The difference between the two is a basis for error. False positives are also accounted.

8.1 Confidence

The definition of confidence used in context to the DMSU software is one of reliability. The reliability of the software to both find tunnels and discriminate between similar subsurface structures that may appear to be tunnels (e.g. vertical dikes or surface changes like sidewalks to soil). As discussed previously, the SF determines a statistical strength of an anomalous signal for each common shot if the minimum anomaly criteria are met. A 'confidence' sliding toggle appears on the 2D Mapping Tool's right hand side. By moving the toggle from 0 to 100 the operator can display all the anomalies (at the 0% setting) to limiting the strongest single anomaly (at the 100% setting). This allows the operator to reduce the anomalies along the survey line appropriately while in the SF Mode (check box). The AARW algorithm uses the sub-array approach to significantly reduce false positives. Similarly, signal strength toggle to assist the operator in limiting the anomalies to the strongest set for selection.

8.2 Comparative Analysis

Figure 8.2 is a screen capture of an operator selecting an anomaly by clicking on that point in the 2D Mapping mode. Note that the Line Distance minus the First Shot is always equal to 17.5m that is the length of the array (11.5m) from the last geophone to the source drop (shot to receiver offset of 6m). Subsequently, Table 8.1 then compares the field measurement to the strongest anomaly location to determine error.

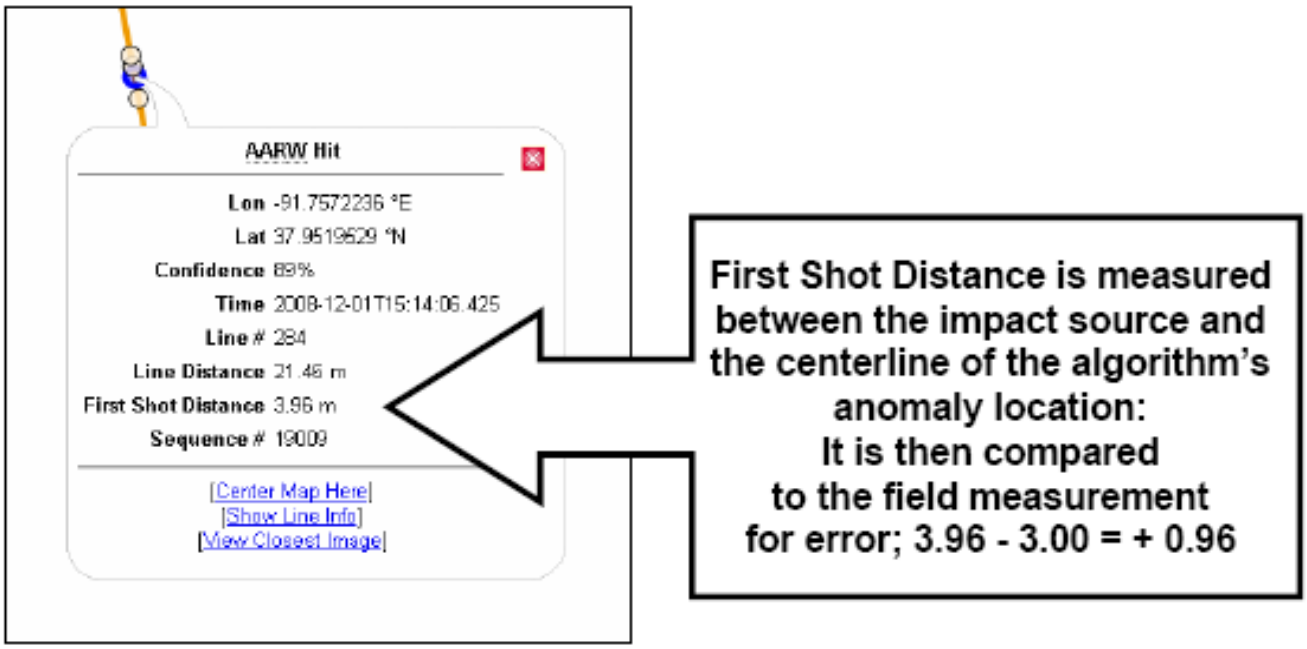

Figure 8.2: The detail 'pop-up' on the 2D Mapping Tool above by selection of a color coded anomaly point. The color code (amber to pink to dark red; weak to strong) is a function of the anomaly strength (or confidence).

	Confidence	First Shot (m)	Tape (m)	Error	CL/Offset/Array
Ber Juan AARW	89	3.96	3	+0.96	3 / 6 / 11.5
Ber Juan SSM	28	11.95	3	+8.95	3 / 6 / 11.5
Physics AARW	97	10.95	11.5	-0.55	11.5 / 6 / 11.5
Physics SSM	65	17.44	11.5	+5.94	11.5 / 6 / 11.5
Tech Soil AARW	97	7.96	9	-1.04	9 / 6 / 11.5
Tech Soil SSM	35	15.44	9	+6.44	9 / 6 / 11.5
Tech Pav AARW	97	7.96	9	-1.04	9 / 6 / 11.5
Tech Pav SSM	33	7.96	9	-1.04	9 / 6 / 11.5
Bishop AARW	97	21.93	17.5	+4.43	17.5 / 6 / 11.5
Bishop SSM	65	21.93	17.5	+4.43	17.5 / 6 / 11.5
Library AARW	79	12.45	6	+6.45	6 / 6 / 11.5
Library SSM	34	2.97	6	-3.03	6 / 6 / 11.5

Table 8.1: The chart depicts the strongest anomaly pick for the SF (or SSM) and AARW. The red error is considered a false positive requiring closer examination and explanation.

8.3 Adjusted Comparative Analysis

As the subsurface becomes more complex (such as in urban environments), the software may interpret the changing behavior of the surface waves in the Earth's subsurface to be indicative of voids. This is the primary reason for the false positives summarized in Figure 8.3. Of particular note was the seeming inability of the DMSU to locate the Bishop Street Student Access Tunnel and the Wilson Library Utility Tunnel on the MS&T campus. The team reverse engineered the problem by superposing the location of the known tunnel on the 2D Mapper. By lowering the confidence strength setting, anomalies of lesser strength would begin to appear. In three cases using SF (SSM), this approach simply offered the operator too many choices of from which to choose. In these cases, it was noted as 'low confidence' since the operator could pick any random anomaly among the set without knowing the actual location of the tunnel.

For the Bishop Street Tunnel Case, the operator noted that a set of anomalies coincided with one edge of the tunnel rather than the center-line. By using the 'TEST Hit' Box the operator inserted the location of the center-line. For AARW and SF the contrast between reflection and attenuation that was the corner was interpreted by the software as a void. The far point identified by AARW as anomalous coincided with a distance of 1.52m from the center-line of the 3.16m void of the tunnel. This yielded an error of virtually 0 when compared to the 'ground truth' centerline. One question becomes, was the reflection and attenuation that the software interpreted as an anomaly from the exterior of the concrete liner's edge (4m wide) or the inner void (3.16m wide)? The data fits more closely to the tunnel's inner void measurement and was used. SF / SSM was categorized s 'low confidence' since the operator could pick any random anomaly among the set without knowing the actual location of the tunnel.

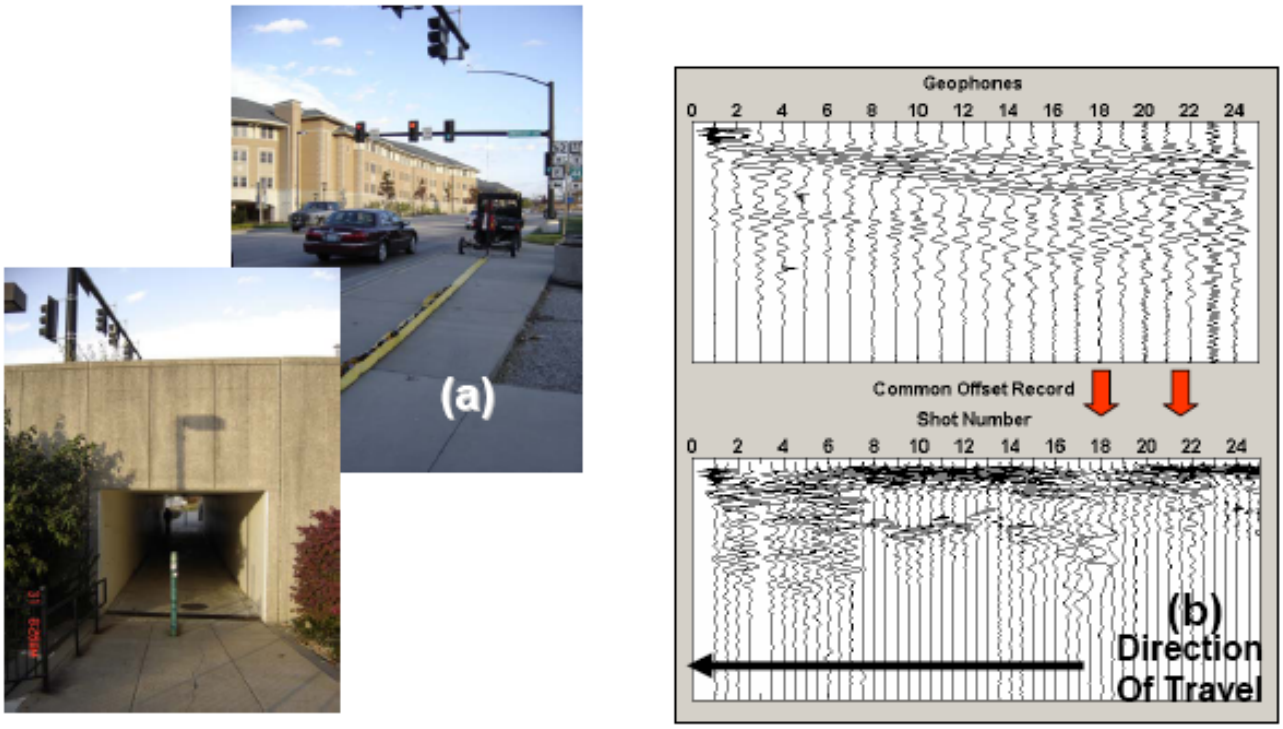

Figure 8.3: (a) DMSU over Bishop Street Tunnel; (b) GUI with tunnel edges marked with red arrows.

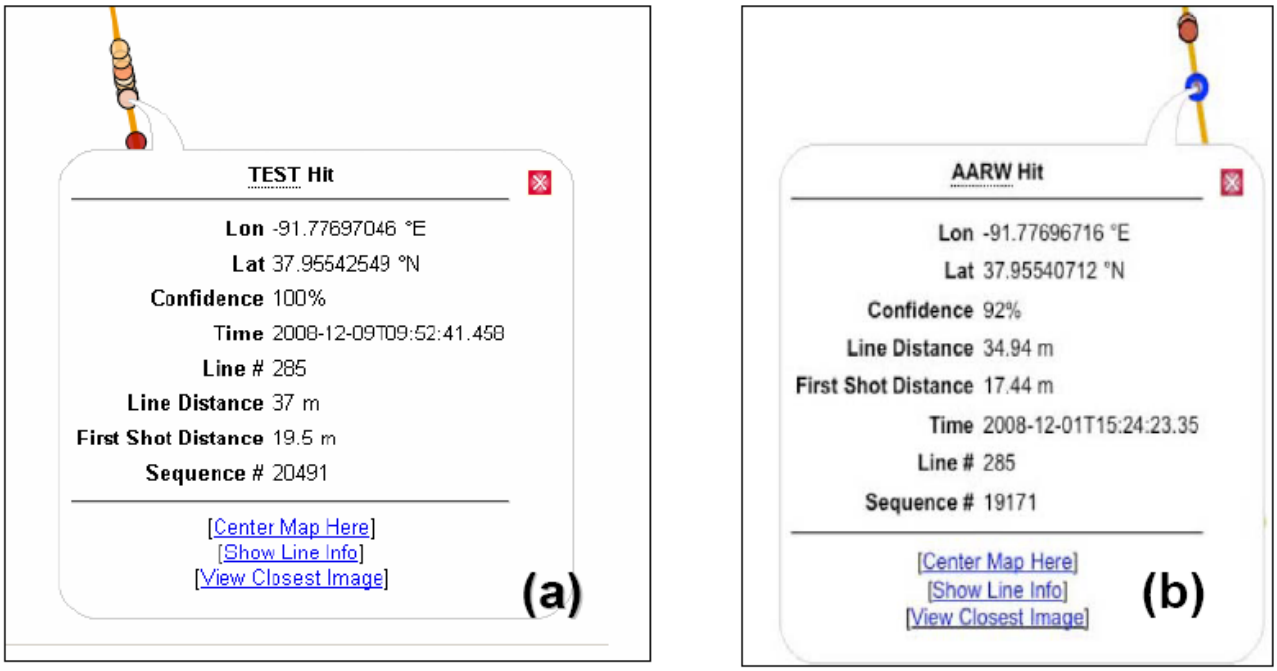

Figure 8.4: Mapping Tool Output considering multiple anomalies. (a) Spiking Filter (SSM) output selecting the anomaly at the field location; (b) AARW output with superposed centerline – note the anomaly (21.93m) was spatially associated with the far edge of a 4m wide box tunnel. The hits displayed in the detail popup are the real location of the tunnel and not actual data for comparison purposes.

For the Wilson Library Case, the superposed centerline of the utility tunnel was the third anomaly pick using AARW and the second pick for SF/SSM. When reviewing the historical GUI from the DMSU, there was initial concern that the poor quality of seismic data observed in the SWCO was due to sloppy advance. This is where the ATV backs up minutely to release tension on the chain as not to induce unwanted vibration 'noise' into the record. It was thought that the first geophone was not being advanced at a consistent 0.5m interval. However, an additional survey using the same geometry and advance using a sledge hammer source and spiked geophones revealed what is best characterized as complex subsurface structure. The difference in quality was attributed to coupling. Figure 8.5(b) shows reflection at two sidewalks as well as the utility tunnel. This corresponds to approximate positions of the anomalies in AARW and SF/SSM as compared to the actual locations of the sidewalks. Again, we see that broadening the anomaly to a set in complex surface / subsurface environments is prudent. In this case, by comparing field notes to the anomalies, one could intuitively discount anomalies at locations where surfaces change significantly (concrete to soil).

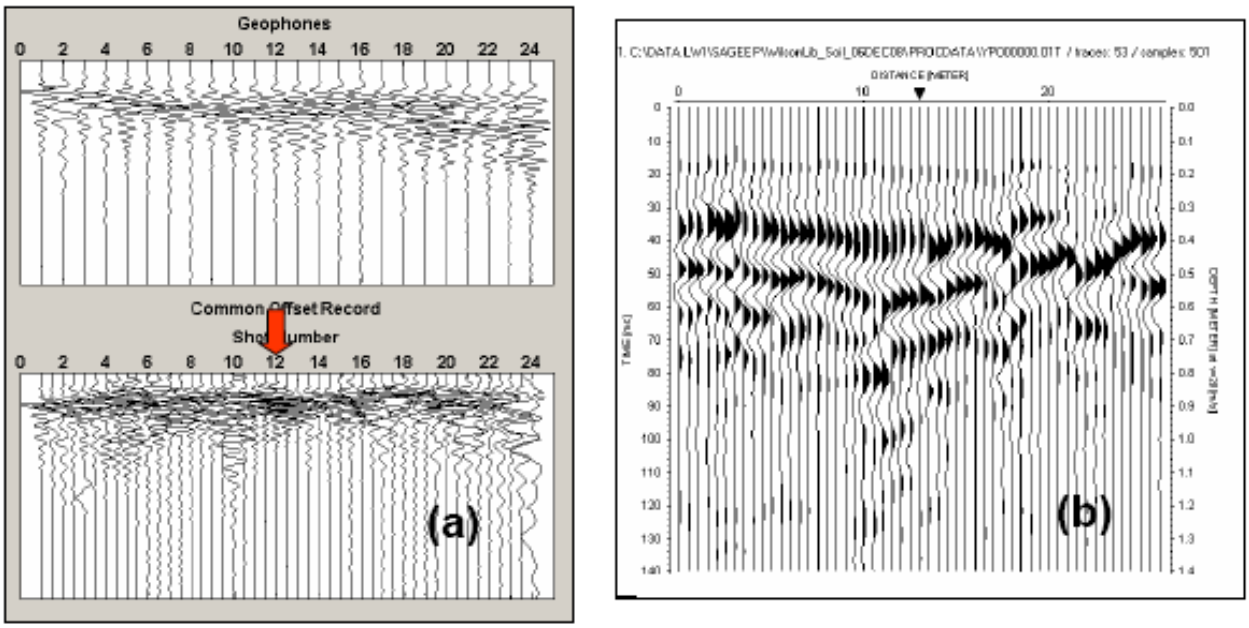

Figure 8.5: (a) GUI of the Wilson Library Tunnel (Soil) where the red arrow is over the tunnel; (b) Identical survey procedure to MSU but using spikes – Although the data is higher quality, there appear to be many reflections typical of more complex soils (urban environments).

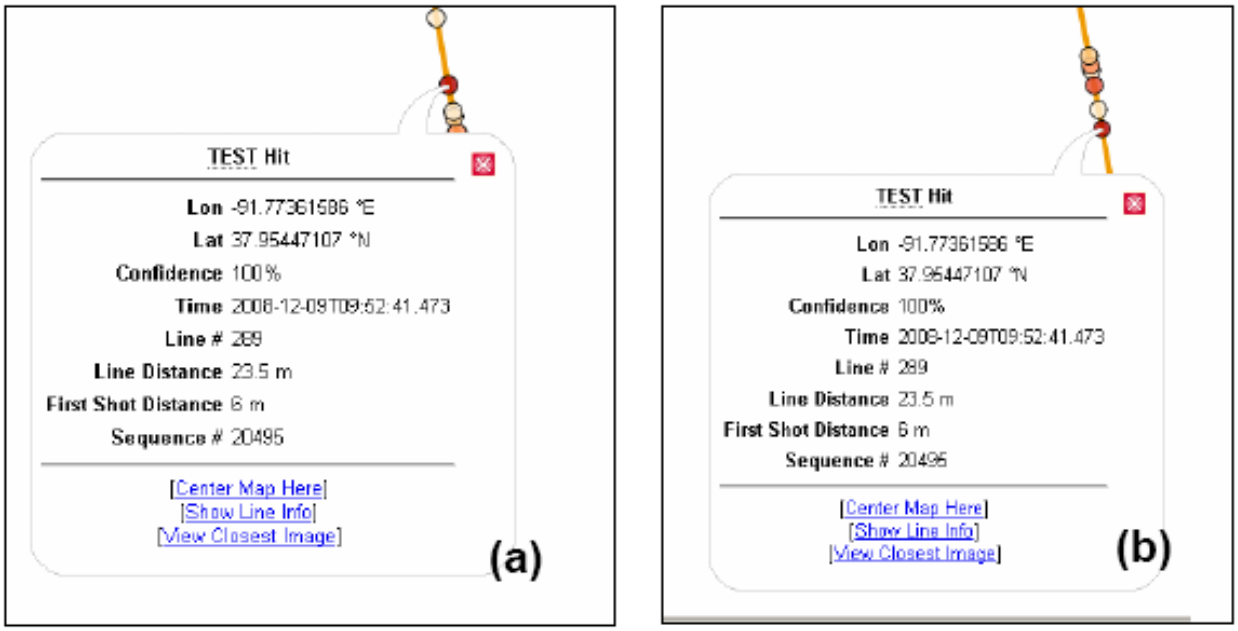

Figure 8.6: (a) A Spiking Filter Anomaly was present at location of the utility tunnel as the operator's second pick, (b) AARW anomaly location as the third pick. Again, the hits displayed in the detail popup are the real location of the tunnel and not actual data for comparison purposes.

Whether the sub-array was more successful at eliminating false positives over SF/SSM was not analyzed. Of note was that an AARW second pick for Ber Juan that happened to corresponded to the first pick of the SF / SSM. The rhetorical question might be asked, 'why wasn't SF/SSM more accurate at Ber Juan before proceeding to the next test location?' The answer was that numerous configurations were at considered, each with advantages. The SF/SSM appeared to work best for the 1m depth tunnel with a 1 to 3m source to receiver offset and geophone spacing at 0.25m. Moreover, selected pristine common shot gathers were used to validate the algorithm suite that best detected the tunnels based on the bounding criteria. The thought process at the outset was that 'if we couldn't see the anomaly at Ber Juan in near perfect conditions, we could not see it anywhere else' (Anderson, 2007). The pristine shot gathers were also used in an experimental excursion to determine the sides, top, and bottom for the tunnel using AARW. Hence, it is a very real possibility that AARW can measure not only the depth to the top of a tunnel, but also the geospatial geometry of its floor and sides (Putnam et al, 2008).

	Confidence	First Shot (m)	Tape (m)	Error	Notes
Ber Juan AARW	89	3.96	3	+0.96	
Ber Juan SSM	28	11.95	3	+8.95	Corresponds to 2nd Pick AARW Cluster
Physics AARW	97	10.95	11.5	-0.55	
Physics SSM	65	17.44	11.5	+1.04	2nd Pick Cluster
Tech Soil AARW	97	7.96	9	-1.04	
Tech Soil SSM	35	15.44	9	+6.44	Low Confidence
Tech Pav AARW	97	7.96	9	-1.04	
Tech Pav SSM	33	7.96	9	-1.04	
Bishop AARW	92	17.44	17.5	-0.06	Two Anomaly's at Edges
Bishop SSM	65	21.93	17.5	+4.43	Low Confidence
Library AARW	79	12.45	6	+0.5	3rd Pick
Library SSM	34	2.97	6	+0.5	2nd Pick

Table 8.2: Adjusted tabulated comparison in operator rank order picks between anomaly and field measurement locations of the tunnel along the survey line. Low confidence setting indicates numerous anomalies available to operator.

8.4 Demonstration

The mobile seismic unit was "officially" demonstrated at Fort Leonard Wood on Saturday, October 4th, 2008. Three external reviewers were in attendance:

1. Larry Allen (ERDC)
2. LTC R. Tucker (MSBL)
3. Stephen Tupper (MS&T-FLW Federal Liaison)

The mobile seismic unit acquired demonstration field data along a ~30m-long traverse that overlaid a known metal culvert (diameter of ~0.6m; depth of ~0.3m). When the mobile seismic unit reached the end of the traverse, the acquired field data were automatically interpreted. The automated interpretation software indicated that there was a high-probability that the traverse was underlain by a single tunnel. The "estimated" location of the tunnel, as calculated by the automated software and displayed on the computer screen, was within 0.5m of the actual tunnel location. No false positives were recorded at the demonstration site.

The external reviewers completed brief questionnaires. All three reviewers circled response B to the question #10: What is your overall recommendation?

A. Deploy and test "as is" (pending training/manual)
B. Good potential; create superior prototype and retest
C. Test demonstration was inconclusive
D. Little potential

9. DISCUSSION AND RECOMMENDATIONS

9.1 Assessment of the DMSU

The DMSU is capable of identifying and locating shallow subsurface tunnels with a reasonably high degree of precision and a minimal number of false positives. The mobile seismic unit is user-friendly and can be operated by non-specialists. Data interpretation is automated; the output is a plan view map (on computer screen) showing the locations of probable tunnels. From the perspective of the external reviewers, the mobile seismic unit (or a modified version thereof) is practical for military operational use in semi-permissive/austere environments and could be operated by a soldier with minimal training.

The current technology (mobile seismic unit complete with interpretational software) could be transferred to military personnel immediately. However, the DMSU Team believes it more prudent to continue to develop the unit with the expectation a significantly superior product will be ready for military use in a matter of months.

9.2 Problem Areas

Depth of Investigation. The man-made tunnels at the six test and/or demonstration sites were no deeper than 1.5m and no less than 0.5m in diameter. We did not attempt to image deeper tunnels because of availability issues and because our current landstreamer (re: short geophone spacing) was designed to image shallow targets. We do not know, with certainty, if our unit is capable of imaging comparable or larger tunnels at significantly greater depths (~5m).

Geological Settings. The mobile seismic unit was tested successfully at six different sites in central Missouri. The unit is capable of imaging shallow tunnels overlain by grass, asphalt or concrete and encased in fairly uniform clayey or silty soils. However, we do not know if our unit is capable of imaging comparable tunnels encased within dry partially-cemented sandy soils.

Depth & Width Estimation. The mobile seismic unit was able to locate all of the tunnels at all of the test sites with an average accuracy of 0.5m. With minimal modifications, the interpretational software should be capable of providing reliable estimates of tunnel widths and tunnel depths.

9.3 Recommendations

The DMSU could be field-tested by non-technical military personnel "as is". However, we recommend that additional period of nine months be resourced to develop and rigorously test a superior prototype that better meets of needs of the military in terms of accuracy, width/depth estimates, robustness, speed, overall utility, defined capabilities, and user-friendliness.
The modified prototype would be significantly superior to the current unit for several reasons:

Accuracy. To improve accuracy and minimize false interpretations, we developed three separate interpretation modules [Surface Wave Common Offset (SWCO) module, Spiking Filter (SF) module, and Attenuation Analysis of Raleigh Waves (AARW) module]. Incoming field data are automatically and simultaneously analyzed by all three modules; tunnel locations are identified on the basis of the statistical analyses of the output of all three modules. At this point in time, AARW provides the most accurate results, in large part because this analytical tool was developed first. It is our opinion that the SWCO approach is extremely promising and that our interpretation system will be significantly improved if we are given more time to further develop and fine-tune this approach. Our SF module will also benefit significantly from "fine-tuning".

Width/depth Estimates. The current unit is capable of estimating tunnels locations to within 0.5m, but is not capable of automatically estimating tunnel widths and depths. We anticipate that our interpretational software, with minimal modifications, will be capable of providing reliable estimates of tunnel widths and tunnel depths.

Robustness. Our current unit functions well under friendly environmental conditions (moderate temperatures, dust-free, sunny skies). We would like to have the opportunity to redesign our unit so that it is capable of functioning well under more difficult environmental conditions.

Speed. The current unit is capable of acquiring about 0.5km of data per day. It is anticipated that the modified prototype will be capable of acquiring more than 1km of data per day.

Utility. Two of the three reviewers indicated that the mobile seismic unit would be of much more utility to the military if the acquired surface wave data could be automatically transformed into shear-wave velocity profiles. These shear-wave velocity profiles would provide military engineers with critical information about the nature subsurface to depths on the order of 15+ m (including shear strength, depth to bedrock, heterogeneity, etc.). If these capabilities are integrated into the existing system, the unit could be used for routine geotechnical investigation purposes (in addition to tunnel detection purposes). The transformation technology (software) is available. It is simply a matter of integrating it into our existing system.

Defined Capabilities. The current unit is capable of imaging shallow tunnels. The proposed modified prototype will be thoroughly tested under diverse field conditions (soil conditions and tunnel depth) so that the potential user is fully aware of the strengths and limitations of the system.

User-friendliness. Our current unit has been successfully operated by non-geophysicists. The system is fairly user-friendly. However, there are a number of modifications that can be made (software mostly) to improve the usability of the mobile seismic unit.

10. REFERENCES

Anderson, N., Thitimakorn, T., Ismail, A., and Hoffman, D., 2007, A Comparison of Four Geophysical Methods for Determining the Shear Wave Velocity of Soils: Environmental and Engineering Geoscience, V. 13, pp. 11-23.

Billington, E. D., Palm R. J., and Grosser, A.T., 2005, MASW Imaging of an Abandoned Minnesota Mine, Washington: 2006 Seattle Annual Symposium on the Application for Engineering and Environmental Problems, Session on Geophysical Studies in Urban Areas. (http://www.x-cd.com/sageep06cd/program.html).

Giles, C., Leparoux, D., Virieux, J., Bitri, A., Operto, S., and Grandjean, G., 2005, Numerical modeling of surface waves over shallow cavities: Journal of Environmental and Engineering Geophysics, 10(2), 111-121.

Miller, R.D., Xia, J., Park, C.B., and Ivanov, J., 2000, Shear-wave velocity field from surface waves to detect anomalies in the subsurface: Geophysics 2000, FHWA and MoDOT Special Publication, 4:8.1–4:8.10.

Miller, R.D., Park C.B., Xia, J., Ivanov, J., and Steeples, D., 2006, Tunnel Detection Using Seismic Methods: 2006 Joint Assembly of the American Geophysical Union, Baltimore: NS21A-07.

Nasseri-Moghaddam, A., 2006, Study of the Effect of Lateral Inhomogeneities on the Propagation of Rayleigh Waves in an Elastic Medium, Canada, University of Waterloo: Ph.D. Thesis.

O'Neill, A., Campbell, T., & Matsouka, T., 2008, Lateral Resolution and Lithologic Interpretation of Surface Wave Profiling: The Leading Edge, V. 27, No. 11, pp. 1550-1563.

Putnam, N.., Nasseri-Moghaddam, A., Kovin, O., Anderson, N., & Grant, S., 2008, Analysis Using Surface Wave Methods to Detect Shallow Manmade Tunnels: Proceedings of the Fifth Highway Geophysics - NDE Conference, Charlotte, NC, pp 404-412, (http://www.ncdot.org/doh/preconstruct/highway/geotech/geophysicsconference/).

Reynolds, John M., 2000, An Introduction to Applied and Environmental Geophysics, England, Wiley & Sons, Ltd..

Sheriff, R., and Geldart, L., 1985, Exploration Seismology (second edition), New York, Cambridge University Press.

Department of the Army, 1999. Materials Testing (Publication No. FM 5-472). U.S. Government Printing Office: Washington DC.

Xia, J., Nyquist, J. E., Xu, Y., and Roth, M. J. S., 2006. Feasibility of Detecting Voids with Rayleigh Wave Diffraction, Pennsylvania: 2006 Philadelphia Annual Meeting of the Geological Society of America, Paper 218-7. (http://gsa.confex.com/gsa/2006AM/finalprogram/session_18007.htm).

Appendix A:
Demonstration Mobile Seismic Unit (DMSU) Operations Manual

Index

General

The content of the DMSU Operations Manual is organized in the order it is likely to be used. For parts, fabrication or software, refer to Appendix B: DMSU Parts Manual. The DMSU was modularized for shipping to a forward staging area in the vicinity of the site of interest. It is assumed that gasoline and electricity is available at the staging area at the end of each day to refuel the ATV and recharge the 2 marine 12 volt batteries using the battery re-charger provided. It cannot be over emphasized that an inventory should be conducted to ensure all components are on hand prior to driving the survey site. The DMSU Operations Manual is not intended to be an exhaustive source nor does it portend to anticipate all technical problems. However, it does provide a concise explanation of how to configure and operate the system in the field and to troubleshoot those problems typically encountered while operating the unit. For planning purposes, the DMSU ATV cab can seat up to 3: A crew consists of the driver and software operator. A safety officer is optional.

Figure A.1: 2 each 12 volt marine batteries should be charged before each survey.

IMPORTANT 	Avoid dropping the geophones or pulling at the geophone cable as they are delicate. Geophones are susceptible to shock and may be damaged. Store the geophones in foam material after every use. Keep the calibration geophone separate for comparison during the RAS-24 dissimilarity test (see page 105).

Survey Pattern

Before conducting a survey, a reconnaissance of the area should ensure that the ground is fairly flat with limited vegetation for coupling and maneuverability. The land streamer may not function effectively when towed across highly irregular surfaces, because some of its geophones may not be effectively coupled to the ground surface. The demonstration unit and its 2 occupants will not be armor-protected. Therefore, security must be provided by the customer.

1. The DMSU is 21m in total length fully configured. The minimum survey line length is site dependent. However, it is recommended the linear distance advanced is at least 12m to allow the algorithms to function properly. The crew must be cognizant that the first and last 5m of the survey line are not used for interpretation as discussed in the technical report. Therefore, the crew should add 5m on each end of the survey line to ensure the surface wave can develop from the impact source to tunnel depth.
2. Standard surveying procedures such as marking / flagging lines and dropping 100m line tapes will assist the driver in advancing the ATV the proper interval in the event the Digi-Roller encounters highly irregular surfaces that cause error.
3. During operation, it is easiest to disconnect the streamer array past the end of a survey line and have the crew drag each half of the array around its center to pivot the firehose 180^{o} for reverse orientation of the unit. This will position the DMSU in the opposing direction for a second survey line.

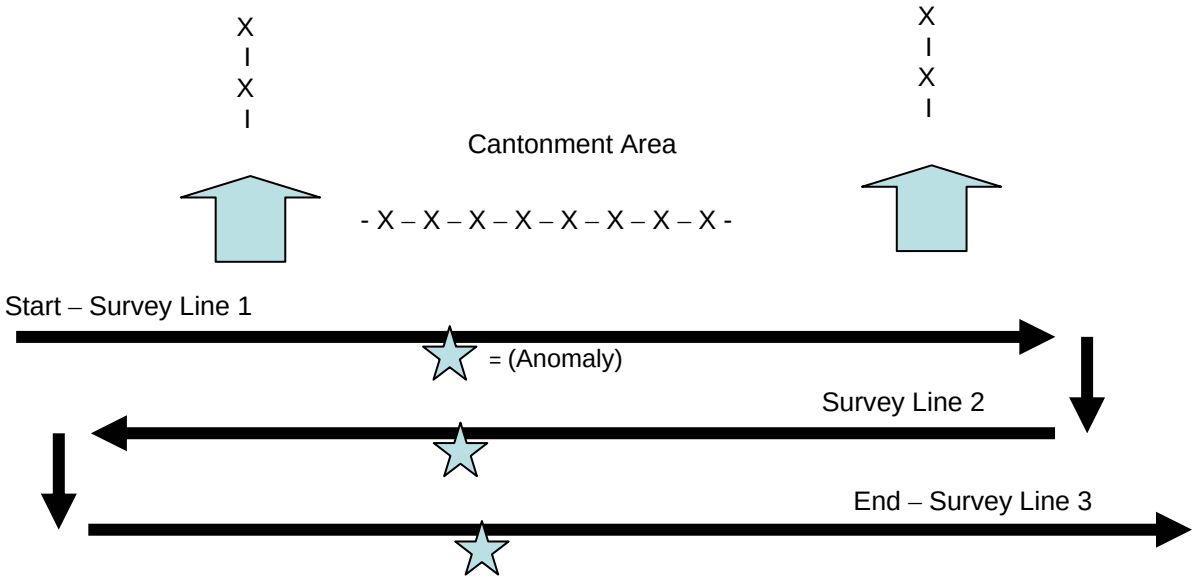

Figure A.2: Diagram of a standard survey pattern used to detect subterranean passageways. The diagram depicts survey lines outside of a fenced cantonment area as example. The star symbols represent anomaly picks for which the survey crew can mark / flag suspect areas on a given line.

Figure A.3: Missouri S&T Student Janely Griffith secures pickets to guide the streamer array on a slope. Terrain with slopes / slippery surfaces (hillside with wet grass) will cause the streamer array to slide down slope diagonally (parallel direction to maximum slope). Short pickets were used to hold the streamer on the survey line trajectory.

Land Streamer

Figure A.4: Pull the geophone cable though the attachment harness ring and front end of firehose to the geophone / plates. A rebar rod can be used to snake the geophone cable through the front portion of the firehose.

1. Unroll the yellow firehose with the attachment harness end toward the trailer.
2. Pull the geophone cable through the harness ring and through the first 5 meters if firehose.
3. Place the second set of cast iron weights on top of the geophone plates. Screw the geophones into the geophone plates. Ensure they are placed in the correct order 1 through 24.
4. Loop the geophone cable once between each geophone to take up the slack of the additional cable inside the firehose. Connect the individual geophone connector cable to the geophone cable. Note that the connector cable has a thin and wide side that only fits in the appropriate configuration.
5. Use 8 inch cable ties to secure the flaps of the firehose between the geophones.

Figure A.5: (a) Geophone screwed into plate; (b) Connecting the individual geophone connector cable to the geophone cable. The excess cable is looped within the 'split' firehose portion that is then secured using 8 inch ties.

IMPORTANT !	A second cast iron weight is placed on top of the first welded cast iron plate; Weight applied downward by the plate to the ground ensures coupling. The geophones will fit through the center of the weights as they are screwed into the plate as seen in Figure A.5.a

6. Use 2 metal shackles to connect the streamer towing clamp to the array tow chain.

7. Connect the geophone cable adapter (cable that splits into 2 each RAS-24 pin connector ends) to the geophone cable.

Figure A.6: 2 metal shackles that connect the streamer towing clamp to the array tow chain.

IMPORTANT 	As the array is pulled by the ATV, the array towing chain remains tight, casing the vibration of the running engine to contribute unwanted noise to the seismic trace. The driver should advance 0.5m accordingly, reverse slightly, and then take the seismic shot. Once a shot is accepted, the driver advances the ATV to the next 0.5m interval and repeats the process.

Seismic Source (GEO-Strike)

1. Determine weather the seismic impact source should use the pavement foot (for thin pavements) or the soil plate with hammer head.
2. Ensure the mechanical foot is in the 'up' position and attach the appropriate foot for the survey. Use the same foot throughout the survey. Alternately, one can adjust the GEO-Strike Elastomere band to lessen the force of the blow if required.

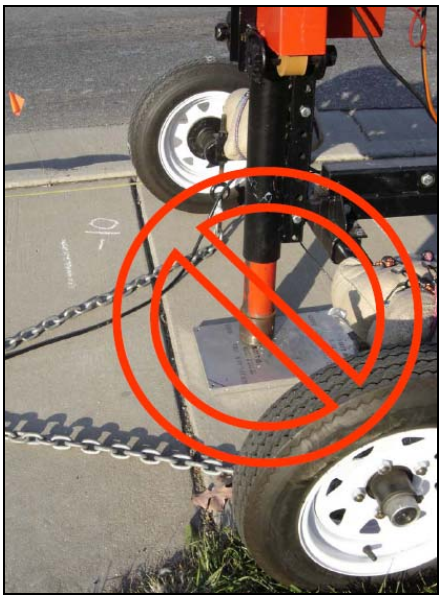

Figure A.7: Hairline cracks are the result of using the plate and hammer head configuration on thin pavements like pedestrian sidewalks.

IMPORTANT 	Thin concrete sidewalks and other pavements can be damaged using the plate and hammer head (Figure A.7). A damage risk assessment should be conducted before the execution of the survey to reduce this risk. The rubber foot is designed for pavements.

Figure A.8: Picture of the hammer (left) and rubber (right) foot. The Wrench with 1.5 inch socket is used to attach either foot to the impact arm using the attachment bolt.

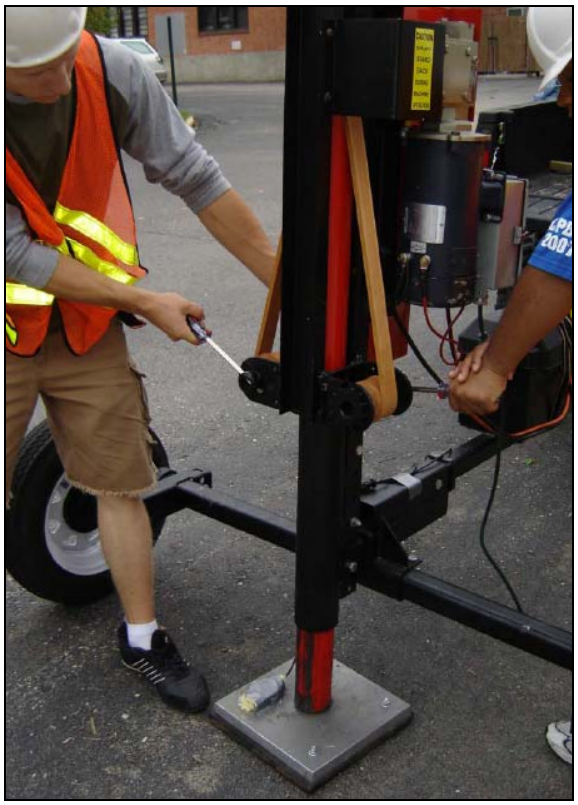

Figure A.9: The Elastomere band is threaded through the top of the arm and opposing cranks that are then tightened in parallel with 18" screwdrivers.

IMPORTANT 	Fasten the GEO-Strike metal safety covers over the bands after tightening. Remember to release the tension and recover the band after the survey.

3. Thread the 'Elastomere' bands through the top of the impact arm and through the mechanical cranks on either side. Tighten the bands simultaneously on either side using 18 inch screwdrivers by hand.
4. Cover the bands with the GEO-Strike cover.
5. (For the Plate and Hammer Configuration) Thread the short towing chain through the center eye-bolt hanging from the trailer towing arm. Screw the chain to either side of the plate ensuring the extended plate is centered and below the striking arm.
6. Secure the geophone and trigger cable to one side of the trailer chassis using vinyl duct tape or 8 inch cable ties. Ensure the battery and firing cables are away from and on the opposite side of the chassis to avoid electrical interference with the trigger cable.

Figure A.10: Seismic Impact Source (GEO-Strike) Trailer configured with plate and hammer head. Sandbags weighted the chassis such that when the source was used, the trailer was not lifted off the ground.

7. Ensure the sandbags are securely fastened on the trailer frame toward each wheel using bungee chords.
8. Plug in the hammer switch cable (red firing button with remote control box) into the female end plug on the GEO-Strike by the fuse box. Extend this cable to the cab.
9. Attach the GEO-Strike power cables to the Marine 12V Battery.

Figure A.11: (a) Attaching power cables to the battery; (b) Shaping and replacing the 80 amp fuse in the fuse box.

TROUBLE SHOOTING	Over tightening the band will cause the fuse to short out. Several 80 Amp fuses should be available for replacement. The fuses are cut for adaptation to fit into the fuse box (Figure A.11.b).

All Terrain Vehicle (ATV)

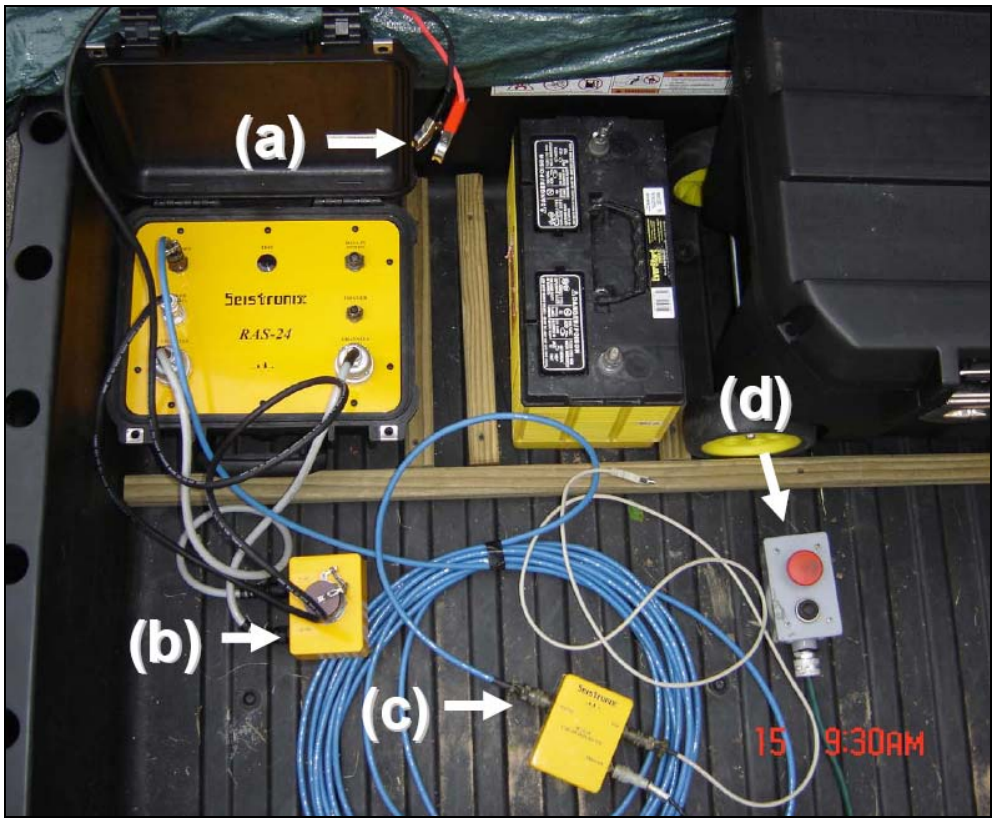

Figure A.12: The RAS-24 connection box in its proper configuration located in the back of the ATV. A waterproof tarpaulin cover is used to shield the electronics from the elements.

1. Connect the power adapter cable (a) to the RAS-24 (unclamped from the 12V Battery).
2. Ensure the geophone cable adapter (b) is properly connected to the RAS-24. They are marked 1-12 and the other 13-24, corresponding to the markings on the RAS-24 pin plug-ins.
3. Ensure the Trigger, RAS-24, and Laptop USB Cables are routed through the USB-100 adapter (c).
4. Hammer switch cable is accessible to the cab (d).

Figure A.13: Attaching the Digi-roller to the rotating adapter housing on the ATV.

5. The Digi-roller PlusII is fit to the circular housing which is then held in place by the circular spring. Use pliers to clamp the spring as you place roller it into the circular housing followed by inserting the circular spring. This allows the Dig-roller to rotate in one direction. Then attach the other wire spring between the ATV chassis and the lower arm of the Digi-Roller. A latch will secure the Digi-roller in the up position. Once the latch is released, the Digi-roller makes contact with the ground to measure distance traveled by the ATV that is held down by the spring.

Figure A.14: (a) Trimble slide and lock receiver mount; (b) hanging camera pedestal.

6. Fasten the Trimble GPS receiver (A.14.a) and digital camera (A.14.b) to their respective mounts. Attach extended 15 pin cable to the GPS and the extended single pin plug-in to the DV-5000G camera.
7. Fasten the GPS hurricane antenna to the exterior mount. Plug in the extended antenna cable to the GPS receiver.
8. The 15 pin GPS cable, camera USB, and RAS-24 USB are plugged into the back of the 'Toughbook' laptop.
9. Plug power for Laptop, GPS and Camera into the 3-way 12V adapter (that is wired into the ATV battery).

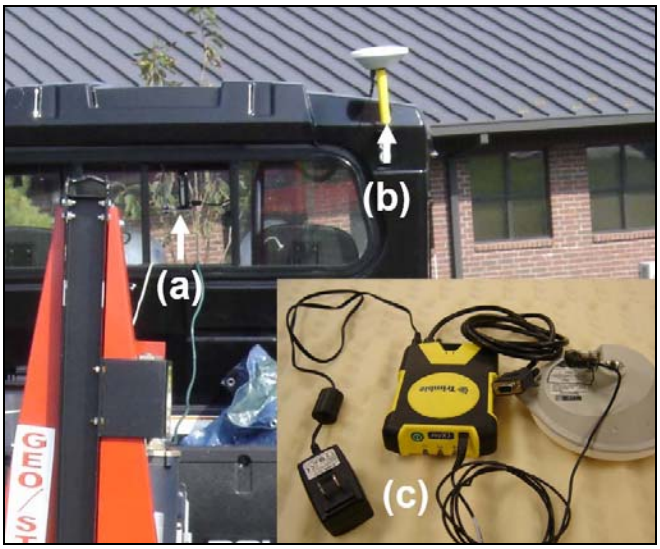

Figure A.15: (a) Digital Camera mounted in rearward viewing position; (b) hurricane antenna; (c) Trimble GPS receiver and antenna.

IMPORTANT	Ensure the 2 Marine 12V batteries are recharged before the next day's survey. One battery powers the seismic source and the other the RAS-24 system. The smaller ATV battery powers the laptop, camera and GPS from the 12V adapter in the cab. The ATV engine should be kept running during operation of the laptop to avoid a drained vehicle battery.

Seismic Software (RAS-24)

1. Ensure all power is connected, the ATV is running, and systems are tuned-on (GPS, Camera, and Laptop).
2. (For reference only) The RAS-24 parameters are as follows:
    - Sample Rate: 1.0ms
    - Shot Count: 1 (No stacking)
    - Gain: 12db
    - Auto-Save: On
    - Record Length: 0.5s

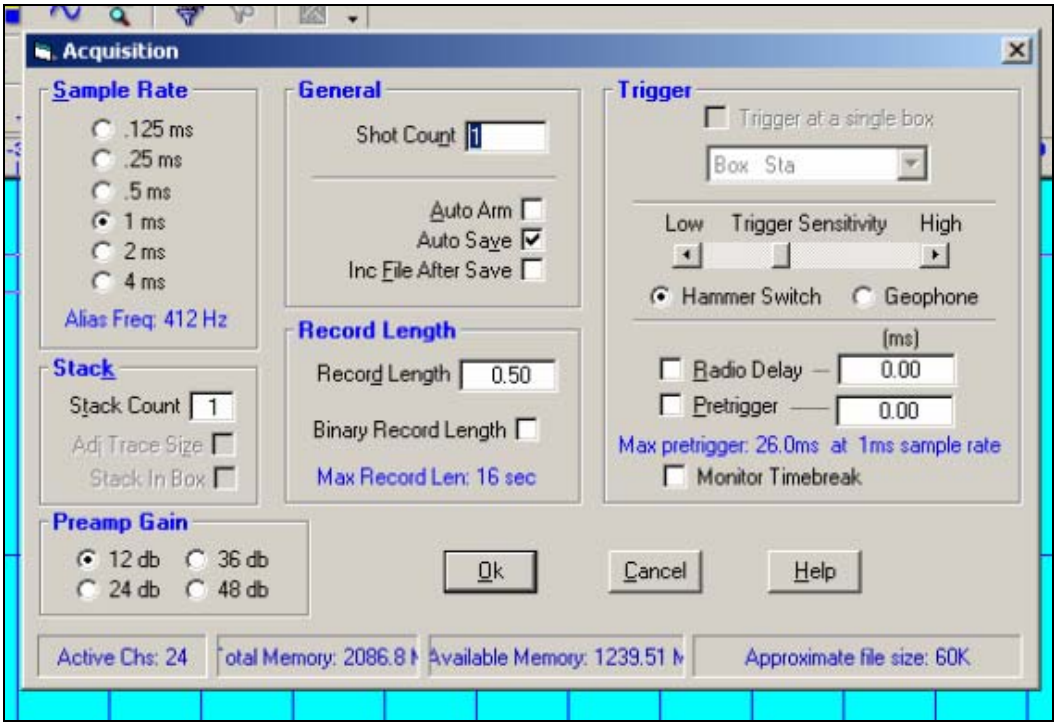

Figure A.16: Screen capture of RAS-24 Setup / Acquisition parameters.

3. For each survey, the software operator must set up a file / folder in RAS-24. Access C:/Seismic and establish a sub-directory with the appropriate title (Figure A.17).

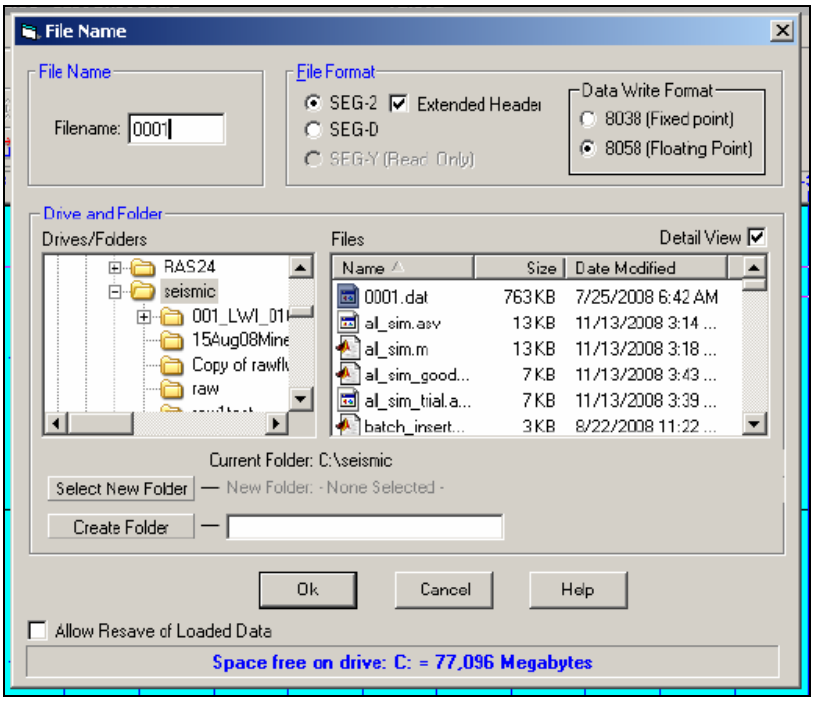

Figure A.17: Screen capture of appropriate file location to start a data folder for a new survey. This folder will store the SEG-2 and floating point format for each seismic record or shot. Note that tunnel304 (MATLAB) and wc2k1_67 (Camera) are files used to communicate to the respective partner software.

Figure A.18: Once all the systems are connected and turned on, pressing the button on the RAS-24 should return '2 beeps'. 2 beeps means the system is connected. 1 beep means there is a disconnected, misrouted, or damaged cable / cable connector.

6. Press the button on the RAS-24 Box. Two beeps means the system is functioning correctly. One beep means there is a disconnected or damaged cable.
7. Take the 'calibration geophone' and replace it with the first geophone. Run the geophone dissimilarity test (Figure A.19). If a geophone is damaged or broken, the test will show a yellow or red bar. Save the test. Now replace the second geophone with the first and run it again (testing the #1 geophone with the reference geophone). Save the test again. Replace any geophone that fails the test as soon as possible: Failure is set at 5% error. Put the 'calibration geophone' away and replace geophone #1 and #2 accordingly.

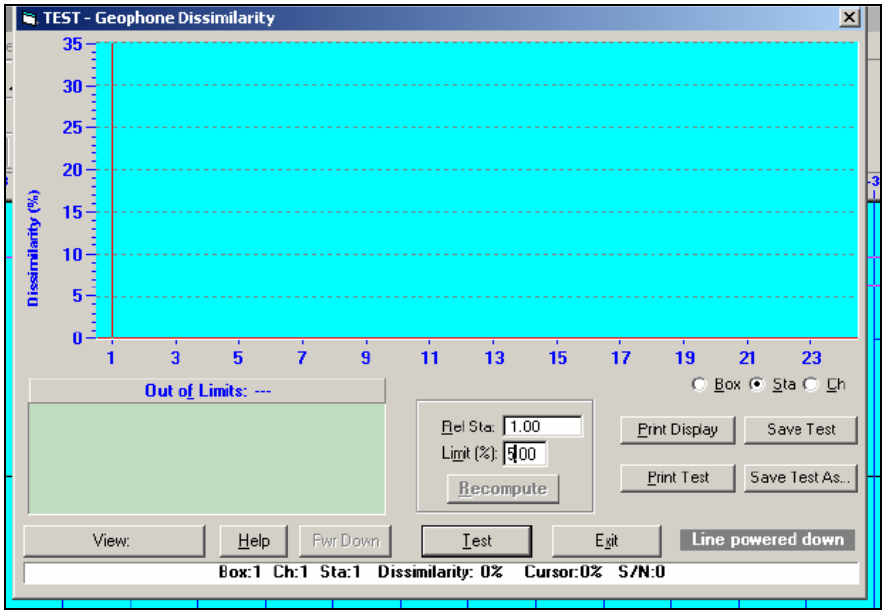

Figure A.19: Screen capture of dissimilarity test operation in RAS-24 under test / geophone similarity. The limit is set to 5%. The test can be saved and displayed in tabular form.

Graphic User Interface (GUI)

IMPORTANT	Allow 5 minutes at the beginning of the survey for the GPS to acquire the location and azimuth before taking the first shot.

1. Connect and switch on the **GPS, Camera, Seistronix units**
2. Start the webcam server from **C:\seismic\wc2k1_67\WebCam2000.exe** with icon

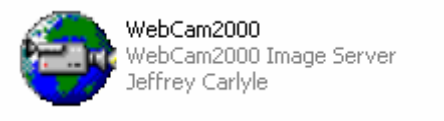

3. Start the firefox web browser. Type in the address "**http://localhost:8989/?random**"
4. Right click on the "**My Computer**" icon and select "**properties**" as shown

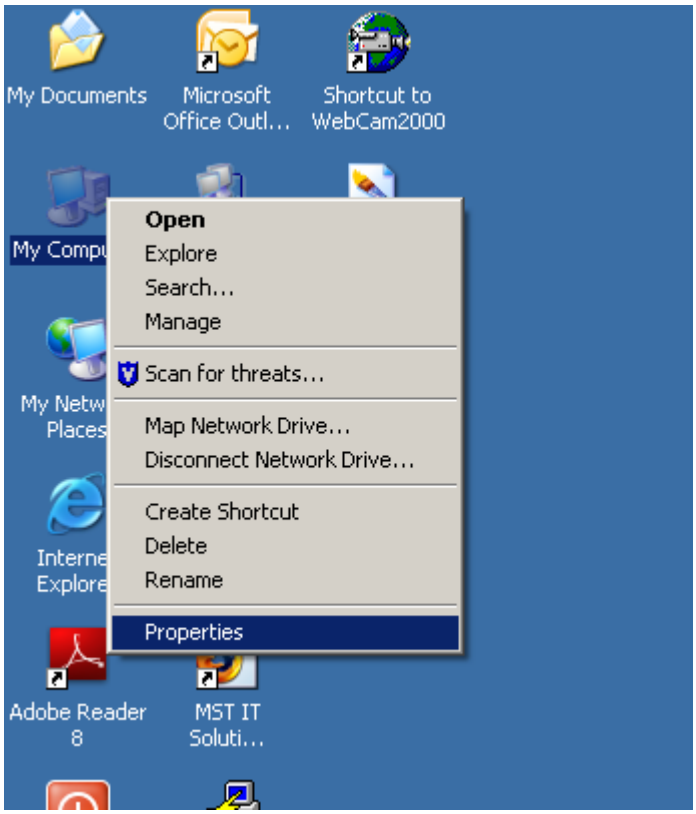

5. Go to "**hardware->device manager**" as shown in

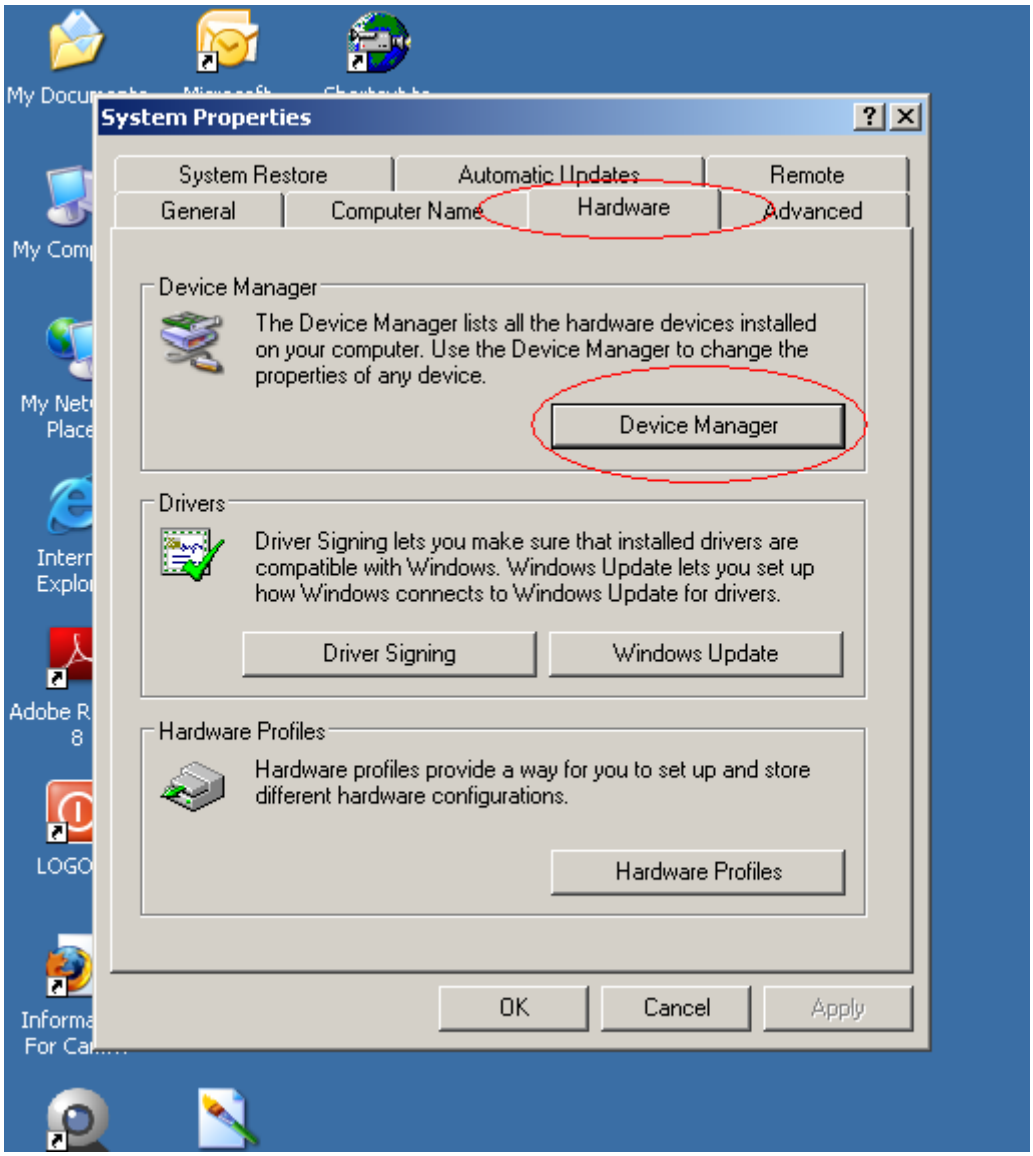

6. Look at the "**Ports(COM & LPT)**" list

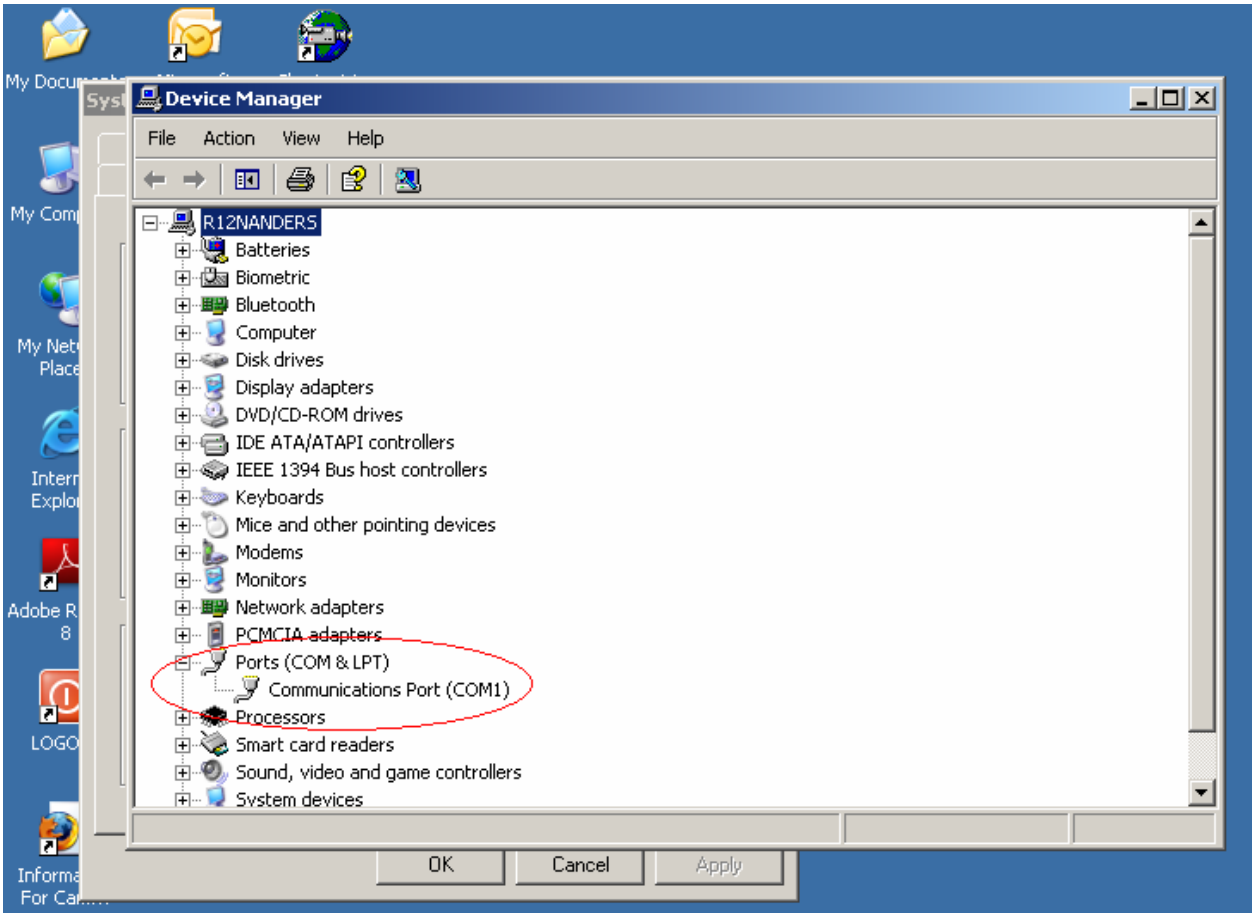

7. There should be another port listed as "**serial adapter COM x**". This '**x**' will be any number. This COM port is the port for GPS. Please note this for GPS setup.
8. Start MATLAB
9. Type in
   cd c:\seismic
   at the MATLAB command window.
10. Type in
    addpath 'c:\seismic\tunnel304'
    at the MATLAB command window.
11. Now start the tunnel program by typing in
    tunnel
    at the MATLAB command window.
12. Press "**Start**" button. Enter the parameters. The start button will be disabled if database has been created. RAS 24 will be started.

13. Please setup RAS 24 to produce a file named **0001** with auto increment disabled. Please set the directory of the file to be "**c:\seismic**". The rest of the settings are standard.
14. **Go to Setup position and follow screen prompts.**
15. Press "**Setup**" button. Enter the parameters. Use the GPS port number found in steps 3-6. **Go to Line Start position and follow screen prompts.** The setup button will be disabled if GPS has started properly.
16. Press "**New Line**" button. Check the GPS parameters and press OK if satisfied. The new line button will turn to end line button when the new line is formed in the database.
17. The system is now set up for use.
18. Please take a shot and wait for data from Seistronix RAS24 to be produced.
19. After the file is produced press "**Shoot**" button. The wheel count value is prompted automatically. Verify the wheel count value (0 for first shot and ideal increments of .5 from then onwards). Press OK. The displays should show the common offset and common shot data.
20. Verify the data and press "**accept**" or "**reject**".
21. Continue until the line is finished.
22. Press "**end Line**" to end the line. Follow prompts on the screen. **If you do not wish to start a new line please use "end" button to finish the current survey.**
23. **Go to New Line Setup position and follow screen prompts. Press OK.**
24. **Go to Line Start position and follow screen prompts.** Press OK followed by "New Line" button.
25. Continue as with the previous line.
26. Use "**end**" button to finish the survey.

TROUBLE SHOOTING 	The program will 'time-out' if it is not being used (e.g. seismic shot taken) for 10 minutes. In effect, this will cause all the respective programs to turn-off for which the program operator must reboot the system. Data will not be lost, but time will be required to queue-up the system.

Seismic Trace Visual Quality Control

Though the software operator is not necessarily a geophysicist, this section is a primer on how to ensure the seismic data collected in each shot is acceptable. Many times, data can be improved by troubleshooting problems based on observations from the traces. Each shot is recorded on a common shot gather trace: It is accepted or rejected by the software operator. Rejecting a shot simply means that you take another shot, look at those traces, and re-evaluate.

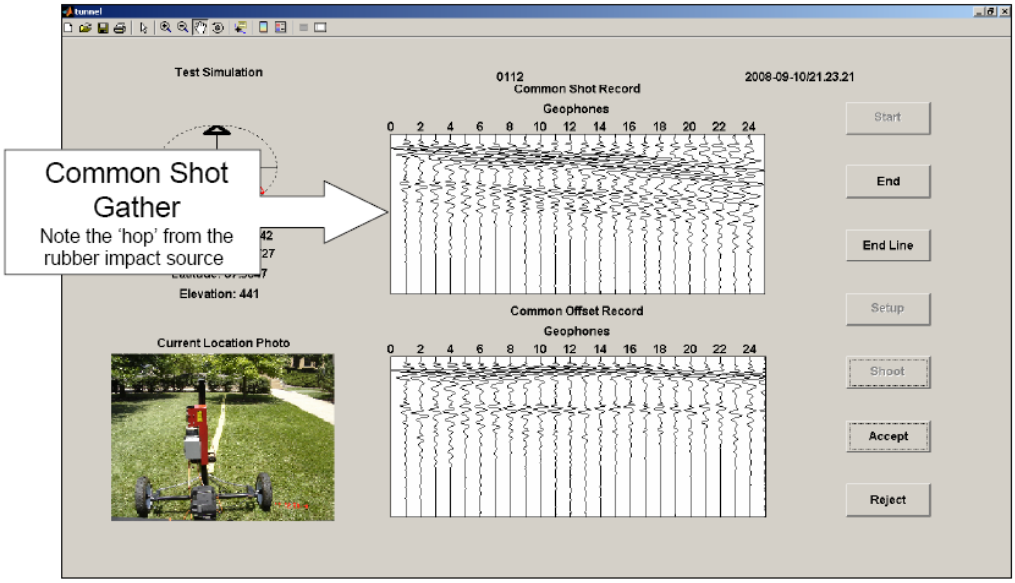

Figure A.20: A screen capture of the Graphic User Interface (GUI) of the DMSU depicted above. The GUI is used by the software operator to accept or reject the seismic shot before advancing to the next shot location.

1. After the RAS-24 processes the shot, ideally you should see:
    - All the traces have wiggles that mean the geophones are connected.
    - The wiggles should have a general 'curvy' pattern which means that high frequency ('sharp little wiggles') vibrations aren't being recorded on top of the surface wave. This kind of vibration is commonly referred to as noise.
    - There is a general linear slope of the peak waves downward from left to right. This means the soil layering is uniform and uncomplicated.
    - The first trace (and perhaps more) does not have a wave beginning at the very top of the graph that looks like it is cut in half. The trace should start with relatively no amplitude at zero or the center of the trace line. That means the trigger is working properly.

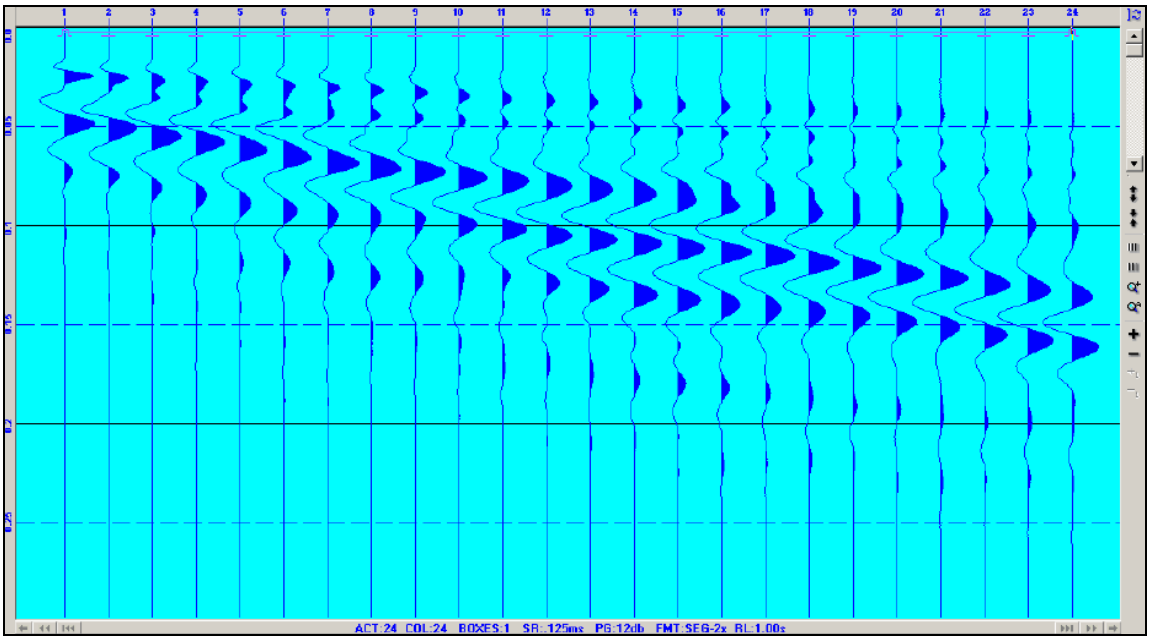

Figure A.21: RAS-24 pristine common shot gather of 24 seismic traces (one per geophone). The screen capture is visually what an excellent trace should look like.

2. Using Figure A.22 as example, there are numerous problem areas. Here is what you can do to improve the quality of seismic data in the field to get the best results given the complexity of the subsurface:
    - Dead or flat traces mean the geophone is either disconnected or poorly coupled. Look at the geophone trace number and proceed back to that geophone to ensure the cables are connected and the geophone is not tipped over or tilted by a rock (for example).
    - If the wavelets look nervous with a lot of squiggles, see if you can wait between traffic or until the wind dies down before you take another shot.
    - If there is a completely random pattern of traces, see if the ground conditions change along the array (e.g. pedestrian sidewalk to soil to asphalt road) and try to re-orient the streamer along same type of surface (e.g. move line over to avoid sidewalk). However, some subsurface are complex (landfills or urban environments).
    - If the trigger is not working or is firing before the weight source hits the ground, check / separate the cables from the battery / remote firing box as electrical interference may be the cause of the problem. If there is no trigger activation, check cables and tighten trigger housing. Replace the trigger last.

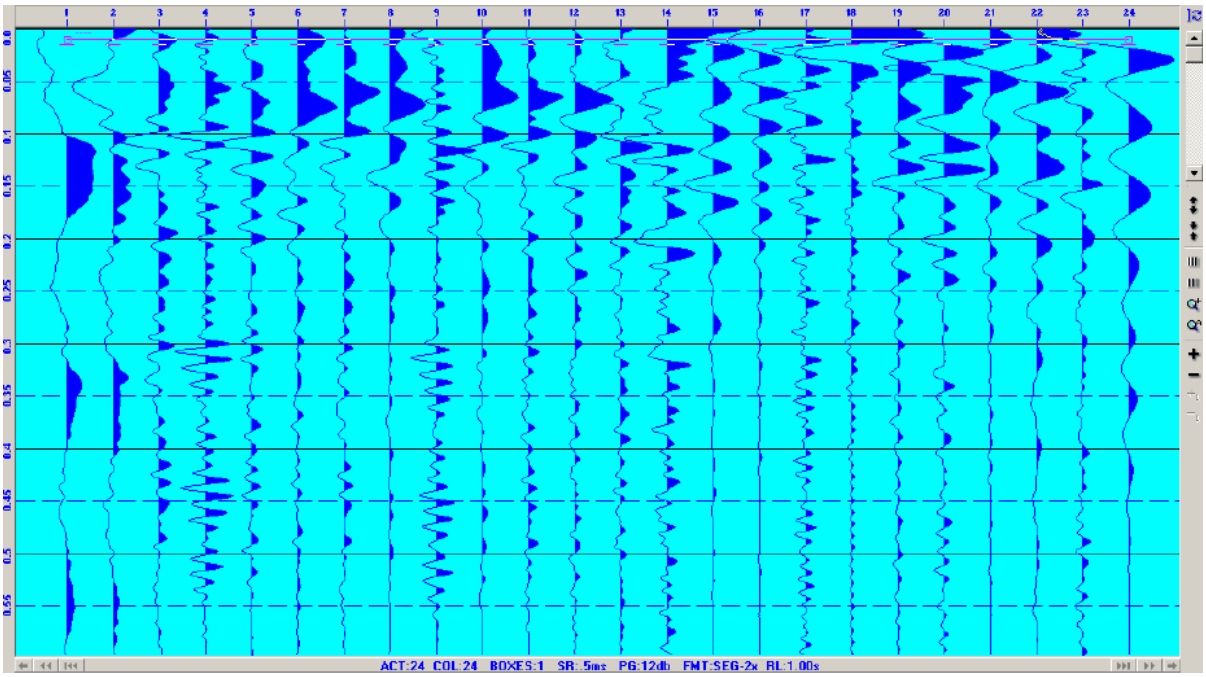

Figure A.22: RAS-24 common shot gather of 24 seismic traces (one per geophone). The screen capture depicts random patterns with some high amplitudes traces. The trigger is not functioning properly. From the first trace we can see energy arriving before time zero (or before the seismic energy is produced by the impact source).

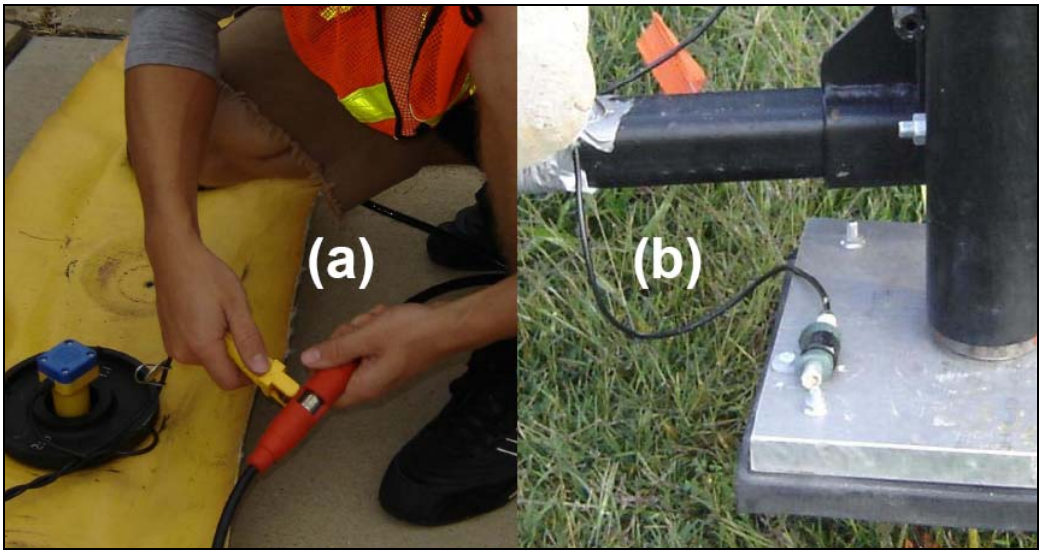

Figure A.23: (a) Checking the connection at a numbered geophone for the corresponding flat trace; (b) Ensuring the trigger is securely fastened to the foot / plate.

TROUBLE SHOOTING	The trigger must be activated at the time the seismic source strikes the ground. If the trigger activates per-maturely, disconnect the trigger cable from the RAS-24 USB-100 box. Engage the impact source - the RAS-24 software should not activate. If it does, then there is likely electrical interference from the weight drop generator. In this case, ensure the battery and remote firing cables are separated from the trigger cable.

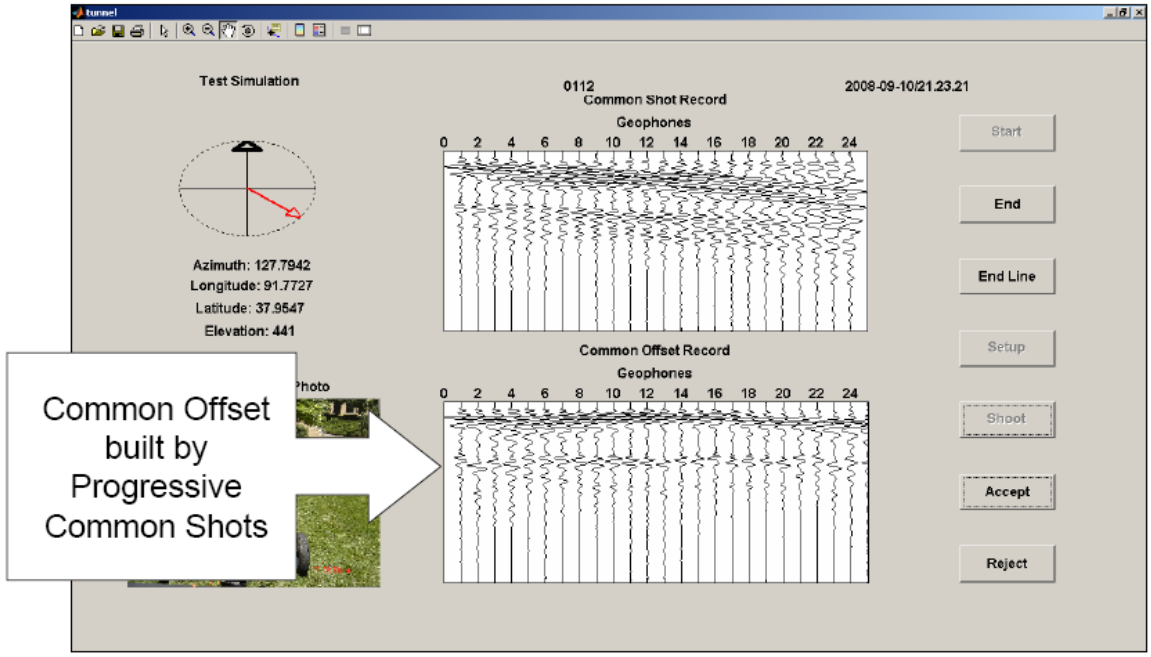

Figure A.24: Surface Wave Common Offset Graphic is constructed by adding a trace from each consecutive shot. This screen will be blank at the beginning of a survey line.

The common offset screen will be blank when you first begin the survey. With each successive shot that is accepted, a trace is added (from the first geophone onto the screen). Once the screen is full, the shots continue to add onto it (Figure A.24). The software operator can scroll left or right on the GUI to view long survey records. The common offset screen is a visual method to locate tunnels. Simplistically, as the source nears a tunnel, the seismic energy is reflected between the host material and air interface of the tunnel wall and is recorded by the geophones. Additionally, when a geophone is over a tunnel, it does not receive some of the energy because it is blocked by the void. This leads us to describe the seismic trace pattern as being 'pulled-up'. Examples are given in Figures A.25 & A.26 to assist the DMSU crew in visually looking for this phenomenon and locate possible tunnels through direct visual interpretation.

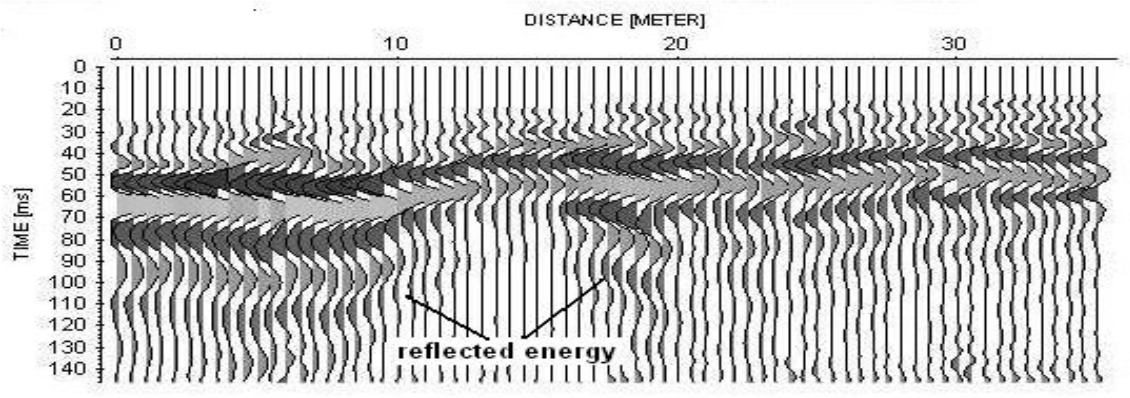

Figure A.24: 2D Rayleigh wave profile above a known 1m embedment depth tunnel. Raw data allows for visual interpretation of tunnel location. Note how the reflected energy is pulled-up toward the center-line of the top of the tunnel.

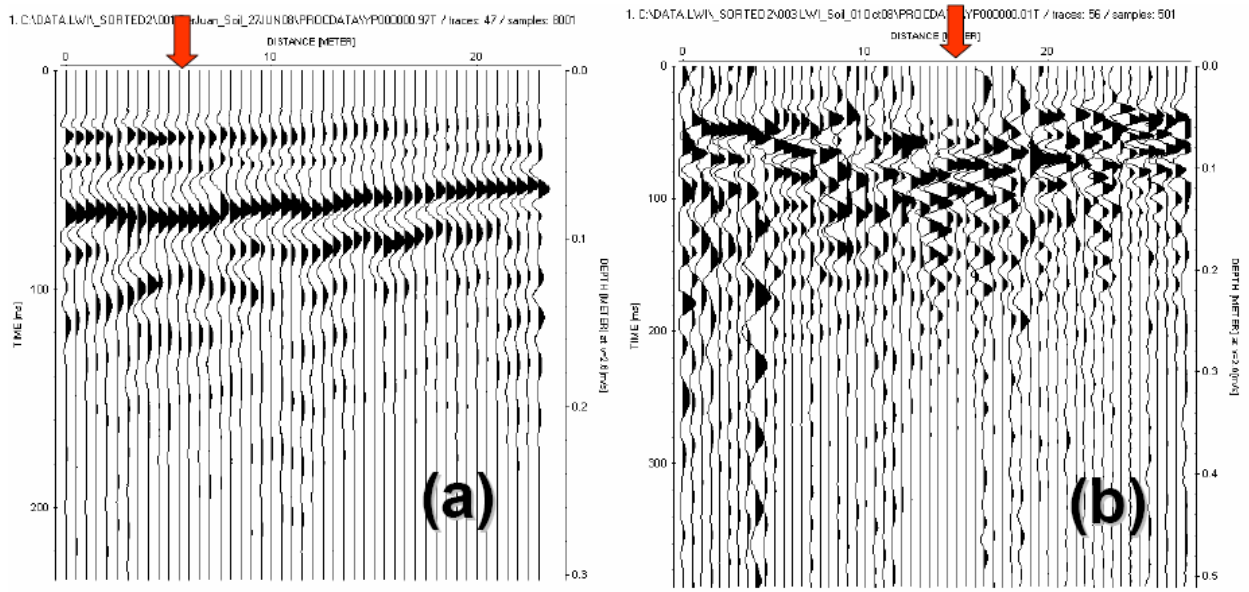

Figure A.25: Common offset profile in soil; (a) red arrow signifies 'ground truth' center-line of tunnel; (b) tunnel is not discernable but the automated software can interpret possible locations.

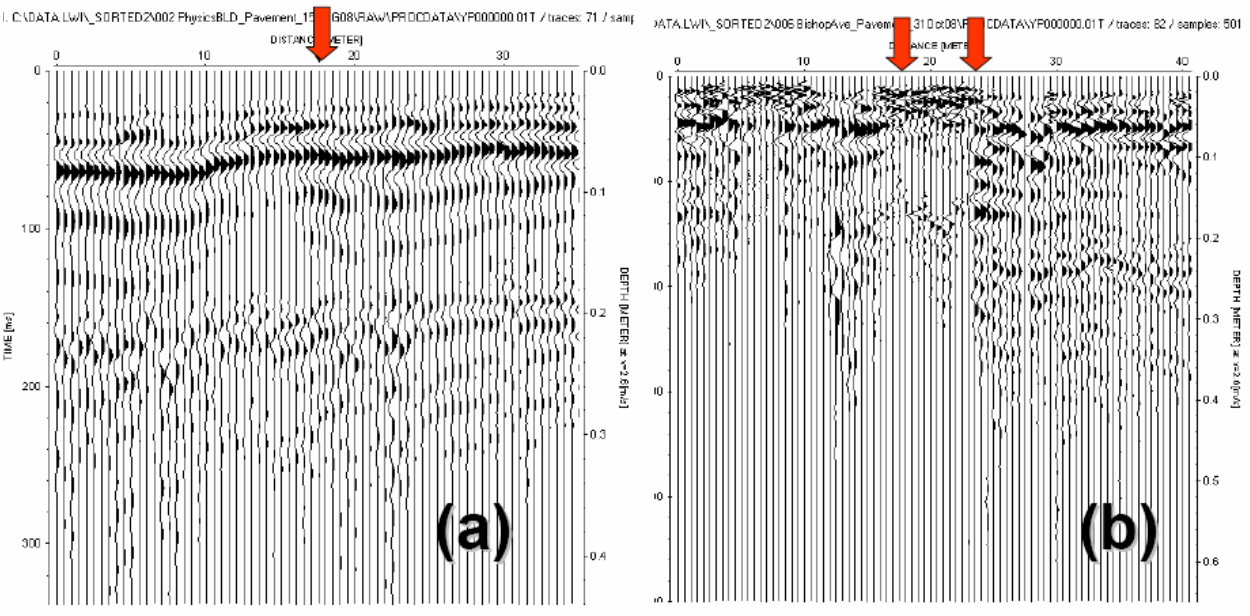

Figure A.26: Common offset profile on pavement; (a) red arrow signifies 'ground truth' center-line of tunnel. Here the tunnel is at an angle, so one might interpret it to be at a slightly different location than it is; (b) a large 3m wide concrete lined box tunnel. Reflections at edges may cause the interpretation software to pinpoint an edge. From the visual interpretation, we might attempt to closely match the interpretation software to common off-set visual interpretation locations.

Interpretation Software

IMPORTANT	For more information about any control, form field, or button, simply move the mouse cursor over it. A **yellow tooltip** popup will appear with more information.

1. Double click on the **Firefox** icon on the Windows desktop to launch the Firefox web browser. The Mapping Software will *not* work in Internet Explorer.
2. Click the **Interactive Viewer** link in the toolbar or enter http://localhost:8080/geoserver/www/index.html in the URL bar. You may click this link at any time to return to return to the main page and start over. The main page is a search engine that will allow you to find the surveys you are interested in viewing, and you can use it just like any other web page.

1. Launch Firefox

3. To display the most recent sweeps that the Mobile Seismic Unit has conducted, just click the **recent sweeps** hyperlink. Otherwise, fill out the search form to find a specific sweep.

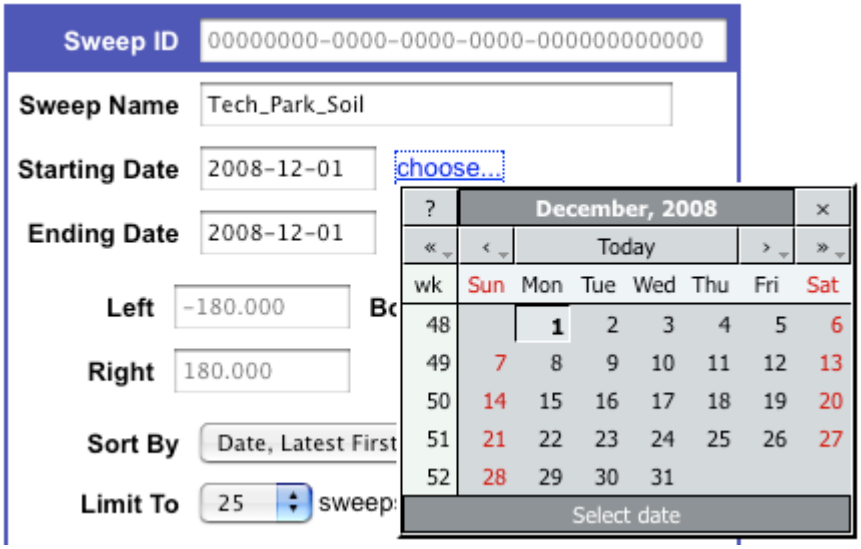

3. Search form with date picker

- Each form field displays examples of valid input in light gray text.
- You may fill out any or all of the form fields, and the search tool will return **only** sweeps that match **all** fields entered. For example, entering a Sweep Name of "Tech Park Soil" and a Starting Date of "2008-12-01" will find only sweeps named "Tech Park Soil" that were conducted after December 1st, 2008.
- The **Sweep Name** field is case-sensitive and matches any part of the sweep name.
- The Starting and Ending Date fields have a "**choose...**" hyperlink that displays a graphical date picker (see above photo) for easily choosing dates.
- The four GPS bounding box fields (**Left**, **Bottom**, **Right**, **Top**) will accept either decimal degrees (such as "-91.78") or degrees-minutes-seconds (such as "91 46 48.00W"). As per convention, positive longitudes are east of the prime meridian, and positive latitudes are north of the equator.
- By default, search results are sorted by date, with the most recent sweeps listed first. You may change this behavior with the **Sort By** menu.

4. Search results will appear in a table on the right side of the page. Each entry lists the sweep name, the starting time, and the decimal degrees longitude and latitude values of the center of the sweep. Click the **name hyperlink** to open a 2D map of the sweep in a

Name	Date	Lon (°E)	Lat (°N)
Tech_Park_Soil_NEW 2008-12-01/15.41.55	2008-12-01T15:41:55	-92.1069	37.7606

4. Click the hyperlink to open a map

new tab.

5. On the map screen, survey **lines** appear as yellow lines, and detected anomalies ("**hits**") appear as varying shades of red dots. Higher confidence hits appear in darker shades of red.

5. Survey line with hits

6. Use any of the following controls to adjust the map view. By default, the map is centered on the middle of the selected sweep, so very little adjustment should be necessary. The map is updated in real-time whenever you press any of these controls.

	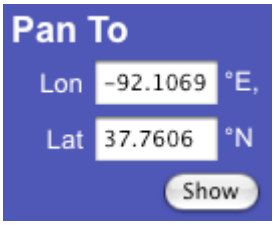	
1. Pan Tool	2. Pan Coordinates	3. Zoom Bar

1. Pan Tool: **Click** the **arrows** to adjust the map view up, down, left, or right. You may also grab and **drag** the **map** with the mouse, just as if you were moving a paper map.
2. Pan Coordinates: Enter a set of coordinates and click the **Show** button to re-center the map on those coordinates.
3. Zoom Bar: **Drag** the slider **up** to zoom **in** or **down** to zoom **out**. You may also use the mouse wheel (if present) to zoom the map. To zoom in on a specific area of the map, **hold** the **shift** key and drag the mouse over the area you wish to zoom in on.

7. Use either of the following controls to adjust the data that is displayed.

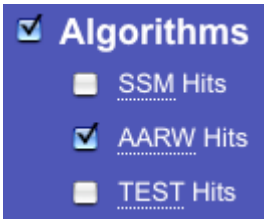	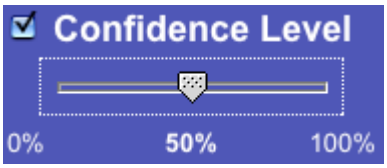
1. Algorithm Selector	2. Confidence Level Slider

1. Algorithm Selector: **Check** the **checkboxes** corresponding to the algorithms you would like to see. The Mobile Seismic Unit uses two different algorithms to find voids, and this control selects which algorithm(s) will be displayed on the map. It is recommended, for the sake of visual clarity, that you only view one algorithm at a time. Be aware of the following limitations when selecting which algorithm to use:
    1. SSM: The Spiking Statistic Method only detects voids that are directly below the drop source during a shot.
    2. AARW: The Attenuation Analysis of Rayleigh Waves method detects voids along the entire geophone array (i.e. from the first geophone to the last geophone).
2. Confidence Level Slider: This tool allows you to filter out low confidence data. **Drag** the slider **right** to **increase** the minimum confidence, and drag the slider **left** to **decrease** the minimum confidence. When the slider is selected, you may also use the **left** and **right arrow keys** to move the slider.

8. Adjust the **confidence level slider** until **one or two clusters** of high-confidence points are visible. This process is highly subjective and requires additional training, but these are some general guidelines

		
1. Confidence too low	2. Confidence too high	3. Confidence just right

1. If the confidence is set too low, there will be too many hits to make sense of, resulting in a very "noisy" image.
2. If the confidence is set too high, there will be very little data displayed, and important information may be missing.
3. If the confidence is set correctly, there will be one or two clusters of high-confidence anomalies very close together. High-confidence clusters like this are most likely underground voids.

This process is similar to focusing a microscope. If the display is "out of focus," the picture will not make any sense.

9. **Click** on any **hit** to display a popup window containing additional details and options.

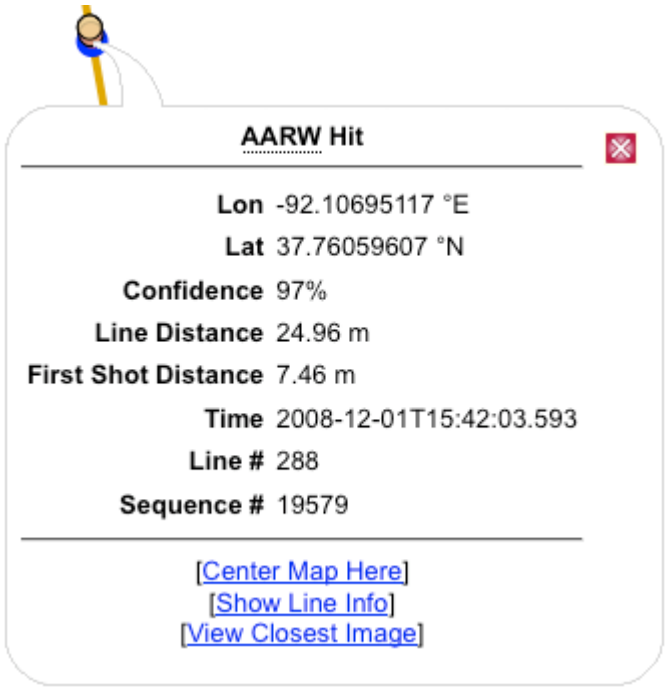

9. Click on a hit to show this popup

The popup window displays

- The algorithm that created the hit and its **Confidence** level
- The exact **longitude** and **latitude** of the anomaly in decimal degrees
- **Line Distance**: The distance of the anomaly in meters from the beginning of the yellow survey line. (i.e., the position of the *last* geophone during the *first shot*.)
- **First Shot Distance:** The distance of the anomaly in meters from the position of the *drop source* during the *first shot*.
- The time the hit was stored in the database and some database identifiers.

- Click the red close box, another hit, or anywhere on the map display to dismiss the popup window.
- The **Center Map Here** link re-centers the map on the selected hit.
- The **Show Line Info** link opens another popup menu with more information about that survey line, including its overall length and GPS coordinates.
- The **View Closest Image** link displays the closest camera image to the selected hit.

10. The **Get Info** control changes what happens when you **single click** on the map screen.

10. The Get Info tool

- **Show Hit Info:** Opens a popup window, as described in Step 9, when you click on any *hit*.
- **Show Line Info:** Opens a popup window with more information when you click on any *line*.

11. To save the current view for later, use the **Permalink** control. **Right-click** on the "**Permalink**" hyperlink and select either **Copy Link Location** to copy it to the clipboard or **Bookmark this Link** to save it in Firefox. Open or visit this link later to restore the map view (complete with selected algorithms and confidence level) to the exact same state it was when you saved it. The numbers underneath the permalink control are the current GPS coordinates of the **mouse pointer**, in decimal degrees.

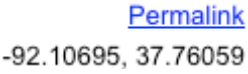

11. The Permalink Control

Operation

1. The crew should decide the most efficient way to the assign tasks in operation of the DMSU. Other than driving and operating the software, it is recommended that the driver operate the remote trigger switch and the software operator take field notes and log each shot.
2. As per previous instructions, it is assumed that all systems are functioning.
3. The software operator uses the GPS to determine the location at the beginning of the survey line.
4. Typically the location of the first geophone is used as the reference on the survey line. When moving the ATV the impact arm should be in the up position.
5. The driver stops at the shot location. Then, the driver backs up slightly to let the tension out of the chain to reduce engine vibration in the streamer.
6. The software operator ensures that the system is charged. The driver then activates the source.
7. Depending on the quality of the shot, the operator accepts or rejects it. In soils, the first shot is used to seat the plate. The second shot is often of better quality and is accepted.
8. The impact arm is raised. The driver and operator communicate in regard to observations. The ATV is moved forward on the survey line trajectory 0.5m.
9. Since the ATV cannot stop exactly at 0.5m every time and we cannot back-up the streamer array, typically a note is made on the log, and the error is subtracted from the next advance (using the Digi-roller) to compensate.
10. At the end of the survey line, the software operator notes the GPS location. The software routine is run and the operator / driver 'pick' suspect tunnel locations on the line. They mark the position on the survey line with paint or flags before preparing to survey the next line.
11. The DMSU is repositioned for the next survey line at sharp turns where the array must be unhooked from the ATV with trailer for rotation or repositioning (of the array). Subsequently, the ATV with trailer is then reconnected to the streamer at the orientation and start of the next survey line.

	Use photo and common off-set interpretation in concert with the mapping tool to locate the suspected tunnel locations before proceeding to the next survey line. It is often difficult to reconstruct or validate the positions of the anomalies on the survey line away from the site.

DMSU Risk Assessment Template

Risk	Control Measure	Residual Rating
1. Accident caused by operation of weight drop	Only DMSU trained personnel operate equipment	
2. Scraping of surface due to streamer dragging or damage due to weight drop	Identify / use approved survey lines coordinated with local authority	
3. Inclement weather (lightning)	Cease work and find shelter	
4. Security: Theft of equipment or data	Laptop in possession at all times / secure unit after survey	
5. Security: OPSEC	No unauthorized wireless transmission of data	
6. Incident	Notify headquarters	
7. Damaged / lost equipment	Protect geophones / recover equipment	
8. Injury	Outline first aid actions for non-life threatening injury or sickness and identify evacuation route	
9. Safety	a. Use hardhats & reflective vests while operating equipment b. Use traffic cones and assign additional safety officer near traffic or construction sites c. Requires area lighting at night	
Prepared By:	Date:	

DMSU Field Notes Template

SURVEY LINE FILE REF	
Date of Survey	
Location	**Name:** **GPS Start:** **GPS End:** **Azuimth:**
Field crew	**Driver:** **Software Operator:** ☐ **Security / Safety Support**
RAS-24 Settings	☐ **Record Length 0.5s** ☐ **Sample Interval 1.0ms** ☐ **Gain 12db** ☐ **Stacking Off**
System Check	☐ **Laptop Communications** ☐ **RAS-24 Button 'beep'** ☐ **Dissimilarity / Visual**
Advance Interval	☐ **0.5m** ☐ **1m**
Topography / Slope	☐ **Less Than 10% Slope**
Site Conditions / Weather	
Surface	☐ **Bare Compact Soil** ☐ **Grassy or Loose Soil** ☐ **Pavement / Asphalt**
Source Configuration	☐ **Rubberized Foot** ☐ **Plate & Hammer**
Structures or Buried Utilities Known	
Line Length	
Background Noise	☐ **Heavy Trucks** ☐ **Intermittent Car Traffic** ☐ **Wind** ☐ **None**
Notification Requirements	
Site Sketch with North Arrow and Approximate Scale	

SURVEY LINE FILE REF		**Page Number**
File Number	**Shot Number**	**First Geophone Location (HIT)**

APPENDIX B: DMSU PARTS MANUAL

The purpose of Appendix B: Parts Manual, is to document information about the purchased and fabricated hardware and electronics used to construct the Demonstration Mobile Seismic Unit (DMSU). It also provides information about freeware & purchased software integrated for use on the laptop. Appendix B is organized in the following manner:

- Modularization of the DMSU
- Commercial-off-the-Shelf Hardware
- Fabricated Hardware
- Software
- Hardware ToughBox Packing List
- Electronic ToughBox Packing List

B.1. Modularization of the DMSU

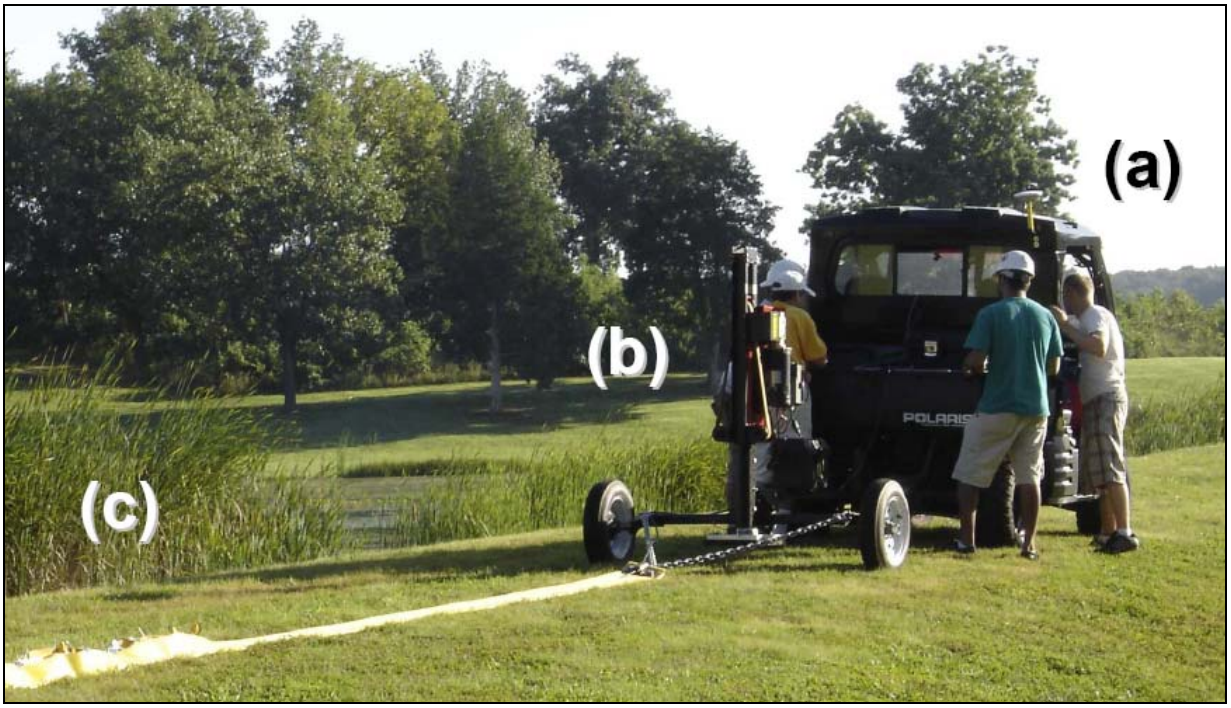

Figure B.1: The demonstration mobile seismic unit (DMSU) consists of (a) an all-terrain vehicle (ATV), (b) a towed trailer with an seismic impact source, and (c) a towed streamer consisting of a fire hose with 24 geophones. The fabricated hardware section is divided by association into these three primary parts.

	DMSU Modularized for Shipping	
No.	**Nomenclature**	**Notes**
1	Polaris Ranger 500 Series ATV 4X4	
2	GEO Strike Seismic Source Trailer	
3	Streamer Array (Firehose with Geophone Adapter Plates attached)	In back of ATV
4	Calculated Industries DigiRoller PlusII	In back of ATV
5	Hardware ToughBox	In back of ATV
6	Software ToughBox	In back of ATV
7	Dell XFR D630 Toughbook	Separate for Information Security
8	Car Batteries (2 each)	HAZMAT (May be shipped separately or procured 'in country')
9	Fuel & Aerosols (Paint & Foam Spray Cans)	HAZMAT (May be shipped separately or procured 'in country')

Table B.1: The DMSU is a self-contained system that can be modularized for shipping. Note that items 3 - 6 (above) are placed into the bed of the ATV.

B.2. Commercial-off-the-Shelf (COTS) Hardware

Table B.2 (below) lists the COTS Hardware that was procured to construct the DMSU. The items are available either 1) on-line at the link provided, or 2) from local retailers (e.g. Radio Shack, Wall-Mart, or Lowe's Stores).

	Commercial Hardware	
No.	**Nomenclature**	**Internet Reference / E-mail**
1	Polaris Ranger 500 Series ATV 4X4	http://www.polarisindustries.com/en-US/Ranger/ Pages/Home.aspx
2	Polaris Ranger Lock & Ride Windshield Kit (PN 287562)	http://www.polarisindustries.com/en-US/Ranger/ Pages/Home.aspx
3	GEO Strike Seismic 100lb Impact Source (PN GS141TFR1A)	bwsgeoph@juno.com
4	GEO Strike Impact Foot for Pavement (PN GS141HMP1A)	bwsgeoph@juno.com
5	Seistronix RAS-24 Seismograph	http://seistronix.com/ras_g.htm
6	USB-100 to RAS-24 Cable	http://seistronix.com/ras_g.htm

7	USB-100 with Hammer Switch Cable	http://seistronix.com/ras_g.htm
8	USB to RAS-24 Interface Cable	http://seistronix.com/ras_a.htm#
9	Seistronix Battery Connector Cable	http://seistronix.com/ras_g.htm
10	Geophone Cable 24 Channel, 1 Meter Spacing	http://seistronix.com/ras_a.htm#
11	Hammer Spread Cable Adapter	http://seistronix.com/ras_a.htm#
12	4.5 Hz Geophones (25 each)	http://seistronix.com/ras_a.htm#
13	Seismic Trigger (6 each) (PN BWSGDCTM1401)	bwsgeoph@juno.com
14	Dell XFR D630 Toughbook	http://www.dell.com/content/products/ productdetails.aspx/ latit_xfr_d630?c=us&l=en&s=bsd&cs=04
15	Law Enforcement Workstation Kit	http://www.ram-mount.com/nodrillsystems/ nodrillbases.htm
16	Trimble GPS Pathfinder ProXT Receiver	http://www.trimble.com/pathfinderproxt.shtml
17	Trimble GPS Pathfinder ProXT Antenna	http://www.trimble.com/hurricane.shtml
18	15 Pin (M/M) Cable Extended 6' GPS to Laptop	http://www.radioshack.com/product/ index.jsp?productId=2484250
19	AGFA Digital Video Camera DV-5000G	http://reviews.cnet.com/digital-camcorders/ agfaphoto-dv-5000g-camcorder/ 4507-6500_7-32869319.html?tag=mncol;rnav
20	USB (M/Camera) Cable Extended Camera to Laptop	http://www.radioshack.com/product/ index.jsp?productId=2809554
21	Car Power Adapter (3 Outlet)	http://www.radioshack.com/product/ index.jsp?productId=2062269
22	Everstart Marine MAXX-29 Batteries (2 each)	Wallmart
23	1 & 7/8 Inch Ball and Hitch (Towing)	Wallmart
24	Calculated Industries Digi-Roller Plus II	http://calculated.com/prd31/ DigiRoller+Plus+II.html

Table B.2: Commercial-off-the-shelf hardware used to construct the DMSU.

B.3. Fabricated Hardware

	Fabrication Hardware	
	ATV	**E-mail**
25	Digital Camera Mount	inskipn@mst.edu
26	Trimble Antenna Mount	inskipn@mst.edu
27	Trimble Receiver Mount	inskipn@mst.edu
28	DigiRoller Plus II Spring Mount Adapter	inskipn@mst.edu

Table B.3: Fabricated items attached to the ATV.

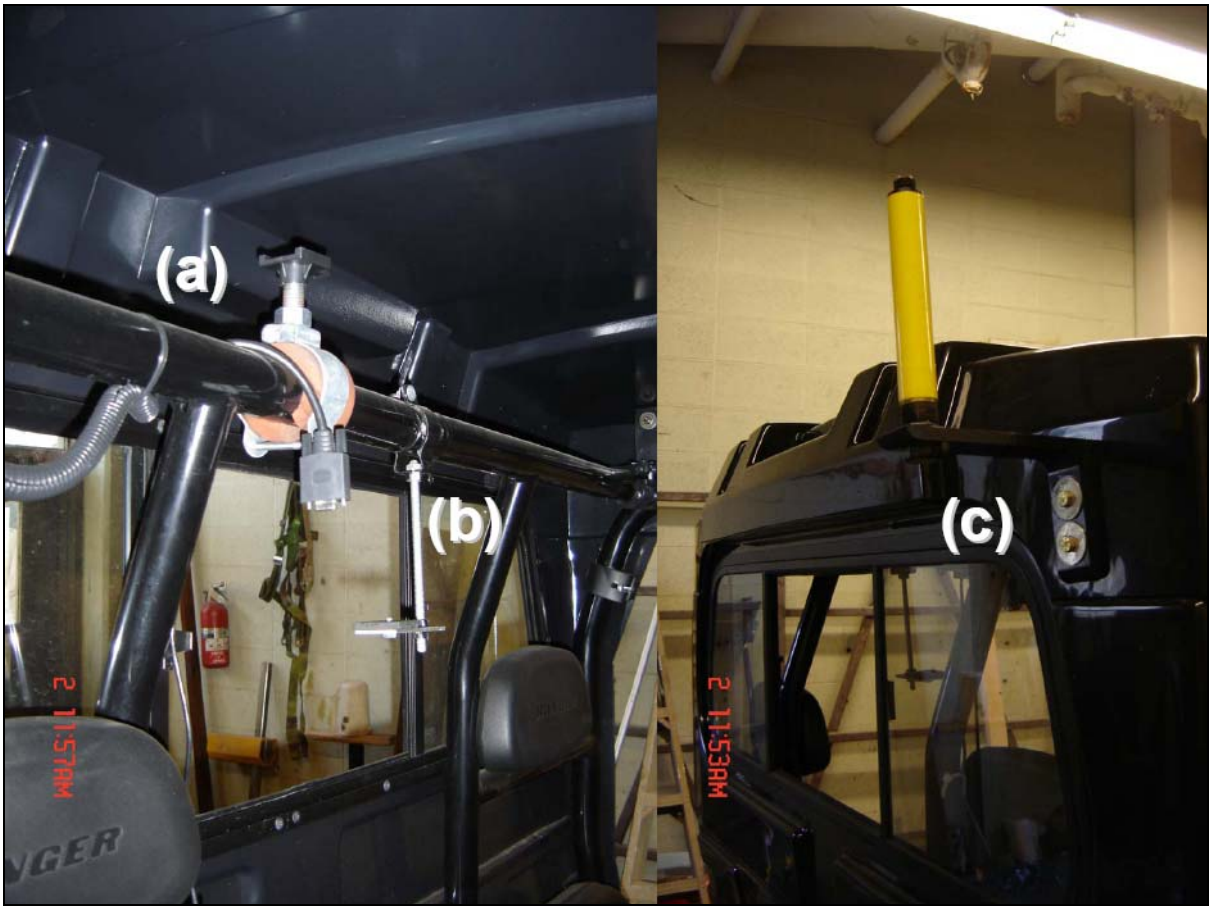

Figure B.2: (a) Slide and lock Trimble receiver mount; cable conduit containing 15-pin Trimble cable, camera & RAS-24 cables from laptop through the rear sliding window, (b) Hanging camera pedestal, and (c) GPS antenna mount.

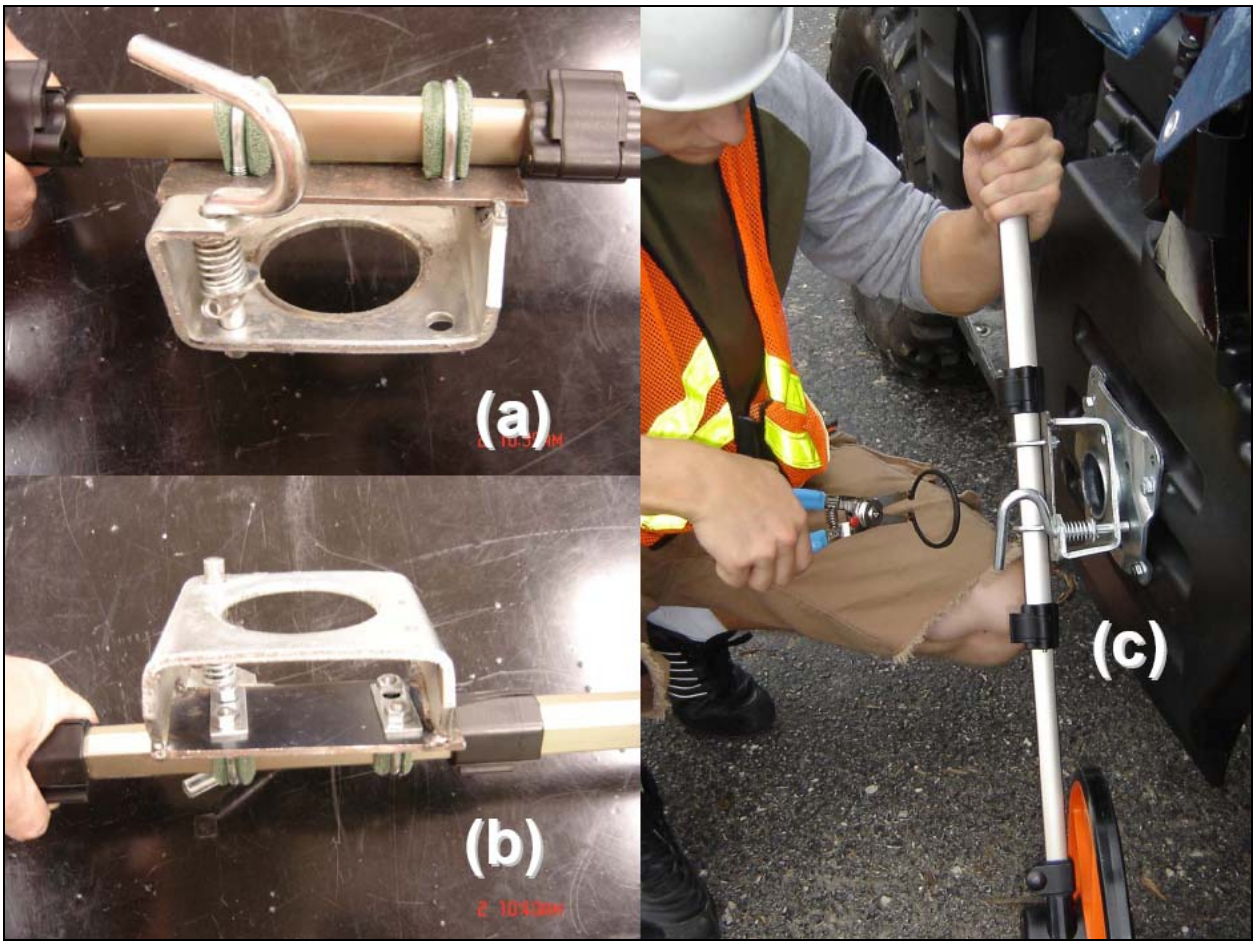

Figure B.3: (a) Outward side of the DigiRoller Plus II spring mount adapter using U-Bolts and housing, (b) Reverse side of adapter, (c) Attaching the roller housing to the vehicle bracket. Note a separate spring plus the upper handle such that the roller makes contact with the ground. The operator measures the interval of advance by using the Digi-roller.

Figure B.4: Law Enforcement Laptop Kit. Note 3-way 12V outlet power adapter and extended USB cables that plug into the back of the Dell XFR D630 Toughbook.

	Fabrication Hardware	
	GEO Strike Source / Trailer	**Internet Reference / E-mail**
29	GEO Strike Metal Plate for Soft Soil (Alloy Steel 4130) 30 x 30x 3cm	http://www.onlinemetals.com/merchant.cfm?pid=9662&step=4&showunits=inches&id=1&top_cat=0
30	Metal Plate Dragging Adapter: Eye Bolt with Hex Nut, 5/16" x 6" Zinc	http://hardware.hardwarestore.com/ 28-447-eye-bolts.aspx
31	Seismic Trigger Housing	inskipn@mst.edu
32	Seismic Hammer Head for Soft Soil (Alloy Steel 4130) from Pipe Fitting taped for 1.5" Bolt	inskipn@mst.edu
33	Chain Link for Dragging Streamer & Plate (Soft Soil)	http://fasteners.hardwarestore.com/ 16-63-chain-specialty/machina-chain-800029.aspx
34	Screw Pin Anchor Shackle, 5/16" (4 each)	http://search.hardwarestore.com/?query=shackle&tId=346
35	Bungee Chords (Assorted)	http://search.hardwarestore.com/?query=bungee&tId=3954
36	Sand Bags (2 each)	http://search.hardwarestore.com/?query=sand+bag&x=8&y=9
37	Twisted Poly Rope, 3/4" x 150' Yellow	http://search.hardwarestore.com/?query=rope&tId=354

Table B.4: Fabricated items used for the GEO-Strike Trailer.

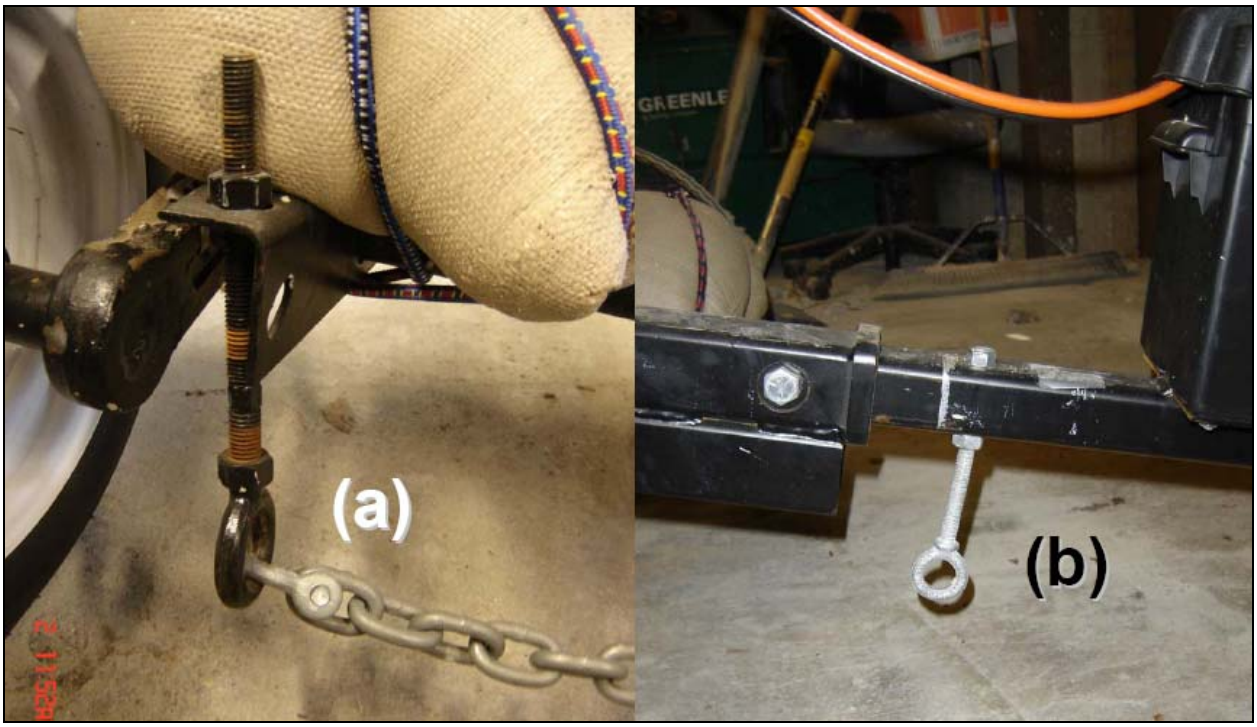

Figure B.5: (a) Eye bolts affixed on the trailer frame near each wheel of the trailer used to drag the chain & streamer array, (b) Eye bolt affixed to the frame to drag the chain & metal plate (for soft soil). Note that a filled sandbag is tied down by bungee chords at each wheel to keep the trailer grounded when the impact hammer is strikes the ground.

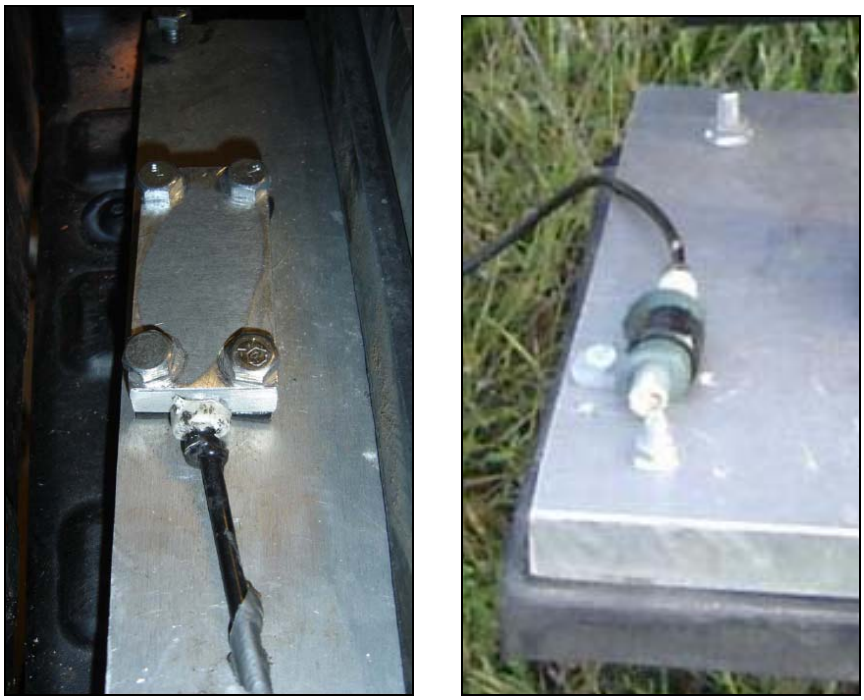

Figure B.6: The metal plate (for soft soil) has an aluminum bracket with a core semi-circular groove that clamps the trigger using standard bolts (left). The rubber foot uses a clamp with foam insulation to house the trigger (right).

	Fabrication Hardware	
No.	**Nomenclature**	**Internet Reference / E-mail**
	Streamer Array	
38	KOCHEK 5" Supply Firehose 100' Split on one side for geophone plates, 3/8" hole punch every 0.5m for plate screw, first geophone hole punch is 6m from source, tow chain included	http://www.chiefsupply.com/Fire%2CRescue/Fire_Hose/Municipal/RC5
39	Streamer Towing Clamp; double over firehose end to prevent tearing	inskipn@mst.edu
40	Geophone Plate Assembly (24 each pair) with 3/8" hole & bolt weld	http://www.iowaspinners.com/fabrication_services.aspx
41	2.5lb. Standard Cast Iron Weights - Barbell (48 each) 2 per geophone plate (one welded / one placed)	http://www.adamantbarbell.com/index.php?main_page=product_info&cPath=76_144&products_id=667

Table B.5: Fabricated items that comprise the geophone streamer array.

Figure B.7: (a) Bottom of streamer towing clamp with anchor shackle used to drag the streamer, (b) upper portion of streamer towing clamp with pipe to route geophone cable.

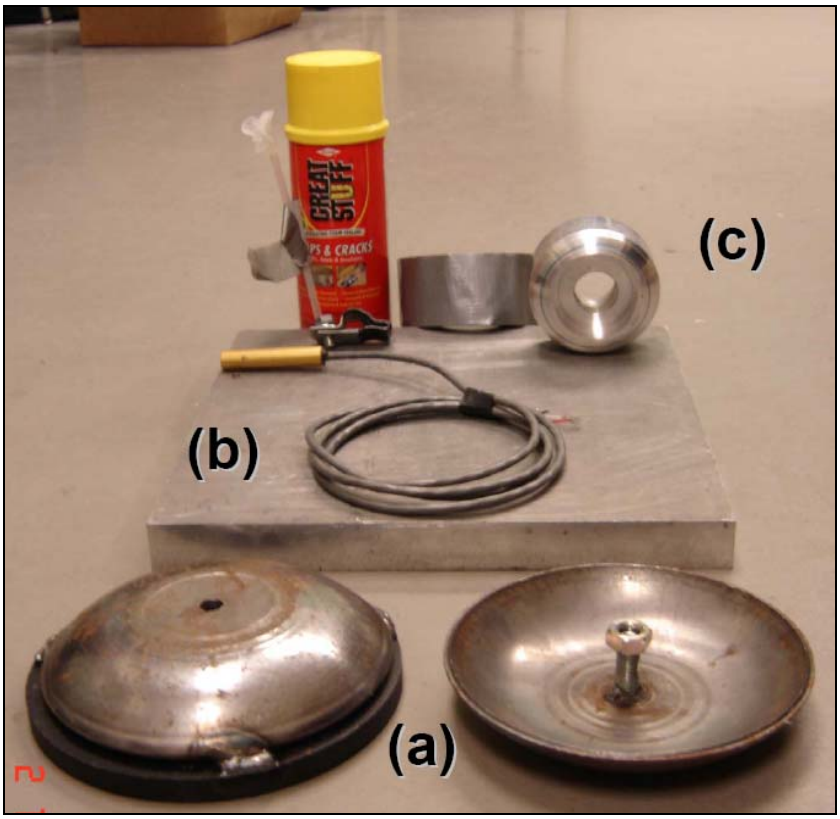

Figure B.8: (a) Geophone coupling plate set where lower plate has 3/8" spot welded bolt and top plate has drilled 3/8" hole with 2.5 lb. cast iron weight spot welded to edges (b) 30 by 30 by 3 cm metal plate (soft soil), (c) Hammer head (soft soil) of pipe fitting from 4130 alloy steel tapped to fit GEO Strike 1.5" bolt.

B.4. Software

	Software	
No.	**Nomenclature**	**Internet Reference**
1	Seistronix RAS-24 Software (Packaged with Hardware)	http://seistronix.com/ras_g.htm
2	Mathworks MATLAB	http://www.mathworks.com/products/matlab/
3	Microsoft Windows XP OS	http://www.microsoft.com/windows/ windows-xp/default.aspx
4	PostgreSQL Global Development Group PostgreSQL	http://www.postgresql.org/
5	Refractions Research PostGIS (PostgreSQL extension)	http://postgis.refractions.net/
6	2D Mapping Tools Shareware (ARCGIS Extension)	http://geoserver.org/display/GEOS/Welcome
7	Trimble GPS Pathfinder ProXT Receiver (Packaged with Hardware)	http://www.trimble.com/pathfinderproxt.shtml
8	AGFA Digital Video Camera DV-5000G (Uses Windows XP Packaged with Hardware)	http://reviews.cnet.com/digital-camcorders/ agfaphoto-dv-5000g-camcorder/ 4507-6500_7-32869319.html?tag=mncol;rnav

Table B.6: Purchased and specially adapted freeware.

B.5. Hardware ToughBox Packing List

The DMSU (ATV with Trailer) is configured to be driven to an area of interest. It is then set up to conduct the survey on-site and broken down upon completion. The Hardware ToughBox Packing List (Table B.7) includes the Geophone Cable, Geophones, and Toolkit. Again, the laptop is carried by the software interpreter and HAZMAT (e.g. Batteries) are joined to the DMSU once it arrives from shipping to conduct systems checks before driven to the area of interest.

Figure B.9: Visual contents of the Hardware Toughbox.

	Hardware ToughBox Packing List
No.	**Nomenclature**
1	De Walt Standard Toolkit
2	4 lb. Blacksmith Hammer
3	3 Inch shortened U Post (10 each)
4	Screwdriver Flathead 18" (2 each)
5	Geo Strike Elastomere Bands All Weather (2 Spare) (PN GS141EB1A)
6	Electrical Tape (6 rolls)
7	Vinyl Duct Tape (4 rolls)
8	100 meter spool measuring tapes (2 each)
9	Environmental Marking Paint (4 Cans)
10	Great StuffBig Crack Foam (1 Can)
11	Surveyor Marking Flags (100 each)
12	USB-100 with Hammer Switch Cable
13	Geophone 24 Channel Cable, 1 Meter Spacing
14	4.5 Hz Geophones (24 each)
15	4.5 Hz Geophone Calibration (Do not use)
16	Fire Control Electronics: Cable& Remote Control Box (PN GS141FCE1A)
17	Impact Strike Metal Plate for Soft Soil (Alloy Steel 4130) 30 x 30x 3cm
18	Impact Plate P/S wave (Pavement) (PN GS141IMPSW1A)
19	1 & 7/8 Inch Ball and Hitch (Towing)
20	Chain Link for Dragging Streamer & Plate (Soft Soil)
21	Screw Pin Anchor Shackle, 5/16" (4 each)
22	Bungee Chords (Assorted)
23	Sand Bags (2 each)
24	Cast Iron 2.5lb weights (25 each)
25	Twisted Poly Rope, 3/4" x 12' Yellow

Table B.7: Hardware used to configure the DMSU at the area of interest.

B.6. Electronic ToughBox Packing List

The Electronic ToughBox Packing List (Table B.8) includes the Seistronix RAS-24, Trimble GPS, Digital Camera, and Electricians Toolkit. Based on historical troubleshooting, it is important to include spare 80 amp fuses, geophone triggers, Elastomere bands, electrical tape and common electronic wire for splicing cables and other expedient field repairs.

Figure B.10: Visual contents of the Electronic Toughbox.

	Electronic ToughBox Packing List
No.	**Nomenclature**
1	Standard Electricians Toolkit
2	Seistronix RAS-24 Seismograph
3	USB to RAS-24 Interface Cable
4	Seistronix Battery Connector Cable
5	USB-100 to RAS-24 Cable
6	Seistronix Hammer Switch Cable Adapter
7	Wrench with 1.5 Inch Socket
8	Dilithium Crystal Seismic Trigger (4 each) (PN BWSGDCTM1401)
9	Trimble GPS Pathfinder ProXT Receiver
10	Pin to Pin for Trimble to Laptop
11	Trimble GPS Pathfinder ProXT Antenna
12	15 Pin (M/M) Cable Extended 6' GPS to Laptop
13	AGFA Digital Video Camera DV-5000G
14	USB (M/Camera) Cable Extended Camera to Laptop
15	Fuses (12 each) for Geo Strike: Bussman 80 Amp Fusible Link
16	Car Power Adapter (3 Outlet)
17	18" Plastic Ties (Bag of 50)
18	12 Volt Battery Charger

Table B.8: Electronic components and cables used to configure the DMSU at the area of interest.